VILNIUS UNIVERSITY
CENTER FOR PHYSICAL SCIENCES AND TECHNOLOGY

Marijus Jurkūnas

Synthesis and Study of Gradient and Diblock Copolymers Containing Phosphorylcholine Moieties

DOCTORAL DISSERTATION

Natural Sciences,
Chemistry (N 003)

VILNIUS 2024

The dissertation was prepared between 2019 and 2023 at Vilnius University.

Academic supervisor – Prof. Dr. Ričardas Makuška (Vilnius University, Natural Sciences, Chemistry – N 003).

This doctoral dissertation will be defended in a public meeting of the Dissertation Defense Panel:

Chairman – Prof. Dr. Saulutė Budrienė (Vilnius University, Natural Sciences, Chemistry, N 003).

Members:
Prof. Dr. Andra Dėdinaitė (KTH Royal Institute of Technology, Sweden, Natural Sciences, Chemistry, N 003),
Assoc. Prof. Dr. Tatjana Kochanė (Vilnius University, Natural Sciences, Chemistry, N 003),
Prof. Dr. Linas Labanauskas (Center for Physical Sciences and Technology, Natural Sciences, Chemistry, N 003),
Prof. Dr. Albinas Žilinskas (Vilnius University, Natural Sciences, Chemistry, N 003).

The dissertation shall be defended at a public meeting of the Dissertation Defense Panel at 14.00 hour on September 2024 in Autitorium of Inorganic Chemistry of the Institute of Chemistry, Faculty of Chemistry and Geosciences.
Address: Naugarduko st. 24, Vilnius, Lithuania.
Tel. +37052193105; e-mail: info@chgf.vu.lt

The text of this dissertation can be accessed at the libraries of Vilnius University and Center for Physical Sciences and Technology, as well as on the website of Vilnius University:
www.vu.lt/lt/naujienos/ivykiu-kalendorius

https://orcid.org/0000-0003-2198-3328

VILNIAUS UNIVERSITETAS
FIZINIŲ IR TECHNOLOGIJOS MOKSLŲ CENTRAS

Marijus Jurkūnas

Gradientinių ir diblokinių kopolimerų, turinčių fosforilcholino fragmentus, sintezė ir tyrimas

DAKTARO DISERTACIJA

Gamtos mokslai,
Chemija (N 003)

VILNIUS 2024

Disertacija rengta 2019–2023 metais Vilniaus Universitete.

Mokslinis vadovas – **prof. dr. Ričardas Makuška** (Vilniaus universitetas, gamtos mokslai, chemija – N 003).

Gynimo taryba:

Pirmininkė – prof. dr. Saulutė Budrienė (Vilniaus universitetas, gamtos mokslai, chemija – N 003).

Nariai:

prof. dr. Andra Dėdinaitė (Karališkasis technologijos institutas, Švedija, gamtos mokslai, chemija – N 003),

doc. dr. Tatjana Kochanė (Vilniaus universitetas, gamtos mokslai, chemija – N 003),

prof. dr. Linas Labanauskas (Valstybinis mokslinių tyrimų institutas Fizinių ir technologijos mokslų centras, gamtos mokslai, chemija – N 003),

prof. dr. Albinas Žilinskas (Vilniaus universitetas, gamtos mokslai, chemija – N 003).

Disertacija ginama viešame Gynimo tarybos posėdyje 2024 m. rugsėjo mėn. 13 d. 14 val. Vilniaus universiteto Chemijos ir geomokslų fakulteto, Chemijos instituto Neorganinės chemijos auditorijoje. Adresas: Naugarduko g. 24, Vilnius, Lietuva, tel. +37052193105; el. paštas info@chgf.vu.lt.

Disertaciją galima peržiūrėti Vilniaus universiteto ir Fizinių ir technologijos mokslų centro bibliotekose ir VU interneto svetainėje adresu: *https://www.vu.lt/naujienos/ivykiu-kalendorius*

CONTENT

ABBREVIATIONS

^{1}H NMR	- proton nuclear magnetic resonance
^{13}C NMR	- carbon nuclear magnetic resonance
ADOPMA	- acetonide-protected dopamine methacrylamide
ATR	- attenuated total reflectance
ATRP	- atom transfer radical polymerization
BMA	- butyl methacrylate
CTA	- chain transfer agent
CTP	- cyanopentanoic acid dithiobenzoate
CS	- chitosan
COF	- coefficient of friction
DFT	- density functional theory
DLS	- dynamic light scattering
DMF	- dimethylformamide
DMSO	- dimethylsulfoxide
DMA	- dodecyl methacrylate
DMAEMA	- 2-dimethylaminoethyl methacrylate
DOX	- doxorubicin
DOPMA	- dopamine methacrylamide
DP	- degree of polymerization
Đ	- molecular weight dispersity (M_w/M_n)
EMA	- ethyl methacrylate
FTIR	- Fourier-transform infrared spectroscopy
HA	- hyaluronic acid
H/D	- hydrogen–deuterium exchange
HEMA	- 2-hydroxyethyl methacrylate
HMA	- hexyl methacrylate
kDa	- kilo Dalton
macroCTA	- macromolecular chain transfer agent
MEA	- 2-methoxyethyl acrylate
MeOH	- methanol
MMA	- methyl methacrylate
M_n	- number-average molecular weight
M_w	- weight-average molecular weight
MPC	- methacryloyloxyethyl phosphorylcholine
NMP	- nitroxide-mediated polymerization
NPs	- nanoparticles
OA	- osteoarthritis

OPEMA	- 2-(2-oxo-1,3,2-dioxaphospholan-2-yloxy)ethyl methacrylate
pBA	- poly(*tert*-Butyl 2-((2-bromo-propanoyloxy) methyl)acrylate)
PC	- phosphorylcholine
PCL	- ε-polycaprolactone
PDA	- polydopamine
PEO	- poly(ethylene oxide)
PEOMEMA	- poly(ethylene oxide) methyl ether methacrylate
pLA	- poly(D,L-lactide)
PMB	- p(MPC-*co*-BMA)
pMPC	- poly(2-(methacryloyloxy)ethyl phosphorylcholine)
PNIPAAm	- poly(*N*-isopropylacrylamide)
PVI/DMS	- poly(vinylmethylsiloxane-co-dimethylsiloxane)
ppm	- parts per million
PSD	- particle size distribution
pSt	- polystyrene
R_p	- polymerization rate
r_1, r_2	- reactivity ratios of monomers in copolymerization
RAFT	- reversible addition-fragmentation chain transfer
RAIRS	- reflection-absorption infrared spectroscopy
SBMA	- sulfobetaine methacrylate
SEC	- size exclusion chromatography
SEIRAS	- surface-enhanced infrared absorption spectroscopy
SMA	- stearyl methacrylate
St	- styrene
UV-Vis	- ultraviolet-visible spectroscopy
WCA	- water contact angle

INTRODUCTION

Biomaterials are substances that has been synthesized and applied to interact with biological systems for medical purposes (therapeutic or a diagnostic). A significant field of biomaterials application is the resistance of protein adsorption and blood coagulation. The pursuit of finding the suitable materials is under the investigation that could potentially possess an ability to prevent certain undesirable biological effects because the unwanted adsorption of proteins and biomolecules can trigger blood clotting, inflammation, immunoreactions, bacterial adhesion, biofilm formation, cell adhesion, and cell differentiation. Addressing this challenge, researchers made a significant progress with the introduction of a synthetic molecule known as 2-methacryloyloxyethyl phosphorylcholine (MPC). Drawing inspiration from the molecular structure of phosphatidylcholine found in eukaryotic cell plasma membranes, MPC possess biologically inert properties, mirroring the characteristics exhibited by endothelial cells in blood vessels. At the core of these properties lies the zwitterionic phosphorylcholine (PC) group. This unique feature disrupts electrostatic interactions and maintains the formation of a thick hydration shell, rich in highly mobile free water around the PC group.

The relevance of the work

Phosphorylcholine polymers are important in biomaterial sciences due to their unique properties – antifouling effect, biocompatibility, biolubrication – and potential applications in biomedical engineering. They are known for mimicking cell membranes, making them suitable for medical implants, coatings, and drug delivery systems. The listed properties of phosphorylcholine polymers make them relevant in various scientific fields, particularly in biomedicine, where their biocompatibility and resistance to biofouling are highly desirable. Poly(2-methacryloyloxyethyl phosphorylcholine) (pMPC) is the most popular and extensively studied zwitterionic polymer, with its precursor MPC monomer being commercially available. The current trend in MPC polymer applications is towards assembling nanolayers of MPC-based polymers rather than conventional single-layer coatings on substrates. In order to achieve the potential to modify surfaces with pMPC in nanoscale, it is necessary to synthesize the diblock copolymers composed of a block of pMPC and a block of another polymer with different non-competing properties. Once synthesized, the MPC-based diblock copolymers are suitable for convenient surface modification of

medical devices with the aim to increase biocompatibility and reduce protein adsorption. It is desirable that another block of the diblock copolymer should possess a moiety capable to stick to a surface. MPC-based copolymers are envisaged to enhance lubrication in aqueous solutions. Such copolymers deliver promising potential for biomedical applications – artificial tears and saliva, biolubrication in human joints.

Scientific novelty

Kinetics of the RAFT copolymerization of the zwitterionic monomer MPC and the macromonomer poly(ethylene oxide) methyl ether methacrylate (PEOMEMA) with rather long PEO chain (19 units of ethylene oxide) was studied and the copolymers p(MPC-*grad*-PEOMEMA) were synthesized for the first time. Reactivity ratios r_1 and r_2 of MPC and PEOMEMA, respectively, in the RAFT copolymerization were determined and gradient structure of the copolymers was established. Hydrophilic diblock copolymers pMPC-*b*-pPEOMEMA and amphiphilic diblock copolymers, containing MPC and dopamine methacrylamide (DOPMA), of well-defined structure were also synthesized by the RAFT polymerization for the first time. Aqueous lubrication by the gradient and diblock copolymers of MPC and PEOMEMA was evaluated in PDMS-glass and cartilage-glass systems. The adsorption behaviour of the diblock copolymers pMPC-*b*-pDOPMA with protected and unprotected catechol groups on gold surfaces was investigated using ATR-FTIR, surface-enhanced infrared absorption spectroscopy (SEIRAS), and reflection−absorption infrared spectroscopy (RAIRS) for the first time. The copolymers with protected catechol groups demonstrated physisorption with rapid adsorption and ultrasound-assisted desorption, while the copolymers with unprotected catechol groups exhibited chemical adsorption with slower dynamics but a stronger interaction with the gold surface.

Main goal and objectives

The main goal of the present research was the synthesis of novel MPC-containing copolymers of well-defined structure and investigation of their solution properties and adsorption. To achieve this goal, the following objectives were set:
1. To study kinetics of the RAFT copolymerization of MPC and PEOMEMA.
2. To synthesize well-defined diblock copolymers of MPC with PEOMEMA and DOPMA.

3. To characterize MPC-containing copolymers and evaluate their solution properties.
4. To study aqueous lubrication by the copolymers of MPC and PEOMEMA.
5. To study adsorption dynamics of the diblock copolymers of MPC and DOPMA on gold surfaces.

The defense statements

1. Copolymers of MPC and PEOMEMA synthesized by RAFT copolymerization possess clearly expressed gradient microstructure.
2. Amphiphilic diblock copolymers of MPC and DOPMA can be synthesized by successive RAFT polymerization of MPC and acetonide-protected DOPMA in methanol.
3. Gradient and diblock copolymers of MPC and PEOMEMA show evident superhydrophilicity and cononsolvency in the solutions of water and ethanol.
4. Gradient and diblock copolymers of MPC and PEOMEMA provide excellent lubrication in the systems PDMS–glass and cartilage–glass.
5. Diblock copolymers of MPC and DOPMA exhibit chemical adsorption on gold surface followed by reorientation of the adsorbed layers.

1. LITERATURE OVERVIEW

1.1. Polymers containing phosphorylcholine moieties: synthesis, properties and application

Phosphorylcholine, a major functional group in polar site of phospholipid, is an electrically neutral, zwitterionic head group. The terminal trimethylammonium cation ($N^+(CH_3)_3$) and phosphate anion (PO_4^{2-}) combined are essential components for formation of phosphorylcholine functional group.

Cells play a crucial role in constructing biological systems, operating independently and responding to chemical and physical signals, often regulated by the cell membrane [1]. This molecular matrix, primarily consisting of phospholipids, proteins, and polysaccharides, provides mechanical strength for cell morphology and regulates chemical concentrations in the cytoplasm. Moreover, cell–cell junctions facilitate communication between neighboring cells. The multifunctionality of the cell membrane makes it an attractive choice for creating nanostructured biomimetic materials in bio-, nano-, and information technology.

Phospholipids within the cell membrane efficiently separate the intracellular cytoplasm and the extracellular environment, serving as a scaffold for glycoprotein receptors and membrane proteins on the cell surface [2,3]. Two components are present in phospholipid molecule: a hydrophobic alkyl chains and a hydrophilic polar head group. Phospholipids spontaneously assemble into a continuous bilayer membrane in an aqueous solution (Figure 1.1).
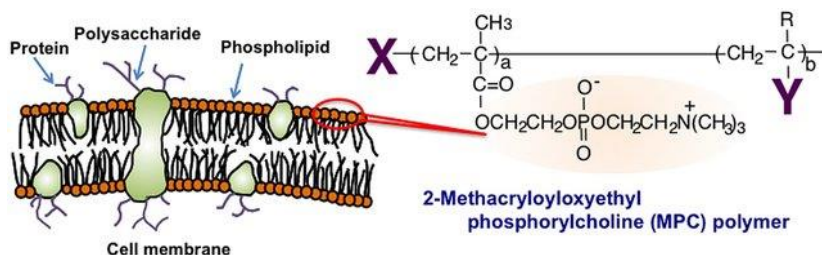
Figure 1.1. Molecular design of 2-methacryloyloxyethyl phosphorylcholine (MPC) polymers by bioinspired concept of cell membrane [4].

While phospholipid molecules have been utilized in biomimetic chemistry for structures like liposomes and Langmuir–Blodgett membranes [5], their molecular assembly faces challenges in chemical and/or physical stability. Addressing this, a proposed solution involves designing a new polymer with phospholipid polar groups, offering improved stability through bonding between phospholipid-like moieties [6].

Phosphorylcholine-based polymers have caught a huge interest in a wide range of applications, including drug delivery systems, coatings for medical devices, and tissue engineering, owing to their ability to interact favorably with biological systems [7]. The bioinspired development of the polymers involves selecting a specific phospholipid polar group and incorporating it into the polymer chain. Phosphorylcholine is a suitable polar group for obtaining a bioinert polymer [4,8]. A variety of molecular structures and material architectures containing phosphorylcholine moieties can be obtained using various methods of polymer synthesis and modification.

1.1.1. Zwitterionic monomers and polymers

The term "zwitterion" is derived from the German words "zwitter" (hermaphrodite or hybrid), and "ion" (charged particle). In the context of chemistry, a zwitterion is a molecule that contains both positive and negative charged groups, resulting with an overall neutral charge [9]. This unique characteristic arises from the presence of functional groups with acidic and basic properties within the same molecular structure [10]. The primitive example of zwitterionic material is aminoacids as molecules containing separated negative ($-COO^-$) and positive charges ($-NH_3^+$) [11]. The first successful synthesis of zwitterionic materials was reported in 1950 [12]. Subsequently, numerous studies have been conducted to investigate the synthesis, solution properties, and applications of these materials. In 1980-1990's, a new ideas were introduced regarding the synthesis of a zwitterionic monomer – an acrylate- or methacrylate-based molecule designed with a functional side group with incorporated both positively and negatively charged groups within its structure [13–15]. Generally, zwitterionic monomers are often used to synthesize zwitterionic polymers [15].

Zwitterionic polymers are polymeric inner salts bearing pairs of cationic and anionic groups in their constitutional repeat units [16]. The three possible anchoring architectures of the zwitterionic groups in polymer has been addressed in Figure 1.2: the zwitterionic groups are anchored to the polymer backbone via the spacer group separating the anionic and cationic groups (A), the zwitterionic polymers designed with a positively charged

trimethylammonium group at the terminal site (B), and polymers with a negatively charged group at the terminal site (C).

A   **B**   **C**
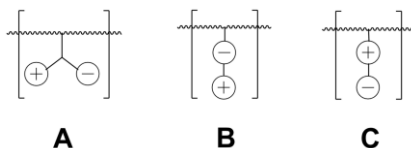
Figure 1.2. A schematic structure of some polyzwitterion with different architectures of the anionic and cationic groups [16].

Three main groups of polyzwitterions are sorted as follows: phosphorylcholine, sulfobetaine, and carboxybetaine [9]. Two primary representative monomers (Figure 1.3) utilized for producing these zwitterionic polymers are sulfobetaine methacrylate (SBMA) and butyl choline phosphate methacrylate [17].

Sulfobetaine methacrylate (SBMA)   Carboxybetaine methacrylate (CBMA)   Butyl choline phosphate methacrylate
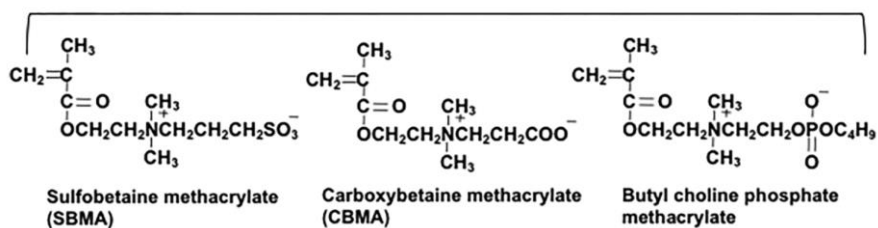
Figure 1.3. The chemical structure of some zwitterionic methacrylate monomers [17].

The first articles describing zwitterionic monomers and corresponding polymers had been published with an ambition to improve the blood affinity of the various phospholipid-based polymers [18–20]. Some of them are presented in Figure 1.4: ω-methacryloyloxyalkyl (with methylene chains of ethylene (n = 2), tetramethylene (n = 4), and hexamethylene (n = 6)) [20], ω-methacryloyloxy (poly(oxyethylene)phosphorylcholine) (MEO$_n$PC, where n = the number of repeating units in poly(oxyethylene)) [21], 2-(acryloyloxy)ethyl phosphorylcholine (APC) [22], 2-[3'-(trimethylammonium) propylphosphoryl]ethyl methacrylate (TPM) [23], 1-methyl-2-methacrylamidoethyl phosphorylcholine (MAPC) [24].
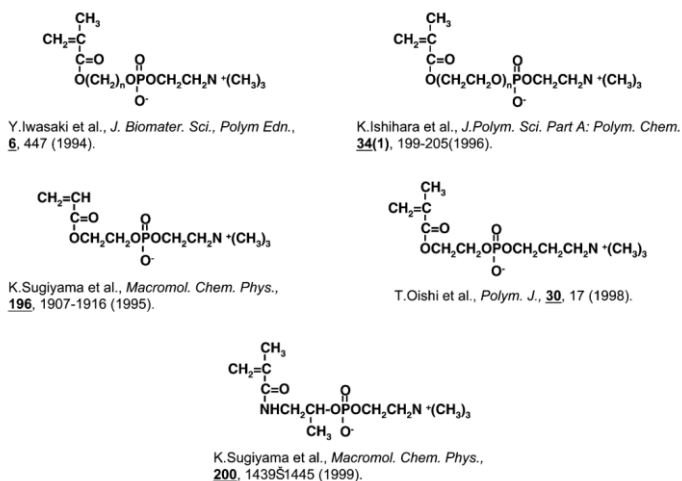
Figure 1.4. Chemical structures of some monomers containing phosphoryl choline group [25].

The above monomers (ω-methacryloyloxyalkyl phosphorylcholine, ω-methacryloyloxy[poly(oxy-ethylene)phosphorylcholine], 2-(acryloyloxy) ethylphosphorylcholine, 2-[3′-(trimethylammonium)propylphosphoryl]ethyl methacrylate, 1-methyl- 2-methacrylamidoethyl phosphorylcholine) basically differ by their type and length of spacers between the phosphoryl choline group and the polymer backbone [25]. These phosphorylcholine-based monomer analogues were used for production of various copolymers (typically with comonomer butyl methacrylate).
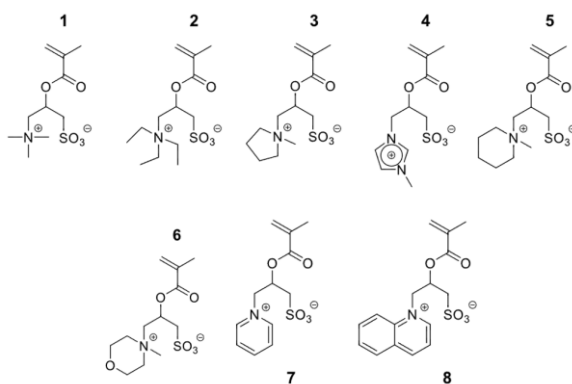
Figure 1.5. Chemical structures of the synthesized sulfobetaine methacrylate monomers [16].

A series of zwitterionic monomers with A-type ionic architecture were synthesized (Figure 1.5) and polymerized using conventional radical polymerization [16].

Recent research emphasizes the profound impact of minor alterations in the chemical structure of polyzwitterions on their efficacy in anti-fouling properties [26]. Numerous articles address the restricted set of commonly employed monomers in antifouling zwitterionic polymers, such as *N*-(2-methacryloyloxy)-ethyl-*N*,*N*-dimethylammonium propanesulfonate (SPE), *N*-(3-methacryloylimino)propyl)-*N*,*N*-dimethylammonium propanesulfonate (SPP), MPC, and a limited selection of carboxybetaine methacrylates [27]. It is not clear which of these monomers units possess superior abilities resulting the need for the development of new polyzwitterion structures to enhance antifouling properties for various applications. However, there currently exist no straightforward rules or guidelines for designing highly effective antifouling polyzwitterions [16]. Among the mentioned monomers, MPC has garnered increased attention due to its notable hydrophilicity, electroneutrality, and minimal interference with hydrogen bonding among water molecules [28–31]. Polymers incorporating phosphorylcholine have emerged as exceptionally promising materials [17,32,33]. Although initial attempts at synthesis of MPC yielded in relatively low quantities [34], subsequently, an efficient synthetic route was developed, resulting in the successful production of MPC and various types of MPC polymers. The establishment of an industrial-scale facility commenced in 1994 and reached its culmination in 1999 [35,36]. Throughout this developmental phase, subtle refinements were incorporated into the synthetic process of MPC, culminating in an enhanced yield of 80% and achieving a purity level of MPC exceeding 98.0%. These refinements in the synthesis method rendered MPC suitable for polymerization and widespread use in the fields of medicine and biology.

1.1.2.Synthesis of polymers carrying phosphorylcholine groups

1.1.2.1. Chemical modification of polymers by phosphorylcholine groups

A detailed heterogeneous synthesis route of a phosphorylcholine-modified chitosan (PC-chitosan) is presented [37]. Chitosan is known as a natural polymer derived from chitin – a substance found in the exoskeletons of crustaceans such as crabs, shrimp, and lobster. Since chitosan is rich with -NH$_2$ functional groups, the amine groups were used as anchors for modification with phosphoryl choline functional groups (Figure 1.6.). Firstly, the amine groups were chemically modified using 2-oxo-1,3,2-

dioxaphospholane. The attached two pholane rings later underwent ring-opening reaction with trimethylamine producing a complete phosphorylcholine functional group (Figure 1.6).
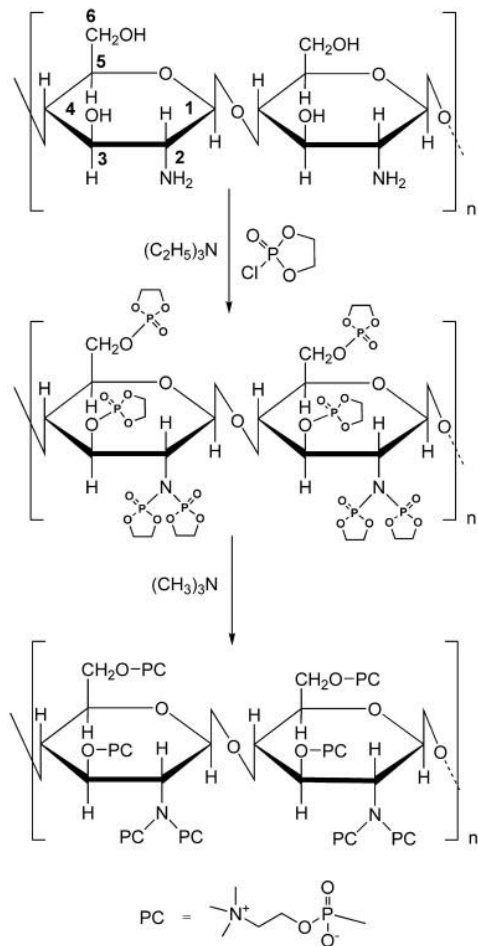
Figure 1.6. Modification of chitosan introducing PC groups [37].

These two reaction steps were used not only for amine groups, but also for modification of the ω-hydroxyl functional group [38]. This method allows a chemical modification of the selected polymer and introduces the desired zwitterion functional group. A phospholipid-mimetic, biodegradable PC-modified ε-polycaprolactone (PCL-PC) was successfully synthesized by incorporating polycaprolactone with zwitterionic phosphorylcholine. Before the synthesis of the terminal phosphorylcholine group, the ω-hydroxyl group of a freshly synthesized poly ε-caprolactone was initially phosphorylated using ethylene chlorophosphate (Figure 1.7). In the final step, the intermediate

ethylene phosphate-terminated PCL undergoes ring opening, employing the nucleophilic base trimethylamine (Me$_3$N) as the ring-opening agent. The properties of the resulting polymer indicated a potential application in biological environments as promising candidate for drug delivery or as temporary coatings for biomaterials in contact with blood.
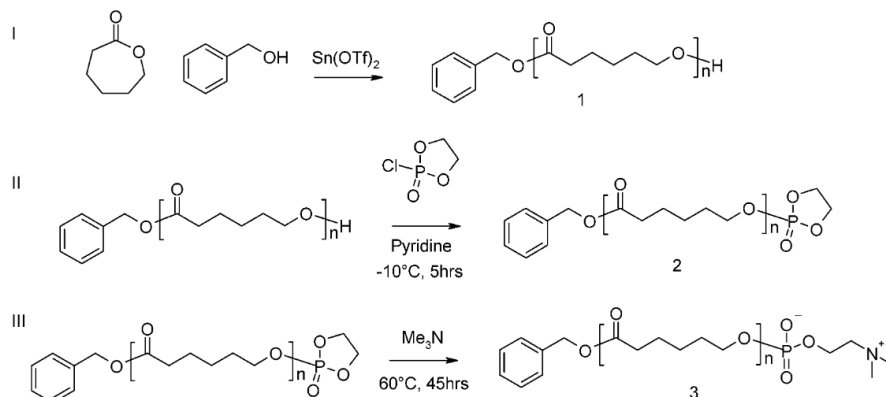
Figure 1.7. Synthesis of phosphorylcholine-terminated polycaprolactone (PCL-PC) [38]

Similarly to the previous study, the poly(ethylene oxide)-poly(ε-caprolactone) (PEO-PCL) diblock copolymers with a phosphoryl choline–terminated group were synthesized through sequential ring-opening polymerization of ethylene oxide and ε-caprolactone [39]. In contradistinction to previous research, the terminal PC group possesses an inverted orientation. Using 2-(dimethylamino)ethanol and Na as initiators, ethylene oxide and CL underwent sequential ring-opening polymerization to produce the dimethylamino-group-terminated PCL-PEO-N(Me)$_2$. This terminal dimethylamino functional group was used for subsequent reaction with 2-methoxy-1,3,2-dioxaphospholane 2-oxide (MEP) which resulted in PC group in (PC)-capped PCL-PEO diblock copolymer, or PCL-PEO-PC for short.

The MPC moieties were grafted onto hyaluronic acid (HA) resulting in a grafted polymer with enhanced lubrication [40–42]. Basically, the HA modification steps included the amidation of carboxyl groups in HA, functionalization of amide groups to thiol groups, and a classical click reaction between thiol and pendant double bond of MPC (thiol-ene click reaction) [42]. In a concise overview, thiolated hyaluronic acid (HA-SH) was firstly prepared from HA using an 1-ethyl-3-(3-(dimethylamino)propyl)-carbodiimide hydrochloride and 1-hydroxybenzotriazole reaction with cystamine

dihydrochloride [41]. Subsequently, HA-MPC was synthesized through a thiol-ene click reaction between HA-SH and MPC. Lubricated PC-modified HA polymers were designed with an intention of the treatment of osteoarthritis.

These above-mentioned PC-modified copolymers hold potential applications in self-assembly and surface modification, leveraging the combination of physical and biological compatibility methods. The approach aims to integrate the advantages of surface coating and utilize the perks of phosphorylcholine functional groups.

1.1.2.2. Synthesis, polymerization and copolymerization of MPC

Many studies regarding synthesis of phosphorylcholine-based polymers were using a monomer known as 2-methacryloylethyl phosphorylcholine (MPC), which is commercially available [7,25]. One of the first detailed descriptions of the synthesis of MPC as a monomer was delivered by Kadoma in 1978 (in Japanese language) [43] and translated to English by Ishihara [44]. A few years later, in 1982, an efficient method for synthesis of MPC was introduced [45]. The original and improved synthesis routes of MPC monomer is presented in Figure 1.8. Basically, an initial step in preparing MPC involves the reaction between cyclic phosphoryl chloride, 2-chloro-2-oxo-1,3,2-dioxaphospholane (COP), and 2-hydroxyethyl methacrylate (HEMA), resulting in the formation of 2-(2-oxo-1,3,2-dioxaphospholan-2-yloxy)ethyl methacrylate (OPEMA). To ensure the purity of OPEMA, triethylamine is employed during the reaction to trap hydrogen chloride as triethylammonium chloride. The presence of water affects the purity, necessitating the use of a high-purity, dry solvent with efficient elimination of triethylammonium chloride. The subsequent step involves the ring-opening reaction of OPEMA with trimethylamine. Due to the heat generated from spontaneous polymerization, it is crucial to suppress heat induction. Additionally, the low boiling point of trimethylamine (4 °C) results in high vapor pressure during heating, requiring an effectively sealed reaction vessel. Upon cooling the reaction mixture, a white precipitate is formed. The subsequent filtration of the precipitate is carried out under dry argon gas, followed by vacuum drying. The synthesis protocol of MPC was formally licensed to NOF Corp. Ltd., a leading Japanese chemical enterprise, with substantive support from the Japan Science and Technology Agency (JST).
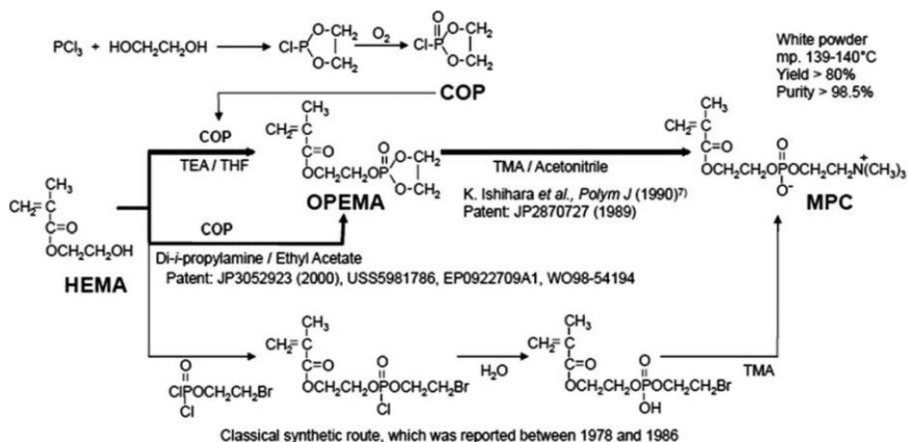
Figure 1.8. Synthetic routes of MPC [44].

Later, a synthetic methodology for the preparation of MPC polymers was elucidated in 1990 [19,28,43]. Kinetics of homogeneous free-radical polymerization of MPC in water using potassium peroxydisulfate (KPS) as an initiator was investigated [46]. The overall activation energy was found to be 12.8 kcal/mol, and the initial polymerization rate (R_p) at 40 °C followed the equation $R_p=k \cdot [KPS]^{0.98} \cdot [MPC]^{1.9}$. The presence of alkaline metal halides accelerated the polymerization, with a larger accelerating effect observed for ions with larger radii. In the presence of NaCl, R_p at 40 °C was expressed as $R_p=k \cdot [KPS]^{0.6} \cdot [MPC]^{1.6}$, and a low overall activation energy of 4.7 kcal/mol was obtained for the polymerization [47]. MPC was polymerized by ATRP to high conversions in both water and methanol. The first-order reaction kinetics, linear M_n vs conversion plots, and relatively narrow molecular weight dispersity ($M_w/M_n = 1.15$-1.35) of the polymers were obtained in both aqueous and alcoholic media at ambient temperature [47]. ATRP rate was notably slower in 2-propanol than in methanol, attributed to the lower polarity of the former solvent. ATRP polymerization of MPC in protic media, particularly in water, was rapid but poorly controlled at ambient temperature. In contrast, polymerization in methanol was slower but better controlled. Factors such as ligand type, target DP, and reaction temperature have been explored, revealing 2,2′-bipyridine as the preferred ligand for the copper catalyst. The living character decreased with higher targeted DP values, and higher polymerization rates were achieved at higher temperatures. Notably, faster rates were also attained at ambient temperature by adding a small amount of water into alcoholic reaction mixture.

Shortly after the discovery of MPC, researchers began using MPC for the synthesis of various copolymers. To develop additional properties of MPC-based polymers, various comonomers were incorporated during the polymerization process [15,19,28]. Typically, MPC was combined with other comonomers that brought different properties to the resulting copolymer. For instance, pMPC is inherently water-soluble and simply does not form micelle-type structures [23,48]. Consequently, copolymer microspheres were created by combining MPC with comonomers (M) such as methyl methacrylate (MMA), ethyl methacrylate (EMA), n-butyl methacrylate (BMA), hexyl methacrylate (HMA), and styrene (St) using emulsifier-free emulsion copolymerization [49]. Kinetic analysis revealed a significant increase in the initial rate of polymerization of MMA with small amounts of MPC. The yield of poly(MPC-*co*-MMA) microspheres decreased with increasing MPC content, while the diameters of poly(MPC-*co*-M) microspheres were smaller compared to corresponding poly(M) microspheres. XPS measurements confirmed the localization of the MPC moiety on the particle surface. The poly(MPC-*co*-M) microspheres exhibited reduced bovine serum albumin (BSA) absorption compared to the control poly(M) microspheres, with the reduction dependent on the hydrophilicity of comonomer M and the MPC composition on the particle surface.

MPC, a hydrophilic monomer, was copolymerized with various monomers, including those of hydrophobic nature [19,49–52]. In this case, a crucial aspect is selecting a suitable common solvent or a compatible mixture of solvents to address monomer solubility. Successful copolymerization yields novel copolymers with properties derived from both MPC and other comonomers. Biocompatible statistical copolymers containing MPC units were synthesized via conventional free-radical copolymerization [53–56]. However, due to the poor solubility of a comonomer and, in many cases, target copolymers in water, the copolymerization of MPC is usually conducted in organic solvents or mixtures of water and water-miscible organic solvents [56,57]. MPC copolymers with styrene [55], alkyl methacrylate [53,58] and other comonomers [59,60] were successfully synthesized. Subject to comonomer, MPC was either a more active or less active monomer in free-radical copolymerization. Thus, reactivity ratios of MPC (M_1) in free-radical copolymerization with styrene and 2-vinyl-4,4-dimethylazlactone were $r_1 = 0.39$, $r_2 = 0.46$ [55] and $r_1 = 0.74$, $r_2 = 1.55$ [56], respectively. Much higher reactivity ratio of MPC (M_1) was in free-radical copolymerization with 2-methoxyethyl acrylate and 2-deoxy-2-methacrylamido-D-glucose, $r_1 = 2.21$, $r_2 = 0.53$ [53] and $r_1 = 1.43 \pm 0.27$, $r_2 = 0.40 \pm 0.14$ [54], respectively.

An MPC-based copolymer with additional photoreactive properties were synthesized [61]. MPC-based copolymer bearing a benzophenone functional group was synthesized for the surface modification of versatile biomedical devices. In this case, poly(MPC-*co*-MHPBP) (PMH) and poly(MPC-*co*-BMA-*co*-MHPBP) (PMBH) were synthesized by a conventional free-radical polymerization method in ethanol. The yield, molecular weight and molecular weight dispersity of all the synthesized photoreactive polymers were determined by GPC. Unfortunately, unpredictable molecular weight and high molecular weight dispersity are expected (but undesirable) outcomes when employing conventional radical polymerization technique.

The controlled/living radical polymerization (CLRP) methods could be also applied for MPC polymerization, but, unlike conventional free-radical polymerization, it offers the ability to synthesize well-defined polymers with low molecular weight dispersity and end-functionalities [62–64]. The three main techniques of CLRP are ATRP, RAFT polymerization, and nitroxide-mediated radical polymerization (NMP) [64]. MPC was polymerized only by two CLRP techniques – ATRP [47,65,66] and RAFT [50,67–72]. Using ATRP, well-defined polymers [47] and various MPC diblock copolymers [50,65,73–75] were produced. Reversible chain-end capping using halogen atoms (usually, Br) ensures, that the instantaneous polymer radical concentration is lower than in conventional free-radical polymerization, which leads to the suppression of termination relative to propagation and hence enables relatively narrow molecular weight distribution ($M_w/M_n \approx 1.1$–1.4) to be achieved [50,73,75]. The main disadvantage of ATRP is the additional purification step of copper removal is required before the application of the synthesized polymers.

RAFT stands out as a robust and versatile approach for controlling radical polymerization [67–69]. By carefully choosing the RAFT chain transfer agent (RAFT CTA) based on the monomers and reaction conditions, it can be applied to a wide range of monomers, including MPC. RAFT polymerization is considered to be undoubtably advantageous method for polymer development compared to radical polymerization. Main requirements of successful and well controlled RAFT polymerization are minimal retardation and a high fraction of living chains [67]. It is also important that the essential material – RAFT CTA – should also have appropriate solubility in the reaction medium. The most reactive RAFT CTA include the dithioesters and trithiocarbonates which have carbon or sulfur adjacent to the thiocarbonylthio group [68]. The use of the modern method of RAFT polymerization enabled to prepare pMPC and its copolymers with controllable molecular weight, relatively low molecular weight dispersity, and of various polymeric

architectures, such as block-type, graft-type and gradient copolymers [50,70–72]. A detailed study of the RAFT polymerization of MPC was published [71]. The inhibition time appeared to be around 2 h in the homopolymerization process which may be due to the inhibitor that the monomer usually contains, if purchased commercially. The rate of the polymerization strongly depended on the concentration of initiator when the RAFT CTA cyanopentanoic acid dithiobenzoate (CTP) is used. A small amount of acetic acid was added to reduce the hydrolysis of CTA. Nowadays MPC is usually polymerized using 3 most popular RAFT CTA: 4-cyanopentanoic acid dithiobenzoate (CTP) [71,76], 4-cyano-4-(thiobenzoylthio)pentanoic acid (CPD) [77,78], and 4-cyano-4-[[(dodecylthio) carbonothioyl]thio]pentanoic acid] (CPA) [79]. RAFT copolymerization of MPC and several methacrylates (2-gluconamidoethyl methacrylamide, 2-lactobionamidoethyl methacrylamide, etc.) yielded 80 % monomer conversion and resulted in copolymers with relatively low molecular weight dispersity (Đ 1.2-1.25) [71]. RAFT copolymerization of MPC and 4-(N-(S-penicilaminylacetyl) amino)phenylarsonous acid methacrylamide resulted in the copolymers with low molecular weight (M_n <13 kDa) and low molecular weight dispersity (Đ 1.12−1.14) [80]. RAFT copolymerization of MPC and 3-formyl-4-hydroxybenzyl methacrylate was carried out in anhydrous DMF, yielding fluorescent polymeric nanoparticles [66]. Despite recent reports on the synthesis of MPC-containing macromolecules, development of novel polymeric structures (e.g., brush-type) and looking forward to their potential application in bio-related fields remains in high demand.

Various copolymers of MPC and hydrophobic alkyl methacrylates, such as *n*-hexyl methacrylate (HMA), *n*-dodecyl methacrylate (DMA), and stearyl methacrylate (SMA), were synthesized by soap-free heterogeneous radical polymerization [81]. The solvent suitable for both monomers was the mixture of water and water-miscible dimethylsulfoxide (DMSO), and the ratio of both components was varied. Aside to heterogeneous polymerization, poly(HMA-*co*-MPC) was synthesized homogenously in methanol:ethanol mixture (3:1, v:v) and it was compared to heterogeneously synthesized poly(HMA-*co*-MPC) which formed micelle structure more easily than homogeneously synthesized one. Several important conclusions were stated: the alkyl methacrylate content of the copolymers is decreasing with increasing the solvent polarity (composition control by control of solvent composition) even though the monomer ratio was not varied; the surface area of the interface had a huge impact for copolymerization; the copolymer composition depended on the specific alkyl methacrylate that was used. In another study, MPC copolymers were synthesized using hydrophobic comonomers and

incorporated into a polyolefin (PEAA) composite as an alternative for blood bag applications [82]. Terpolymers of MPC, hydroxyethyl methacrylate (HEMA), and lauryl methacrylate (LMA) with varying monomer ratios were synthesized in THF:EtOH (7:3, v:v). The copolymers were blended with polyolefin to maintain the original mechanical properties of PEAA while enhancing blood compatibility.

1.1.2.3. Synthesis of block and graft copolymers containing pMPC chains

Graft and block polymers, particularly those incorporating pMPC chains, have gained significant attention in the field of polymer chemistry and biomaterials. Synthesis of the graft polymers involves the attachment of polymeric chain of MPC units onto a polymer backbone, resulting in unique structures with diverse properties. Grafting involves the introduction of side chains onto an existing polymer, while block polymers are synthesized by extending the already synthesized polymer with different kind of another polymer block.

A typical graft polymer example is a cellulose membrane that was developed through the synthesis of a cellulose-based graft copolymer HPC-*g*-PMPC (hydroxypropyl cellulose graft poly(2-(methacryloyloxy) ethyl phosphorylcholine); a principal scheme of the graft polymerization is presented in Figure 1.9 [83].
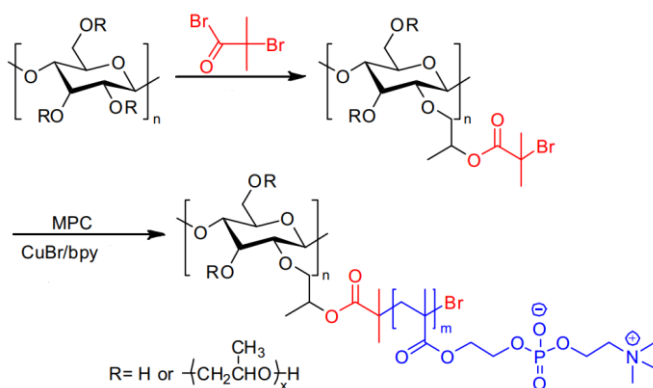
Figure 1.9. Synthesis of the macroinitiator HPC-Br and graft copolymer HPC-*g*-pMPC [83].

The following synthesis procedure started by dissolving cellulose in a dimethylacetamide/LiCl solution and reacting it with 2-bromoisobutyryl bromide to synthesize a macroinitiator, which was later used for polymerization of MPC from the cellulose backbone in a DMSO/methanol solution [84]. Characterization using FT-IR, NMR, and GPC confirmed the formation of a well-defined graft copolymer (cell-pMPC). Protein adsorption studies demonstrated that cellulose membranes modified with cell-pMPC exhibited good resistance to protein adsorption.

Diblock copolymers with different block lengths, consisting of cationic poly(trimethylammonium ethyl methacrylate) (pTMAEMA) block and zwitterionic pMPC block, were synthesized by RAFT polymerization [85]. The representative synthesis procedure of the diblock copolymer pTMAEMA-*b*-pMPC via RAFT method is demonstrated in Figure 1.10. The process involves polymerizing MPC from pTMAEMA as macromolecular chain transfer agent (macroCTA). Cationic macroCTAs with degrees of polymerization of 20, 40, and 100 were synthesized, and MPC polymerization targeted different [MPC]/[TMAEMA] ratios. The resulting cationic-zwitterionic diblock copolymers exhibited >90% monomer conversion, and were characterized by ^{1}H NMR spectroscopy and size exclusion chromatography (SEC). Well-defined diblock copolymers with very low molecular weight dispersity Đ = 1.15 were prepared.
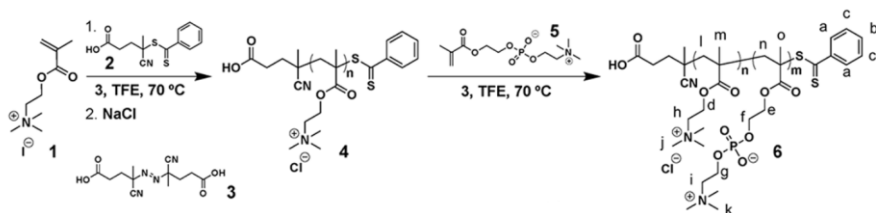
Figure 1.10. Synthesis route to the diblock copolymers pTMAEMA-*b*-pMPC [85].

1.1.2.4. Surface modification by pMPC chains

Two established strategies for polymer immobilization onto diverse substrates involve the "grafting to" method through physical adsorption and the "grafting from" approach via surface-initiated polymerization (Fig. 1.11) [86].
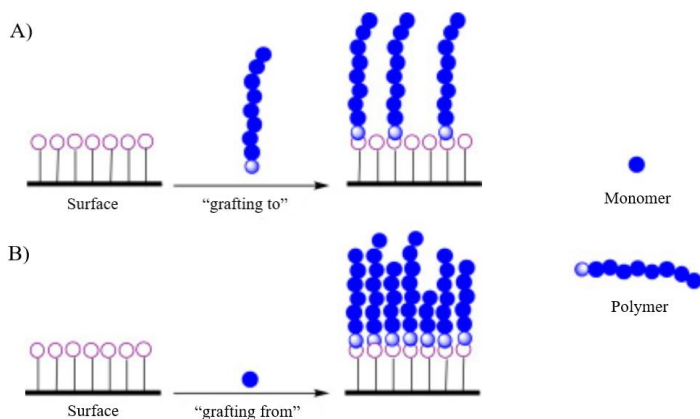
Figure 1.11. Two main grafting techniques for surface modification with polymers: "grafting to" (A) and "grafting from" (B) [86].

Surface-initiated living radical polymerization of MPC was demonstrated to form polymer brushes with unique properties arising from the high density of polymer graft chains [87–89]. To control the polymer characteristics when grafting polymers from a surface, some techniques could be applied, such as photo-induced polymerization, atom transfer radical polymerization (ATRP), NMP, and reversible addition-fragmentation chain transfer (RAFT) polymerization [90–93]. One of many typical examples of "grafting from" technique is pMPC growth on thermoplastic poly(ether-etherketone) (PEEK) via self-initiated surface polymerization [94,95]. This method is relatively simple since PEEK is sensitive to UV radiation and when it is exposed to photo-irradiation the semi-benzopinacol radicals (i.e., ketyl radicals) are formed. Those radicals act as photo-initiators and could initiate the graft-from polymerization using MPC as a monomer. Due to the presence of a nanometer-scale pMPC layer, the water wettability and lubricity of the PEEK surface grafted with pMPC were significantly enhanced compared to the untreated PEEK surface, primarily attributed to the highly hydrophilic nature of MPC. Instead of the organic substrate, the inorganic surfaces were grafted as well. For example, polyphenolic tannic acid (TA) was beneficially employed on the surface of stainless steel as the unique surface anchor for the preparation of zwitterionic polymer brushes [96]. A primer initiator (brominated TA – TABr) was synthesized by partially replacing the trihydroxyphenyl groups in TA molecules with alkyl bromide. The remaining unreacted trihydroxyphenyl of TABr was utilized to anchor the initiator primer to the stainless steel (SS) surface, forming tridentate complexes. This bifunctional primer served as initiation sites for the subsequent surface-

initiated atom transfer radical polymerization (SI-ATRP) of zwitterionic MPC (Figure 1.12). Among other polymer-grafted surfaces, SS-*g*-pMPC performed expected abilities such as low bacterial adhesion, good resistance against *Amphora coffeaeformis* (microalgae) attachment and settlement of barnacle cyprids.
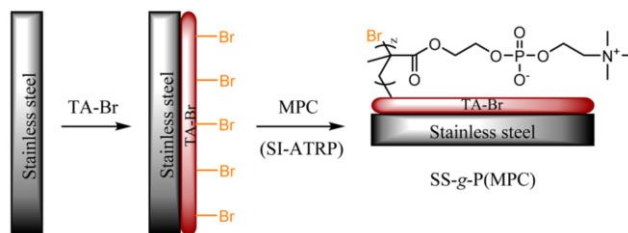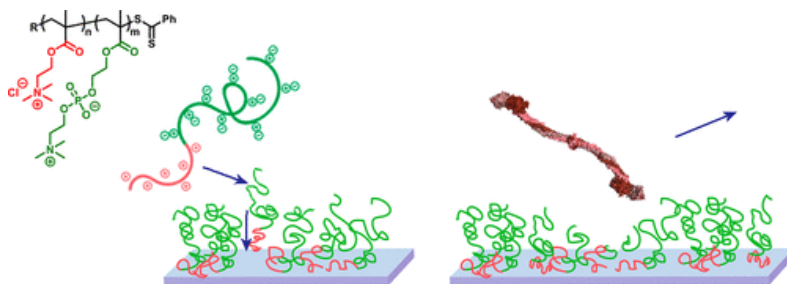

Figure 1.12. The schematic representation of stainless steel surface functionalization with cationic and zwitterionic polymer brushes through the "grafting-from" approach [96].

"Grafting from" technique is preferential in many cases giving chemically bonded layer with high graft density. However, this approach usually is more complicated since it involves pre-treatment of chemically inert surfaces to create active sites initiating or controlling chemical grafting reactions, the surface polymerization is not currently scalable. Important to mention another disadvantage which is the inaccuracy or impossibility to characterize basic characteristics of grafted polymer – molecular weight, degree of polymerization and molecular weight dispersity.

In turn, "grafting to" is more convenient from the practical point of view providing an opportunity to synthesize particular polymers in advance and decorate surfaces of complex configuration in a simple manner. Unfortunately, MPC does not have an ability to covalently attach to surfaces, thus the "grafting to" method requires additional groups that are responsible for anchoring MPC units onto the surface [97,98]. Such an example of "grafting to" technique was demonstrated using the copolymer consisted of both catechol containing dopamine methacrylamide (DOPMA) and MPC units. For example, randomly synthesized p(DOPMA-*co*-MPC) was covalently grafted onto the amino rich polyethylenimine/polydopamide codeposited surface to obtain stable antifouling surface [99]. The anchoring catechol groups are well known for forming a covalent bonds with various surfaces [100–102]. Codeposition of the p(DOPMA-*co*-MPC) copolymers and dopamine resulted in ultrasmooth polyelectrolyte coatings with excellent

lubricating properties [103]. Another "grafting to" approach was achieved with MPC-based diblock copolymers containing cationic block of pTMAEMA as anchoring block [85]. The diblock copolymer pTMAEMA-*b*-pMPC was synthesized via RAFT polymerization, and its nanometer-thick layers were produced due to electrostatic attachment between cationic pTMAEMA block and negatively charged silica surface (Fig. 1.13). Interestingly, the most protein-repellent layers (with protein adsorption of 0.01 mg/m^2 or less) were produced by using the diblock copolymer containing of about 20 TMAEMA units and 100-140 MPC units.

Figure 1.13. The schematic representation of surface modification with the diblock copolymers pTMAEMA-*b*-pMPC (left) and visualization of the repelled lysozyme (right) [85].

In summary, through the integration of appropriate surface coating techniques, polymers incorporating MPC units demonstrate considerable potential for the creation of durable, non-fouling materials, particularly in the context of medical device development for long-term applications such as joint cavities to enhance interfaces with damaged cartilage. Moreover, MPC polymers not only possess the capability to significantly reduce the undesired adsorption of proteins onto biomedical devices but also manifest essential properties pertaining to the lubrication of material interfaces. Consequently, they contribute to the mechanism of interfacial interactions between medical devices and biological materials.

1.1.3. Properties of polymers containing MPC units

1.1.3.1. Solubility, solution properties and aggregation

pMPC can be dissolved in water, methanol, ethanol, and propanol. Other solvents such as acetone and THF do not dissolve pMPC completely. Usually, acetonitrile, acetone, and THF are used for precipitation of pMPC [104]. The

solubility of pMPC in aprotic solvents such as *N,N*-dimethylformamide (DMF) and dimethyl sulfoxide (DMSO) is poor, whereas protic solvents are good solvents for pMPC, except for isopropanol [105].

Although pMPC is soluble in water and ethanol, separately, but the polymer in ethanol-water solution exhibits properties of cononsolvency. The pMPC is known to be not soluble in certain compositions of ethanol-water solutions (60–92 vol% ethanol) [106]. To enhance comprehension of this feature, it is necessary to investigate the interactions between the zwitterion group and water. Firstly, inner salt formation results in the proximity of the trimethylammonium cation and phosphate anion, where three methyl groups are bound to the nitrogen atom of the MPC unit outside the polymer chains, water molecules take on a more stable, ice-like clathrate structure that surrounds the poly(MPC) chain due to hydrophobic hydrations. Methyl groups that are next to the nitrogen atom of ammonium group are located on the outer surface of the poly(MPC) molecule. These regions are locally hydrophobic and, as a result, hydrophobic hydration is more likely to appear. This configuration creates a site that conducts favorable interactions with water through hydrophobic hydration, leading to a more ordered water structure. Several investigations support the hydration hypothesis [107–109]. The phosphorylcholine groups were found to possess a hydrophobic hydration layer that do not disturb the hydrogen bonding between the water molecules of the clathrate structure around ammonium group (Figure 1.14).
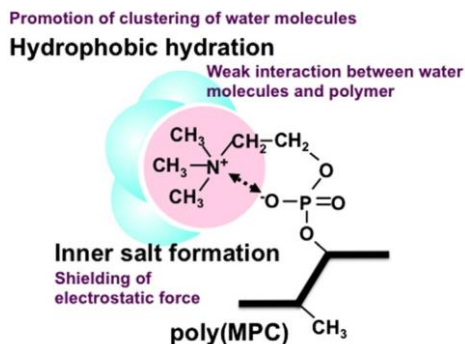
**Figure 1.14.** Illustration of speculative image of hydration of phosphorylcholine groups in the side chain of pMPC [106].

In contrast to common polyelectrolytes, pMPC maintains consistent molecular morphology and solubility in aqueous solutions regardless of pH or ionic strength. Unlike typical polyelectrolytes, which exhibit a rapid increase in viscosity as polymer concentration decreases due to counterion binding and

electrostatic shielding effects, pMPC shows a different behavior. The polymer state of pMPC only partially depends on concentration, as electrostatic repulsion and spreading of the molecular chain are limited in the absence of counterions [110].

The solubility properties of MPC-based copolymers depend on three key aspects: the nature of comonomer in the copolymer, the composition of the resulting copolymer and molecular weight. For instance, the solubility properties of most popular MPC-based copolymer p(MPC-*co*-BMA) (PMB) could be influenced by the composition [19,22,50,57,70,111]. For instance, achieving a MPC unit composition of 30% and above, the copolymer facilitates an easy dissolution in water, decreasing the stability of physically immobilized polymer. Random copolymer of MPC and BMA is well-studied and widely used for preparation of coatings [28,48,50,70]. p(MPC-*co*-BMA) with 30% MPC units and molecular weight of more than 500 kDa were generally used for the surface coating. For example, PMB37 (MPC molar content 37%) was synthesized to a high degree of polymerization, resulting in large molecular weight product ($M_w > 5.0 \cdot 10^5$) [61]. The increased molecular weight prevents PMB37 from dissolving in aqueous solutions, making it suitable for coating materials due to the robust physical interaction between the alkyl methacrylate (BMA units) and the host materials. The copolymer was used for modification of cyclic polyolefin and silicon surfaces. Other synthesized copolymers containing both phosphorylcholine and photoactive benzophenone groups ($M_w < 1.0 \cdot 10^5$) were easily dissolved in both ethanol and water. Worth to mention that these copolymers were rich in MPC units. Instead of BMA with butyl side group, the copolymers with a similar architecture were randomly synthesized using a monomer with 3-times longer substituent such as dodecyl methacrylate (DMA) [51,112].
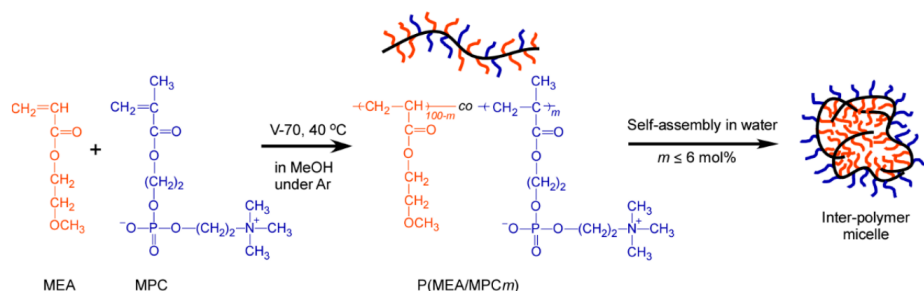

Figure 1.15. Synthesis scheme of the random copolymers p(MEA/MPC) and micelle formation in aqueous solution of these copolymers [53].

Regarding the formation of micelles, another illustrative case involves the copolymerization of hydrophobic monomer 2-methoxyethyl acrylate (MEA) with hydrophilic monomer MPC in a common solvent methanol [53]. The resulting p(MEA/MPC) copolymer exhibits the capability to form micelles, especially when the copolymer comprises less than 6 mol% of MPC units (Figure 1.15). This characteristic makes it potentially suitable for biomedical applications. Polymerization modifications might be applied in order to synthesize a MPC-based copolymers with yet additional property – biodegradability [51,111].
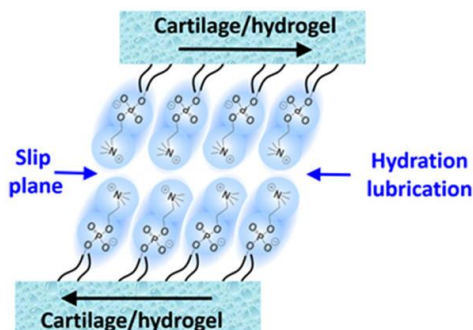
1.1.3.2. Hydration lubrication

pMPC has long been recognized to be a biocompatible compound with the optimal performance for reducing the coefficient of friction (COF) and therefore enhancing joint lubrication by increasing the viscosity of a synovial fluid [113–115]. The main explanation of the significant COF reduction between the surfaces lies behind the unique property of pMPC – hydration lubrication, which was firstly mentioned in 2003 [116,117] and extensively investigated after 10 years [118]. Hydration lubrication has been accepted as the primary reason dominating the superlubrication property of the articular cartilage under pressure [119]. Basically, the two main aspects of hydration lubrication must be addressed. Firstly, the tenacious attachment of water molecules to the enclosed ionic charges forms a hydration shell surrounding the zwitterionic charges (PO^{4-}, $N^+(CH_3)_3$) of the phosphorylcholine group due to the nature of dipole of water molecules (12−19 water molecules per MPC headgroup) [106,120–122]. Ishihara et al. proved the formation of inner salt between the trimethylammonium cation and phosphate anion in aqueous solutions where water molecules are arranged into a 'clathrate' structure around the trimethylammonium group [106,120]. In the hydration layer, the part of water that is bound around the phosphorylcholine group is called a non-freezing water (N_{NFW}) – water which is non-crystallizable due to strong molecular interactions with the matrix polymer. The amount of non-freezing water in pMPC hydration layer was found to be approximately 50%, which is similar to the values for various kinds of polysaccharides [123]. The other part of water in hydration layer is known as intermediate water. This finding was later supported when a specified molecular model was suggested with a conclusion that each monomer unit in pMPC contained 8.8 molecules of intermediate water (N_{IW}) and 9.4 molecules of non-freezing water (N_{NFW}) (Figure 1.16) [124].
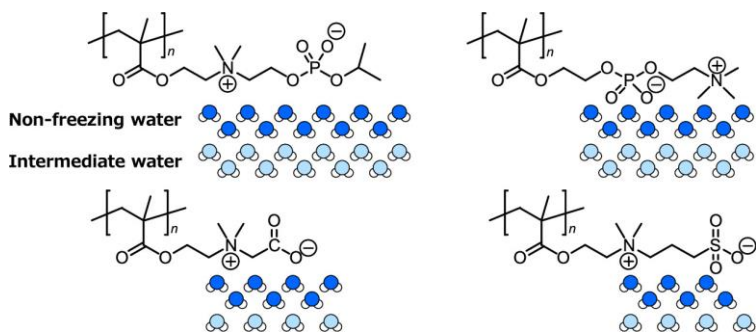
Figure 1.16. The schematic representation of the maximum amounts of non-freezing water and intermediate water for each monomer unit in the zwitterionic polymer [124].

The strong bound water molecules are formed, which possess the resistance to dehydration and therefore lead to their ability to support a large pressure (Figure 1.17) [116]. The second aspect of hydration lubrication mechanism is rapid exchange between the water molecules in the hydration layer and adjacent free water molecules because that does not involve a permanent loss of water from the hydration shell (the exchange time can be as short as nanoseconds) [118,125,126]. This enables very rapid relaxation of the hydration shell, meaning that it has a high fluidity [125]. This property leads to ability to behave fluidly when sheared at rates lower than these exchange (relaxation) rates [122]. Such hydrated shells of MPC are tenaciously bound to the charges but are at the same time very fluid, and so serve as efficient lubricating layers.

Figure 1.17. Hydration lubrication mechanism between cartilage surfaces [125].

A polysaccharide-based biolubricant was synthesized by grafting hydrophilic pMPC and natural antimicrobial polypeptide nisin (N) onto the backbone of chitosan (CS) [127]. The enhancement of CS-N with pMPC side chains significantly reduced COF from 0.067 and 0.060 for CS and CS-N to 0.038 for CS-MPC-N, respectively. Due to the hydration lubrication of pMPC, the lubricant CS-MPC-N possessed excellent lubricating properties with its COF close to the level of usual synovial fluid present in the articular cartilage interface. Taking into account some drawbacks of natural lubricant hyaluronic acid (HA), related to rapid clearance and degradation in vivo [128], researchers have examined tribological properties of chemically modified HA. The COF value of MPC-modified HA (HAMPC) (∼0.025) is lower than that of HA (∼0.065), with a reduction of about 62 % [41,129]. HAMPC demonstrated a better anti-inflammatory effect, excellent cell viability, showed almost no cytotoxicity and improved lubricating properties compared to HA. The copolymers of MPC and DMA were used for the elimination of reactive oxygen species and lubrication enhancement [130]. COF value at the loading force of 35 MPa decreased from 0.018 to 0.009 with the increase of the P(DMA-*co*-MPC) copolymer concentration from 0.1 mg/mL to 1.0 mg/mL, respectively. Compared with pure poly(*N*-isopropylacrylamide) (PNIPAAm), the zwitterionic pMPC endowed PNIPAAm-pMPC composite nanospheres with better lubricating effect [131]. The value of COF decreased from 0.05 to 0.02 with an increase in MPC content in the PNIPAM-pMPC nanospheres in aqueous suspension and remained stable regardless of temperature and pressure. pMPC brushes efficiently decreased abrasive wear and enhanced lubrication between the contact tribopairs. The MSNs-NH_2@PMPC formed a thin adsorption film on the Ti_6Al_4V surface, which can function as a protective boundary film to achieve boundary lubrication between two sliding surfaces [132]. The antifouling characteristics inherent in MPC polymers render them conducive for the formulation of surfaces endowed with antithrombotic and antimicrobial attributes.

In particular, it is difficult for the hydration shells to overlap with each other due to the steric effect [133]. The lower Gibbs free energy of water molecules within these hydration shells hinders their deformation, making them resilient to significant normal pressure. On the contrary, the swift exchange of water molecules within the hydration shell with adjacent free water molecules leads to a fluid-like response when subjected to shear forces. Consequently, this results in a decreased coefficient of friction at the sliding interface.

1.1.3.3. Antifouling and protein repelling

Whitesides et al. [134] examined the protein adsorption behavior of self-assembled membranes and proposed four requirements for inhibition of protein adsorption: hydrophilicity; charge neutrality; presence of hydrogen-bonding acceptor groups; absence of hydrogen-bonding donor groups.

The authors also concluded that inert surfaces based on charged groups have two main advantages compared to those based on ethylene glycol: better stability to oxidation and increased sensitivity to pH and ionic strength. It is clear that polymers with phosphorylcholine groups conveniently meet these requirements and therefore they are well-known for creating a non-fouling surface that resists protein adsorption and cellular attachment [60,135,136]. The "protein-resistant" behavior helps to maintain the integrity of the material's surface, reducing the risk of biofilm formation and potential infections in medical applications. Polymers with MPC moieties have unique property to repel proteins compared to other hydrophilic polymers. To clarify the reason for the reduced protein adsorption on the MPC polymer, the water structure in the hydrated polymer was examined with attention to the free water fraction [121]. Authors selected MPC, acrylamide (AAm) or N-vinyl pyrrolidone (VPy) moieties as a hydrophilic fraction of the copolymer and pHEMA or pBMA were used as a hydrophobic part of copolymer. Polymer membranes were prepared by a solvent evaporation method from a 10% alcohol or DMF solution on a quartz plate. Polymer-coated plates then were immersed in protein solution, rinsed, and dried. Protein adsorption test was carried using circular dichroism (CD) and ultraviolet (UV) spectroscopy. Theoretically, protein adsorption starts with protein trapping by a network structure of water molecules on the surface [137]. The longer the contact of a protein on the surface, the greater is the chance of the protein's interacting with the surface, undergoing a conformational change, and inducing irreversible adsorption. Furthermore, MPC copolymers absorbed fewer proteins with their original conformation. Authors concludes that, unlike other hydrophilic polymers, proteins can contact the MPC surface reversibly because of high free water fraction on MPC surface [121].

The mechanism underlying the unique antifouling property is still of significant interest. The recent explanation of pMPC antifouling mechanism was introduced by Ishihara [135]. Since the MPC unit is electrically neutral, the phosphate anion and trimethylammonium cation are in close proximity, causing an outward orientation of the three methyl groups attached to the nitrogen atom. This establishes a favorable site for hydrophobic hydration (Fig. 1.18). It is energetically advantageous for water molecules to adopt a

clustered structure around hydrophobic functional groups as they form hydrogen bonds with other water molecules instead of interacting with the hydrophobic functional groups [135]. It has been reported that the $-N^+(CH_3)_3$ ion of phosphatidylcholine weakly binds to water molecules in both the primary and secondary hydration layers, thereby increasing the hydrogen bonds between water molecules [138].
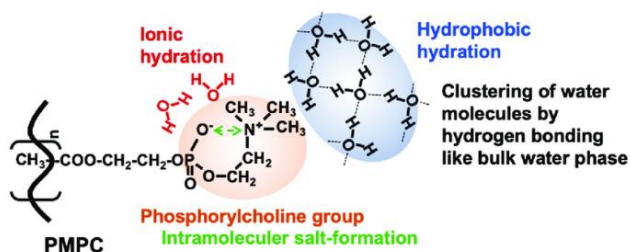
Figure 1.18. Schematic representation of hydration state of pMPC [135].

Non-fouling mechanisms of both hydrophilic and polyzwitterionic materials are based on creating a hydration layer near the surface and steric repulsion. The hydration layer formed by hydrophilic polymers such as PEO and their derivatives, is maintained by weak hydrogen bonds. On the other hand, the hydration layer formed by zwitterionic polymers is more tightly bound through electrostatic interactions which makes these polymers more effective in resisting the adhesion of fouling agents [139]. The hydration layer not only plays a crucial role in providing antifouling properties but also serves as effective lubrication mechanism between surfaces, giving attention to yet another distinctive property of MPC known as hydration lubrication.

1.1.3.4. Biocompatibility

One of the most remarkable properties of phosphorylcholine-based polymers is their exceptional biocompatibility. Yu et al. investigated the toxicity and biocompatibility of pMPC using several methods including unscheduled DNA synthesis test, Ames test, micronuclei test, and animal implantation [140]. The results of mutagenicity and potential carcinogenicity of phosphorylcholine-containing extracts were negative, including no DNA damage, nor gene mutations. The animal implantation illustrated no toxicity and good resorption. Due to perfect biocompatibility MPC polymer-containing commercial eye drops were tested for cytotoxicity and compared with similar products [141]. MPC product contains approximately 0.1%

lipidure-PMB (copolymer of MPC and butyl methacrylate, NOF Corporation, Tokyo, Japan). Authors concluded that MPC-based eye drops were tolerable to ocular surface cells. The product was comparable to single doses of clinically approved drugs containing sodium hyaluronate. This study gives a discussion that MPC-containing artificial tears have a potential to treat patients who suffers dry-eye disease and need ocular comfort. Future applications of MPC for ophthalmic medications would include antiglaucoma ophthalmic solutions, antiallergic ophthalmic solutions, and other drugs for long-term use when cell protection and inert properties are advantageous. MPC was used for implantable medical device surface modification providing advantageous hydrophilicity and antifouling properties [10,11]. Due to their non-thrombogenic nature, phosphorylcholine containing polymers are used in various cardiovascular applications, such as coatings for stents and vascular grafts. Their ability to resist platelet adhesion and activation helps prevent clot formation, reducing the risk of thrombosis. For example, chitosan, a natural polymer, was modified with phosphorylcholine (PC) which increased water absorption and reduced bovine serum albumin adsorption [37]. PC-chitosan exhibited improved hemocompatibility in full human blood, showing prolonged activated partial thromboplastin time. In cell interaction tests with human umbilical vein endothelial cells, PC-chitosan demonstrated good biocompatibility and cytophilicity, with minimal impact on cell differentiation and multiplication compared to native chitosan.

In tissue engineering, phosphorylcholine-based polymers are utilized as scaffold materials for growing cells and tissues. Their non-fouling properties minimize unwanted interactions between cells and scaffold, allowing for better cell adhesion and growth.

1.1.4. Application of polymers containing MPC units

The phosphorylcholine functional group is renowned for its ability to replicate the structure of phospholipids found on the outer surface of cell membranes, making it a favorable polar group for the development of various bioinert polymers. Thanks to its hydrophilicity, electroneutrality, and minimal impact on the hydrogen bonding between water molecules, polymers containing phosphorylcholine have emerged as exceptionally promising materials, particularly among other zwitterionic polymers [17,70,71]. This is especially evident in their efficacy for surface modification of clinically utilized devices, such as guide wires, stents, oxygenators, left ventricular assist devices, and microcatheters [17,28,72]. Polymers containing phosphorylcholine moiety have gained significant attention in the field of

biomaterials and medical applications due to their exceptional biocompatibility and unique surface properties. Phosphorylcholine plays a pivotal role in imparting these polymers with their distinct characteristics. Their ability to interact favorably with biological systems, such as reducing friction in natural joints, underscores their versatility and potential impact in various fields.

In natural joints, the cartilage on sliding surfaces is crucial for smooth movement. Anatomical studies reveal that hydrophilic proteins and polysaccharides (proteoglycans) combine to form a complex, further covered by a phospholipid molecular membrane on the top surface [143]. A healthy human joint is the most typical superlubricated system with the coefficient of friction (COF, defined as [force to slide]/[compressive load on surfaces]) between two sliding articular cartilages at a level as low as 0.001−0.01 under physiological joint pressures (4−10 MPa) during routine activities [144,145]. Unfortunately, knee osteoarthritis (OA) is a highly prevalent disorder and a leading cause of disability worldwide, with a high possibility to increase over the coming decades [145,146]. Meanwhile, injecting natural (e.g., hyaluronic acid) or synthetic bio-macromolecule lubricants into joint cavities to enhance damaged cartilage interface lubrication performance has been regarded as an effective strategy in treating arthritis [147–149]. The materials that are inspired by the bottle-brush structure feature of polysaccharide aggregates in synovial fluid, synthetic brushed biolubricants with good interface hydration and adsorption capacities get considerable attention. Intraarticular injection of hyaluronic acid (HA) based viscosupplements has long been a popular approach to treat complications associated with OA. Emerging studies are searching for an alternative to HA using new polymer designs by taking inspiration from the molecular structures present in native synovial fluid, which consists of four main components: hyaluronic acid, lubricin, aggrecan and phospholipids [125]. Between such alternative materials are synthetic zwitterionic polymers. The most extensively studied zwitterionic polymer is pMPC which is known for its biocompatibility and ability to mimic the above mentioned phospholipids [28,150,151]. Because of unique properties, MPC-based polymers are used in promising application fields, including biomedical devices, coatings, and lubricants [7,35,57,60,114,121,124,152].

Some medical devices used in biomedical and clinical fields need to be exceptionally good in terms of lubrication and bacterial resistance. Polymers with MPC moieties have a unique structure that imparts excellent lubricating properties providing steric repulsion, preventing close contact and adhesion between surfaces, and thus reducing friction [7,35,153,154]. MPC polymers has been commonly used to enhance lubrication and reduce friction

[116,154,155]. Various types of copolymers containing MPC units were synthesized and explored including graft-derivatives of natural (e.g., chitosan [37,127] or hyaluronic acid [41,129]) and synthetic (e.g., PDMS [90,156], PNIPAAm nanospheres [131]) polymers as well as amphiphilic statistical [48,53,157,158] and block [48,50,159] copolymers. COF of pMPC modified PDMS was 90% lower than those of the unmodified PDMS [90]. The triblock ABA-type copolymers composed of two pMPC blocks (A) and a central poly(vinylmethylsiloxane-*co*-dimethylsiloxane) (PV$_l$D$_m$MS) block (B), were attached to PDMS surface via hydrosilylation of the silicone block [156]. By increasing the ratio of MPC to PV$_l$D$_m$MS in the copolymer, the coefficient of friction was decreased from 1.4 to 0.01. A similar strategy has been reported for functionalization of a titanium alloy surface, where the surface-anchoring site was designed by mussel-inspired dopamine methacrylamide (DMA) units [160]. Titanium alloy substrate, typical for biomedical implants, coated by DMA-MPC copolymer showed enhanced lubrication and bacterial resistance. COF was significantly reduced from 0.124 for neat titanium alloy to 0.051 for DMA-MPC copolymer coated surface, moreover, COF was almost independent of frequencies and pressures.

The phosphorylcholine groups contribute to the hydrophilic nature of these polymers, leading to their excellent water absorption capacity. This property is advantageous for applications involving controlled drug release, as the polymers can absorb water and swell, releasing the entrapped drug over time. The diblock copolymers pLA-*b*-pMPC containing a block of p(*D,L*-lactide) were introduced as pH-sensitive, biocompatible and biodegradable polymersomes that have advantages in delivery of hydrophilic drugs for cancer therapy [161]. The release behavior, which strongly depends on the pH, is ascribed to the hydrolysis of pLA-*b*-pMPC. The polymersome-to-micelle transition was mainly driven by hydrolytic degradation of the pLA block. The hydrolysis leads to a change in structure from polymersomes to micelles, triggering the release of encapsulated anti-cancer drugs like the hydrophobic doxorubicin (DOX) and the hydrophilic doxorubicin hydrochloride (DOX·HCl). pH-sensitive drug release behavior was demonstrated by using hydrophobic doxorubicin as the release drug [162]. The drug was loaded into polydopamine-core (PDA) nanoparticles, which were modified with a diblock copolymer of MPC and (2-dimethylamino)ethyl methacrylate (DMAEMA) (PDA@MPC$_{87}$-*b*-DMAEMA$_{18}$). The modified PDA nanoparticles exhibited not only the anticipated characteristics of colloidal stability and biocompatibility but also displayed remarkable near-infrared photothermal properties and pH-sensitive drug release behavior. Another drug release control mechanism was introduced using DOX loaded

pMPC-glutathione nanogels that were prepared via reflux precipitation polymerization [163]. Due to presence of glutathione, the pMPC nanogels possessed redox-responsive manner. The DOX-loaded pMPC nanogels remained stable under physiological conditions with low release of DOX (13% in 24 h), but rapid release of the drug occurred in a reduction environment (82% in 24 h).

In summary, materials incorporating MPC are gaining prominence in drug delivery systems, artificial joints, and the surface modification of medical devices, attributed to their biocompatibility and capacity to minimize protein adsorption and cell adhesion. Polymers containing phosphorylcholine groups demonstrate a unique combination of biocompatibility, non-fouling and biolubrication properties, hydrophilicity, and stability. These attributes are vital for expanding the utility of MPC-based polymers in living organisms, avoiding immune responses. Such characteristics position them as valuable materials for a broad spectrum of biomedical and biotechnological applications where artificially synthesized MPC-based polymers eventually interact with living systems.

1.2. Catechol-containing polymers: synthesis and properties

In recent times, there has been considerable interest in developing adhesives inspired by mussel adhesive proteins [164–168]. The adhesion properties of mussels in wet conditions are attributed to the presence of catechol-containing amino acid 3,4-dihydroxyphenyl-L-alanine. To replicate these adhesive properties, various synthetic polymers with catechol groups have been synthesized and investigated [101,164,169]. The broad range of polymers containing catechol groups offers a rapid and effective method for applying coatings through "grafting to" on surfaces of diverse origins (Figure 1.19). Typically, a simple immersion of the substrate in the polymer solution is sufficient to establish a protective layer.

Dopamine methacrylamide (DOPMA), a widely used monomer with a catechol moiety, has been copolymerized with commercially available monomers such as acrylamide [170], 2-hydroxyethyl methacrylate [171], N-isopropylacrylamide [172], methylmethacrylate [173], alkyl (meth)acrylates or (meth)acrylamides with short (methyl-, n-butyl-) or long (decyl-, dodecyl-) alkyl chains [174,175], styrene [176], etc. DOPMA has been copolymerized also with long chain-length (M_n from 6000 to 25 000 g mol^{-1}) PEOMEMA resulting in terpolymer poly(dopamine methacrylamide)-co-(methyl methacrylate)-co-(poly(ethylene glycol) methyl ether methacrylate) [177].
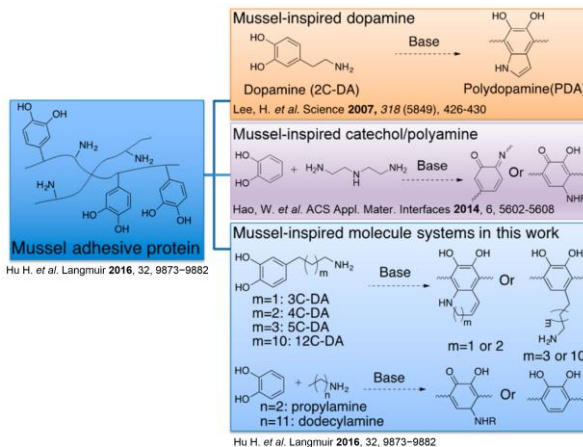
Figure 1.19. Overview of mussel-inspired materials with proposed polymer structures [164].

Di- and triblock copolymers were obtained through RAFT polymerization using DOPMA and (2-(dodecylthiocarbonothioylthio)-2-methylpropionic acid terminated PEO as macroCTA [178]. RAFT polymerization of acetonide-protected DOPMA and dopamine acrylamide resulted in homopolymers and block copolymers [102]. Furthermore, RAFT copolymerization of acetonide-protected DOPMA with PEOMEMA produced statistical copolymers of various compositions [179]. It was demonstrated [180,181] that the adsorbed layers of statistical catechol copolymers p(DOPMA-*co*-PEOMEMA) exhibited high underwater wear resistance, while diblock copolymers pDOPMA-*b*-pPEOMEMA showed exclusively high corrosion protection performance.

The copolymers of DOPMA and MPC have been synthesized through conventional free-radical copolymerization [99,103,130,160,182–184]. The copolymers p(DOPMA-*co*-MPC) were covalently grafted onto amino-rich polyethylenimine-polydopamide codeposited surfaces to produce stable antifouling surfaces [99]. The codeposition of p(DOPMA-*co*-MPC) copolymers resulted in ultrasmooth polyelectrolyte coatings with excellent lubricating properties [103]. These copolymers, possessing both adhesion and antifouling properties, were employed for various applications, including the fabrication of lubricating microspheres [182], the modification of biodegradable mesoporous silica nanoparticles for dual functionality [183], the enhancement of lubrication and bacterial resistance on titanium alloy surfaces [160], and the preparation of efficient scavengers for reactive oxygen

species [130]. It is worth to note that all mentioned examples utilized statistical copolymers of MPC and DOPMA.

## 1.3. Polymethacrylate-type brush copolymers with PEO side chains

Numerous naturally occurring and synthetic polymers, including starch, cellulose derivatives, polyesters, polyanhydrides, and more, are currently utilized in drug delivery systems [185]. The United States Food and Drug Administration (US FDA) has approved several biodegradable polymers for this purpose, such as *N*-(2-hydroxypropyl) methacrylamide (HPMA), poly(ethylene glycol) (PEO), poly(*L*-lactic acid) (PLA), poly(glycolic acid) (PGA), poly(*D*,*L*-lactic-*co*-glycolic acid) (PLGA), and polycaprolactone (PCL) [186]. The most versatile polymer among them is PEO due to its variable molecular weights ranging from 200 Da to 8 000 kDa that could be employed in numerous pharmaceutical applications. Moreover, oligo-(ethylene glycol)-based polymers are known as neutral, water-soluble, non-toxic materials, and are the most applied synthetic polymers in the biomedical field [187]. These PEOs have been examined to be safe for cosmetic use by the Cosmetic Ingredient Review Expert Panel [188]. Beyond its cosmetic applications, PEO stands as a benchmark and a preferred polymer. Since 1977, when PEO was first attached to bovine serum albumin and liver catalase proteins, numerous studies have demonstrated PEO's efficacy in enhancing drug delivery [189,190]. Additionally, higher-density PEO coating reduces protein adsorption on nanoparticles (NPs), endowing densely PEO-coated NPs with superior stealth properties in animal models [191].

PEOs, also referred to as polyethers, consist of repeating ethylene glycol (or ethylene oxide) units [-$(CH_2CH_2O)_n$-]. These derivatives are primarily characterized by their molecular weights. Unlike linear PEO, polymethacrylate-type copolymers featuring poly(ethylene oxide) (PEO) side chains and acrylate-based backbone are marked as a new category of materials with a unique brush-like architecture [192]. Compared to linear polymers with PEO in the backbone, brush polymers possess superior properties such as reduction of side effects, improvement of cellular uptake, and enhancement of biodistribution [193]. These side chains endow the copolymers with distinctive traits such as flexibility, hydrophilicity, and heightened solubility in aqueous environments. The brush-like architecture, characterized by densely packed PEO chains, facilitates interactions with water molecules and bio-macromolecules, positioning them as promising candidates for diverse applications in drug delivery, biomaterials, and surface modifications. For

example, the synthesized polymers via polymerization of oligo(ethylene glycol) (meth)acrylate featured surface active properties and thermo-responsive properties [194–196]. pH and/or temperature sensitive copolymers were usually synthesized using PEO_xMEMA containing PEO chain of a certain length with other comonomers, such as methacrylic acid (MAA) [194], hydroxyethyl acrylate [195], or 2-(dimethylamino)ethyl methacrylate (DMAEMA) [197,198]. Additionally, a water-soluble poly(ethylene oxide) methyl ether methacrylate with short PEO side chain of 5 units (PEO_5MEMA) was copolymerized with hydrophobic styrene using well controlled RAFT copolymerization, yielding copolymers with relatively low molecular weight dispersity (Đ 1.15-1.70), desired composition, and a broad range of molecular weights (M_n 2-21 kDa) that correlated with theoretically calculated values [199]. The synthesized copolymers p(St-*co*-PEO_5MEMA) showed thermoresponsive properties with potential to be used as drug delivery systems in biofields. A pH-responsive comb copolymer, poly(diethylaminoethyl methacrylate-*co*-poly(ethylene glycol) methacrylate), facilitated the preparation of emulsions and dispersions with particle sizes ranging from 1 to 10 μm [197]. Easily scalable copolymer, with its well-suited composition and structure for systematic variation, demonstrated the pH-responsiveness to both emulsions and dispersions. Diblock PEO-based brush copolymers were synthesized, incorporating repeating units of PEO_xMEMA in both blocks but with varying lengths of PEO chains (x = 5, 9, 19, 43) [200]. The study demonstrated the potential to synthesize diblock brush copolymers reaching very high conversions of the monomers (q > 97%), and a very low molecular weight dispersity (Đ < 1.1), showcasing the versatility of the approach and contributing to a deeper understanding of the polymerization process (Figure 1.20). Utilizing four PEO methacrylates with different molecular weights, coupled with variations in the order and succession of monomer addition during RAFT polymerization, provided new insights into the reactivity of these monomers. In order to get diblock brush copolymers with low molecular weight dispersity by RAFT polymerization, PEO methacrylate with shorter PEO chains should be polymerized first [200].

In addition to thermo- and pH-responsive properties, the antifouling ability significantly contributes to the interest in field of biomedicine. The study of antifouling polymers is rapidly expanding, with various methods and new polymer designs aimed at surface modification with ability to repel proteins and other biomaterials [201]. PEO brushes have been a primary choice for creating such antifouling surfaces. It's been so widely used for this purpose that it's often referred to as the top choice, or the "gold standard," of antifouling polymers [201]. For example, polymer brush thin films by spin-

casting a solution of well-defined amphiphilic graft copolymer (pBA-*g*-pSt)-*co*-pPEOMEMA were fully characterized and tested with protein solutions (bovineserum alumin and cytochrome) [202]. The films resisted BSA better due to differing protein interactions via hydrogen bonding. Cell adhesion experiments were performed by using human keratinocyte cell line (HaCaT) and it was discovered that polymer brush films possessed good antifouling ability. Furthermore, shorter pSt side chains and higher pPEOMEMA content resulted in better low-fouling behavior.
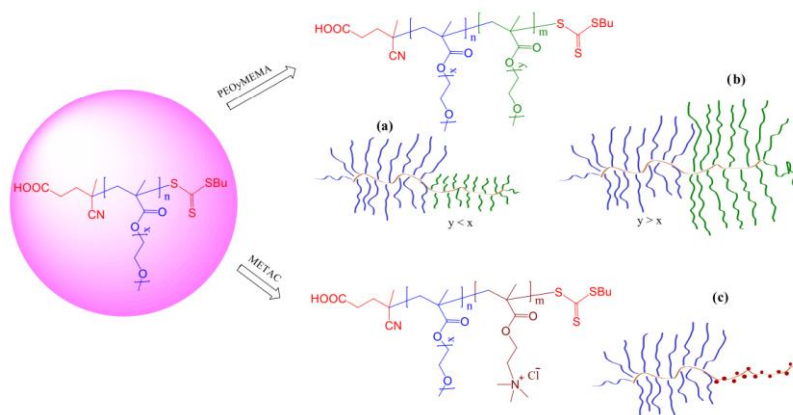
Figure 1.20. Graphical illustration of possible chain extension of pPEO$_x$MEMA-CTA: (a) by PEO$_y$MEMA with shorter PEO side chains; (b) by PEO$_y$MEMA with longer PEO side chains; (c) by cationic monomer METAC [200].

Brush copolymers containing PEO side chains are also know for complex interactions with surfaces. The random copolymer of PEOMEMA and cationic monomer methacryloyloxyethyl trimethylammonium chloride p(PEOMEMA-*co*-METAC) was synthesized via conventional free-radical copolymerization, and the adsorption behavior of the cationic copolymer p(PEO$_{45}$MEMA-*co*-METAC) onto silica was examined under varying pH and ionic strength conditions using reflectometry, Quartz crystal microbalance with dissipation monitoring (QCM-D), and contact angle measurements [203,204]. The main purpose of this study was to evaluate adsorption of the copolymer on silica driven by both electrostatic and nonelectrostatic polymer−substrate interactions. It was observed that the surface adsorption decreased with increasing pH at constant ionic strength, and with increasing ionic strength at constant pH, contrary to typical polyelectrolyte behavior. The

decrease in adsorption was attributed to reduced nonelectrostatic affinity between PEO chains and silica, along with competition between small ions and polyelectrolyte charges at the silica surface. Hydrogen bonding between ether groups in the polymer side chains and protonated silanol groups at the silica-water interface facilitated nonelectrostatic affinity. Electrostatic interactions between the polymer charges and the surface also played a role, with side chains enhancing sensitivity to added electrolyte. Reflectometry and QCM-D techniques revealed a high content of water in the adsorbed layer, at pH>6 resulting in less compact conformations of the polymer and increased water content. These findings shed light on the complex interplay between polymer-surface interactions and solution conditions in adsorption processes. In many applications envisaged for bottle-brush polymers with PEO side chains a large PEO content at the solid−liquid interface is considered to be favorable [204].

The interactions between PEO side chains and surface are closely related to lubrication of the surface, which plays a huge role in biomedical applications. It has been shown by Spencer et al. that poly(L-lysine) containing PEO grafts adsorb onto silica surface due to electrostatic interactions and form dense brush layers providing good lubrication [205]. Low friction between polymer-coated surfaces was explained by boundary lubrication which is defined as the lubrication of surfaces by molecules themselves by holding on to a thin layer of water e.g., lamina splendens of articular cartilage surface [206]. It was demonstrated by Claesson et al. [207], that bottle-brush polymethacrylate-type copolymers with randomly distributed PEO side chains and positively charged backbone in aqueous media are firmly attached to the surfaces creating highly hydrated PEO layer and providing very low friction between coated surfaces. The lowest coefficient of friction, 0.006, was observed using the copolymer with low charge density and high density of PEO chains confirming strong contribution of the extended conformation of the adsorbed layer [208]. Excellent lubricity was explained by several factors such as low interpenetration of the opposing brushes, high fluidity of the hydration layers, and differences in osmotic pressure in the brush and outside of it [31]. Thus, for excellent lubrication, the polymer layers on a surface should be dense, stretched to prevent interpenetration between the opposing layers, and sufficiently hydrated to form a fluidic interface. In order to understand the surface behaviour and effect of PEO side chains, a detailed study was carried out focusing on adsorption of the brush copolymers p(PEO$_{45}$MEMA-co-METAC) containing 45-units-long PEO side chains. The possibility of exchanging adsorbed layers of p(PEO$_{45}$MEMA-co-METAC) brush polyelectrolytes with a highly charged

linear polyelectrolyte was investigated [209]. A real-time study, tracked by changes in the mass and viscoelastic properties of the p(PEO$_{45}$MEMA-*co*-METAC) polymer layer, revealed that the copolymer with less content of METAC units disposed as an extended layer, facilitating pMETAC chain diffusion at the interface, while the compact layer of the preadsorbed copolymer p(PEO$_{45}$MEMA-*co*-METAC) with higher content of METAC units remained unaffected. This study complementary supports the local stretching of the PEO side chains that are enforced by the polyelectrolyte architecture [210]. Composition of the copolymers p(PEO$_{45}$MEMA-*co*-METAC) has a huge role in the adsorption mechanism – at low charge densities (0-10 mol% of METAC) adsorption of the copolymers primarily depended on the PEO side chains, while at charge densities of the copolymer 25 mol% or higher, adsorption predominantly relied on electrostatic interactions [211]. Furthermore, this study was supplemented by proving that the alignment of the backbone of the uncharged bottle-brush polymer p(PEO$_{45}$MEMA) was parallel to silicon oxynitride surface, which maximized favourable interactions between side-chains and surface [212]. For highly charged copolymer with the excess of METAC units, electrostatic forces took the main part in the adsorption, resulting formation of the METAC layer at the surface and outer layer with many extended PEO side chains [207,212]. Diblock copolymers of PEOMEMA and METAC adsorbed parallel to the surface, and, as adsorption progressed, PEOMEMA chains were later replaced by cationic chains on the surface, which finally resulted in the formation of a thick brush-like layer rich in 45-unit-long PEO side-chains, providing strong steric repulsion, low friction forces, and high load bearing capacity [213]. Diblock copolymer p(METAC)$_m$-*b*-p(PEO$_{45}$MEMA)$_n$ not only featured strong adsorption on silica, but also demonstrated excellent lubrication, including significant reduction of shear ice adhesion strength (>90%) compared to bare silica, and stronger attachment to the silica compared to the bottle brush polymer pPEO$_{45}$MEMA or pMETAC [214]. Interestingly, the bottle-brush polymer pPEO$_{45}$MEMA did not perform as well as the diblock copolymer due to the weaker surface attachment and lower adsorbed amount. Cationic anchoring block enhanced not only the attachment to the surface but also the load bearing capacity [215]. In pure water, low friction forces were observed up to 50 MPa due to strong steric repulsion and minimal layer interpenetration, while friction increased in high ionic strength solutions due to reduced electrostatic affinity [215]. The friction decreased with decreasing load, indicating the self-healing properties that are undoubtedly unique to self-assembled layers. In addition to the lubrication and self-assembling properties, the adsorbed layers of the cationic bottle-brush copolymers p(PEO$_{45}$MEMA-

co-METAC) demonstrated antifouling properties preventing adsorption of both anionic BSA and cationic lysozyme [216].

1.4. Final remarks and summing-up

The literature review presents the most important aspects related to the chemistry of phosphorylcholine-based materials. The study begins with the inspiration from the natural source of phospholipids followed by synthetic compounds carrying PC groups including synthesis, properties and applications. While kinetics of free-radical polymerization of MPC has been examined and numerous MPC-based copolymers were synthesized, limited articles provide insights into copolymerization kinetics and reactivity ratios of monomers, particularly, in RAFT copolymerization. This situation is challenging a detailed study of kinetics and microstructure of the copolymers containing MPC units. Furthermore, only few articles covered the synthesis of diblock copolymers containing pMPC as one of the blocks. This is unsurprising, giving the fact that synthesis of a proper diblock copolymer usually requires an advanced polymerization technique (RAFT, ATRP, etc.) and some additional steps during the synthesis route.

Literature delves into bio-inspired materials, with a notable focus on developing adhesives inspired by mussel adhesive proteins, particularly those containing catechol groups. It's noteworthy that these applications utilized statistical copolymers of MPC and DOPMA, demonstrating the versatility of these synthetic polymers in mimicking mussel adhesion properties. Unfortunately, among the list of MPC-based diblock polymers, the copolymers with both MPC and DOPMA units are still absent in scientific literature. The absence of such diblock copolymers might be explained by difficulties related to successive polymerization of the monomers with distinctly different hydrophilicity, and also additional requirements for protection of catechol groups during polymerization [179]. The block structure of these copolymers is expected to ensure excellent adhesion by the pDOPMA block while allowing the pMPC block to stand away from the surface, providing exceptional lubricating and antifouling properties. Moreover, the protection of the catechol functionality enables long-term storage of the copolymers without concerns about oxidation.

The literature also covered the effect of some PEO- and MPC-based copolymers that exhibited prominent antifouling ability and effectively inhibited the adhesion of proteins and human platelet cells. Although a few scientific articles described PEO-MPC copolymers, they cannot be attributed to brush type polymers because of linear structure of a PEO block. The

literature clearly lacks information about the synthesis of MPC-based brush copolymers containing PEO side chains. In other words, the combination of pPEOMEMA brush-type block and pMPC block may possess better antifouling and biolubricating performance than that of single pPEOMEMA or pMPC. By realizing this idea, an ideal copolymer candidate for various biomedical applications could be introduced.
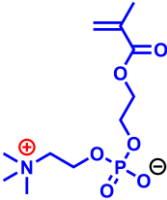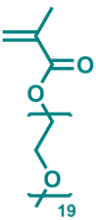
Many articles describing the antifouling properties of MPC-based copolymers introduce several methods of surface modification with these copolymers. In most cases, a solvent evaporation method is used to create polymer-coated substrates, which are then immersed in a protein solution. Although the interactions between the phosphorylcholine moiety and proteins are extensively studied, there is potential to better understand these interactions if the orientation and conformation of the copolymers on the surfaces are established. The orientation of the MPC-based diblock copolymer pMPC-*block*-pBMA on a polypropylene substrate was once analyzed by AFM proving that the pMPC block is oriented from the substrate towards the aqueous phase [98]. Unfortunately, neither the interactions between substrate, nor the conformational changes of the diblock copolymer during the adsorption process were investigated. It is evident that an in-depth study of the adsorption mechanism and the surface orientation of copolymers with a hydrophilic pMPC block is essential and promising.
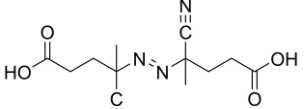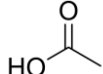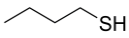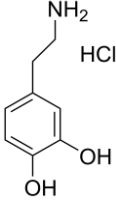
2. EXPERIMENTAL SECTION

2.1. Materials and reagents
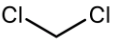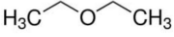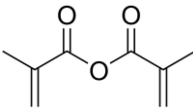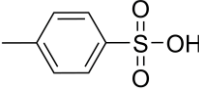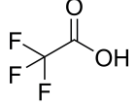
2.1.1. Monomers

Name	Properties	Producer	Formula
Acetonide-protected dopamine methacrylamide (ADOPMA) IUPAC: *N*-(2-(2,2-dimethylbenzo[*d*][1,3]dioxol-5-yl)ethyl) methacrylamide	M 261.14	Synthesized according to [179] (*see section 2.2.2*)	
2-Methacryloyloxyethyl phosphorylcholine (MPC) IUPAC: 2-(Methacryloyloxy) ethyl 2-(trimethylammonio) ethyl phosphate	M 295.27 T_m 143-148 °C	Contains ≤100 ppm MEHQ, 97% *Sigma-Aldrich*	
Poly(ethylene oxide) monomethyl ether methacrylate (PEO19MEMA) IUPAC: 2,5,8,11,14,17,20,23,26,29,32,35,38,41,44,47,50,53,56-nonadecaoxaoctapentacontan-58-yl methacrylate	M ~950 d_4^{20} 1.1 g/cm^3 n_d^{20} 1.455 T_m 38 °C	Passed through a chromatographic column filled with basic Al_2O_3 *Sigma-Aldrich*	
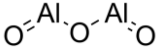
Poly(ethylene oxide) monomethyl ether methacrylate (PEO₉MEMA) IUPAC: 2,5,8,11,14,17,20,23,26-nonaoxaoctacosan-28-yl methacrylate	M ~475 d_4^{20} 1.08 g/cm³ n_d^{20} 1.496 T_m -2 °C	Passed through a chromato-graphic column filled with basic Al_2O_3 *Sigma-Aldrich*
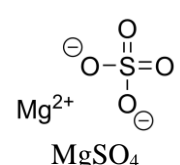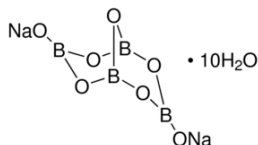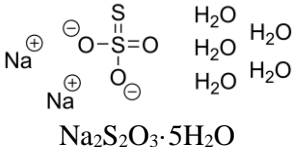
2.1.2. Organic materials

Name	Properties	Formula
4,4'-Azobis-(4-cianovaleric acid) (ACVA) *Fluka*	M 280.1 T_m 118-125 °C	$C_{12}H_{16}N_4O_4$
Acetic acid *Eurochemicals*	M 60.05 d_4^{20} 1.049g/cm³ n_d^{20} 1.371 T_b 118.1 °C	$C_2H_4O_2$
1-Butanethiol *Sigma-Aldrich*	M 90.19 d_4^{20} 0.842 g/cm³ n_d^{20} 1.443 T_b 98.2 °C	$C_4H_{10}S$
Carbon disulfide *Riedel-de-Haen*	M 76.1 d_4^{20} 1.26 g/cm³ n_d^{20} 1.627 T_b 46.24 °C	S=C=S CS_2
Dopamine hydrochloride *Sigma-Aldrich*	M 189.64 T_m 245 °C	$C_8H_{12}ClNO_2$
Dichlormethane (DCM)	M 84.93 d_4^{20} 1.326 g/cm³	
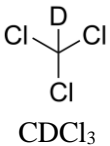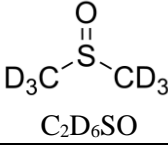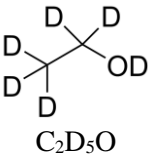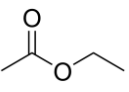
	n_d^{20} 1.424 T_b 39.6 °C	Cl $\diagup$ Cl CH_2Cl_2
Diethyl ether (ethoxyethane) *Eurochemicals*	M 74.12 d_4^{20} 0.713 g/cm³ n_d^{20} 1.353 T_b 34.6 °C	$H_3C \diagup O \diagdown CH_3$ $C_4H_{10}O$
2,2-Dimethoxypropane (DMP) *Sigma-Aldrich*	M 104.15 d_4^{20} 0.85 g/cm³ n_d^{20} 1.378 T_b 83 °C	$C_8H_{10}O_3$
Methacrylic anhydride *Sigma-Aldrich*	M 154.165 d_4^{20} 1.035 g/cm³ n_d^{20} 1.453 T_b 87 °C	$C_5H_{12}O_2$
p-Toluenesulfonic acid monohydrate (TSA) (4-methylbenzenesulfonic acid) *Sigma-Aldrich*	M 190.22 T_m 104.5 °C	$C_7H_8O_3S \cdot H_2O$
2,2,2-Trifluoroacetic acid (TFA) *Roth*	M 114.023 d_4^{20} 1.489 g/cm³ T_b 72.4 °C	$C_2HF_3O_2$
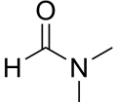
2.1.3. Inorganic materials

Name	Properties	Formula
Aluminum oxide (basic) *Roth*	M 102 d_4^{20} 3.95-4.1 g/cm³	$O=Al\diagdown O \diagdown Al=O$ Al_2O_3

Hydrochloric acid (35% solution) *Eurochemicals*	M 36.5 d_4^{20} 1.49 g/cm³ n_d^{20} 1.254	HCl
Iodine *Reachim*	M 36.5 d_4^{20} 4.933 g/cm³	I—I I_2
Magnesium sulphate *Roth*	M 120.36 d_4^{20} 2.66 g/cm³	$MgSO_4$
Sodium bicarbonate *Sigma-Aldrich*	M 84.01 d_4^{20} 2.20 g/cm³	$NaHCO_3$
Sodium hydride (60 % suspension in oil) *Sigma-Aldrich*	M 23.99 d_4^{25} 1.2 g/cm³ n_d^{20} 1.470 T_b 800 °C	NaH
Sodium nitrate *Sigma-Aldrich*	M 84.98 d_4^{20} 2.26 g/cm³	Na_2NO_3
Sodium tetraborate decahydrate *Sigma-Aldrich*	M 381.42 d_4^{20} 1.73 g/cm³	$Na_2B_4O_7 \cdot 10H_2O$
Sodium thiosulphate *Merk*	M 158.11 d_4^{25} 1.667 g/cm³ n_d^{20} 1.489 T_m 48.3 °C T_b 100 °C	$Na_2S_2O_3 \cdot 5H_2O$
Sodium hydroxide *Sigma-Aldrich*	M 39.99 d_4^{20} 2.13 g/cm³	NaOH

2.1.4. Solvents

Name	Properties	Formula
Deuterated chloroform (CDCl₃) *Merk*	M 120 d_4^{20} 1.50 g/cm³ n_d^{20} 1.444	CDCl₃
Deuterated dimethyl sulfoxide (DMSO-*d6*) *Merck*	M 78 d_4^{20} 1.19 g/cm³ n_d^{20} 1.476	C₂D₆SO
Deuterium oxide (D₂O) *Merck*	M 20.3 d_4^{25} 1.107 g/cm³ n_d^{20} 1.328 T_b 101.4 °C	D₂O
Deuterated methanol (MeOD-*d4*) *Merck*	M 36.07 d_4^{20} 0.888 g/cm³ n_d^{20} 1.327 T_b 65.4 °C	C₂D₅O
Methanol (MeOH) (> 99.9%) *Merck*	M 32.04 d_4^{20} 0.792 g/cm³ n_d^{20} 1.329 T_b 64.7 °C	CH₃OH CH₄O
Ethanol (EtOH) (95%) *VWR International*	M 46.07 d_4^{20} 0.789 g/cm³ n_d^{20} 1.361 T_b 78.37 °C	CH₃CH₂OH C₂H₆O
Ethyl acetate (EtOAc) (> 99.5%) *Honeywell*	M 88.11 d_4^{20} 0.897 g/cm³ n_d^{20} 1.373 T_b 74-75 °C	C₄H₈O₂
Tetrahydrofuran (THF) (> 99.9%)	M 72.11 d_4^{20} 0.887 g/cm³ n_d^{20} 1.407 T_b 66 °C	

Eurochemicals		C_4H_8O
Hexane (> 99.5%) *Eurochemicals*	M 86.18 d_4^{20} 0.655 g/cm³ n_d^{20} 1.375 T_b 68 °C	C_6H_{14}
N,N-dimethyl formamide (DMF) (> 99.8%) *Honeywell*	M 73.1 d_4^{20} 0.948 g/cm³ n_d^{20} 1.430 T_b 153 °C	C_3H_7NO

2.2. Synthetic procedures

2.2.1. Synthesis of RAFT chain transfer agent (CTA)

RAFT CTA 4-(((butylthio)carbonothioyl)thio)-4-cyanopentanoic acid was synthesized according to the general procedure described previously with few adjustments [217]. To a cold (0 °C) solution of 1-butanthiol (2.89 g, 32.0 mmol) in anhydrous diethyl ether (70 mL) 1.45 g NaH (60% in mineral oil, 36.3 mmol) was continuously added. After 30 min of stirring, 12.18 g of CS_2 (160 mmol) were added dropwise at 0 °C. The cloudy yellow reaction mixture containing the formed sodium butyl carbonotrithionate was allowed to warm to room temperature. Later on, the mixture was 30 min purged with N_2 gas, then 5.08 g of iodine (20 mmol) were added in one portion, and the reaction mixture was stirred for 1 hour at room temperature. The formed precipitate of insoluble NaI in diethyl ether was removed by filtration, and the filtrate was washed several times using 1 M $Na_2S_2O_3$ aqueous solution to remove unreacted iodine. The combined organic layers were dried with $MgSO_4$, and the solvent was removed under reduced pressure giving 6.0 g of yellow viscous oil of bis-(butylsulphanylthiocarbonyl) disulfide. 4,4-Azobis(4-cyanovaleric acid) (ACVA) (13.44 g, 48.0 mmol) was added into three-neck round-bottom flask containing 6.0 g of bis(butyltrithiocarbonate) dissolved in 150 mL of EtOAc, and the solution was stirred overnight under reflux in N_2 atmosphere. The solution was washed with water (3×100 mL) to remove unreacted ACVA, and concentrated using rotary evaporator. The product was purified using flash column chromatography (eluent hexane:EtOAc:AcOH = 4:1:0.01 (v/v), R_f 0.2), and the solvent was removed resulting in yellow solid

4-(((butylthio)carbonothioyl)thio)-4-cyanopentanoic acid (BCPA). Overall yield 8.29 g (89%). Analytical data of BCPA: m.p. 41-45 °C;

^{1}H NMR (400 MHz, CDCl$_3$, Fig. 2.1) ppm: 0.96 (t, J = 7.4 Hz, 3H), 1.45 (m, 2H); 1.71 (m, 2H), 1.91 (s, 3H), 2.36–2.60 (m, 2H), 2.71 (t, J = 7.8 Hz 2H), 3.36 (t, J = 7.5 Hz, 2H);

^{13}C NMR (100 MHz, CDCl$_3$, Fig. 2.2) ppm: 13.59 (-$\underline{C}$H$_3$), 22.10 (-$\underline{C}$H$_2$-), 24.86 (-CN-C-$\underline{C}$H$_3$), 29.49 (-$\underline{C}$H$_2$-COOH), 29.70 (C-$\underline{C}$H$_2$-C), 33.48 (-CN-C-$\underline{C}$H$_2$), 36.78(-C-S-$\underline{C}$H$_2$-), 46.20 (-CN-$\underline{C}$-CH$_3$), 118.90 (-$\underline{C}$≡N), 177.12 (-$\underline{C}$OOH), 216.79 (-S-$\underline{C}$S-S-).
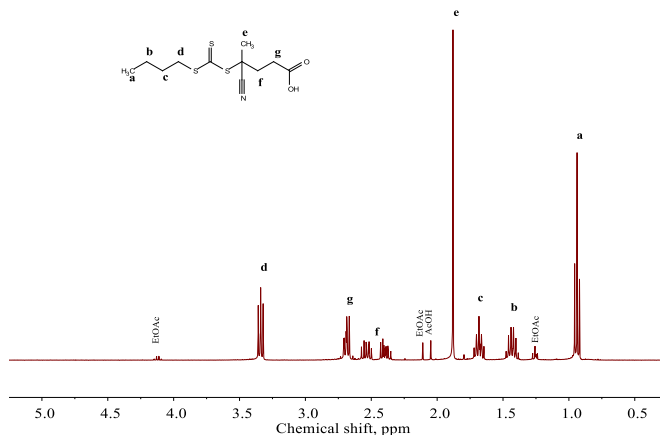
Figure 2.1. ^{1}H NMR spectrum of 4-(((butylthio)carbonothioyl)thio)-4-cyanopentanoic acid (BCPA) in CDCl$_3$ at 22 °C.
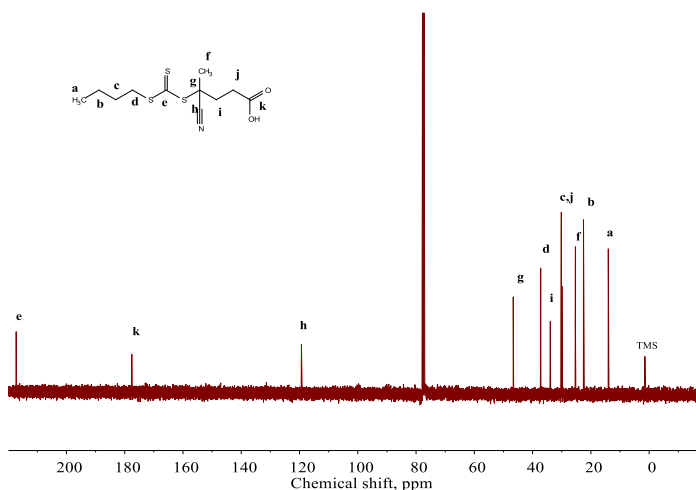
Figure 2.2. ^{13}C NMR spectrum of 4-(((butylthio)carbonothioyl)thio)-4-cyanopentanoic acid (BCPA) in CDCl$_3$ at 22 °C.

2.2.2. Synthesis of acetonide protected dopamine methacrylamide (ADOPMA)

DOPMA was synthesized according to the procedure published before [179]. 20 g (52.44 mmol) of sodium borate decahydrate ($Na_2B_4O_7 \cdot 10H_2O$) and 8 g (95.23 mmol) of sodium bicarbonate ($NaHCO_3$) were dissolved in 200 mL of deionized water, the solution was bubbled with N_2 for 30 min, and then 10 g (52.8 mmol) of dopamine hydrochloride were poured to the aqueous mixture of sodium borate/sodium bicarbonate under nitrogen flow. After that, 9.5 mL (58.1 mmol) of methacrylic anhydride dissolved in 50 mL THF was added dropwise under constant stirring. During the reaction between 3,4-dihydroxyphenethylamine hydrochloride and methacrylic anhydride, pH of the solution was kept moderately above 8 by adding 1 M aqueous NaOH solution. After stirring for 24 h at room temperature under N_2, the aqueous reaction mixture was washed twice with 100 mL of ethyl acetate to remove residual methacrylic anhydride and then acidified to pH < 2 with concentrated HCl. After extraction (three times with 100 mL of ethyl acetate), the combined brown organic phase was dried over $MgSO_4$. The solvent was removed using rotary evaporator, and the product was crystallized and recrystallized from hexane–ethyl acetate mixture (7:3, v:v). The obtained slightly greyish powder was dried in a vacuum-oven overnight at room temperature, yield 11.1 g, 95%.

The hydroxyl groups of DOPMA were protected by the formation of a five-membered acetonide ring during the reaction of DOPMA with 2,2-dimethoxypropane in the presence of the catalyst p-toluenesulfonic acid. To carry out the synthesis, 150 mL of anhydrous toluene was introduced into a three-neck round-bottom flask and purged with N_2 for 30 minutes. Subsequently, 9.2 g (44.0 mmol) of previously synthesized DOPMA and 0.3822 mg (2.2 mmol) of p-toluenesulfonic acid were added. The mixture was then refluxed for 1 hour under a nitrogen flow. Afterward, the solution was cooled to room temperature, and 54.6 mL (440 mmol) of 2,2-dimethoxypropane were introduced. The resulting inhomogeneous mixture was gradually heated to its boiling point and vigorously stirred for approximately 4 hours until the precipitate dissolved, resulting in a dark brown solution. The solution underwent a series of washes: first with sodium bicarbonate (pH 8), followed by deionized water. The solution was then dried over $MgSO_4$. The solvent toluene was removed using a rotary evaporator, yielding dark orange viscous oil. The final product was purified using flash column chromatography, utilizing a hexane–ethyl acetate mixture (9:1, v:v) as an eluent. Subsequent solvent removal by rotary evaporation yielded a white solid powder, X g, 92% yield. ^{1}H NMR (250 MHz, DMSO-d6, Fig. 2.3)

δ(ppm)): 8.12 (t, 1H, -NH-C=O), 6.56-6.74 (m, 3H, Ph), 6.21 (dd, 1H, -C$\underline{H}$=CH2), 6.05 (dd, 1H, C$\underline{H}_2$=CH-), 5.56 (dd, 1H, C$\underline{H}_2$=CH-), 3.30 (q, 2H, -CH2-C$\underline{H}_2$-NH-), 2.63 (t, 2H, -C$\underline{H}_2$-CH$_2$-NH-), 1.61 (s, 6H, (CH$_3$)$_2$-C-).

^{13}C NMR (400 MHz, DMSO-d$_6$, Fig. 2.4) δ(ppm)): 164.6 (1C, -NH-C=O), 146.8 (1C, $\underline{Ph}$-O(C(Me)$_2$)), 145.2 (1C, $\underline{Ph}$-O(C(Me)$_2$)), 132.6 (1C, -$\underline{C}$H=CH$_2$), 131.8 (1C, $\underline{Ph}$-CH$_2$-), 124.8 (1C, -CH=$\underline{C}$H$_2$), 120.9 (1C, Ph), 117.6 (-$\underline{C}$(CH$_3$)$_2$), 108.7 (1C, Ph), 107.6 (1C, Ph), 40.4 (1C, -$\underline{C}$H$_2$-NH-), 34.7 (1C, -80 $\underline{C}$H$_2$-CH$_2$-), 25.5 (1C, ($\underline{C}$H$_3$)$_2$-C-).
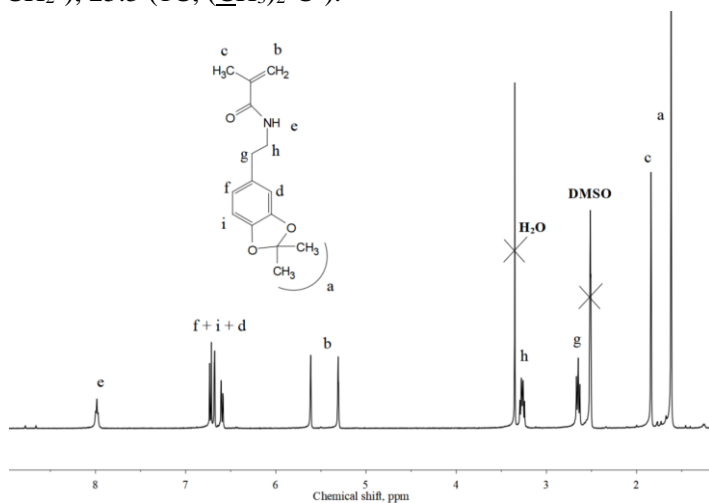
Figure 2.3. ^{1}H NMR spectrum of ADOPMA in DMSO-d$_6$ at 22 ºC.
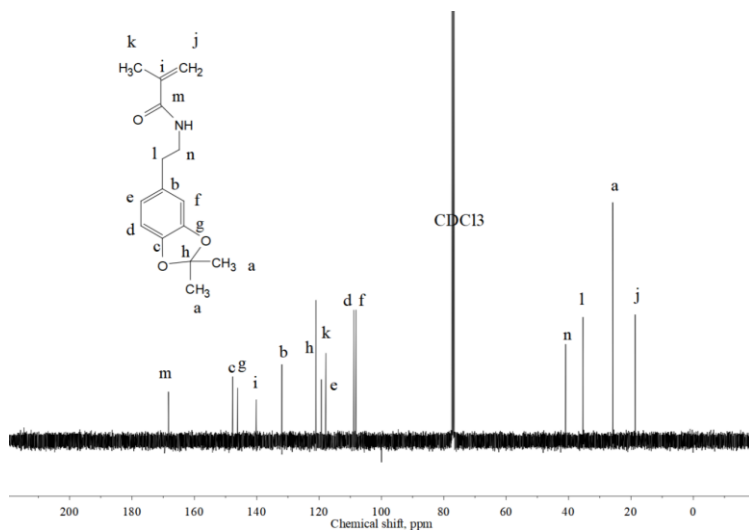
Figure 2.4. ^{13}C NMR spectrum of ADOPMA in CDCl$_3$ at 22 °C.

2.2.3. RAFT copolymerization of MPC and PEOMEMA

For the synthesis of the copolymers, MPC and PEOMEMA were copolymerized at different molar ratios (75:25, 50:50, and 25:75, respectively). The initial molar ratio of CTA to the initiator was kept constant ($[CTA]_0/[I]_0 = 3/1$). The copolymerization procedure of MPC and PEOMEMA at an initial monomer molar ratio of 50:50 is presented below ($[M]_0/[CTA]_0/[I]_0 = 240/3/1$): MPC (0.59 g, 2.0 mmol), PEOMEMA solution (3.8 g, 2.0 mmol), RAFT CTA (14.5 mg, 0.05 mmol) and ACVA (4.67 mg, 0.0166 mmol) were placed in 50 mL round-bottom flask and dissolved in 22.8 mL of MeOH and 4.3 mL of water (MeOH/water = 3/1 v/v). Copolymerization was carried out at 70 °C for 24 hours and then stopped by quenching the flask to liquid nitrogen. The copolymers were purified by dialysis through a 12-14 kDa MWCO cellulose membrane against water, and the copolymer was obtained by freeze-drying, giving the white powder (practical yield 2.63 g, 60%).

2.2.4. RAFT copolymerization of MPC and PEOMEMA in NMR tubes

For the kinetics study, copolymerization of MPC and PEOMEMA in a mixture of deuterated solvents MeOD-*d4* and D_2O (3/1 v/v) was carried out in NMR tubes. 0.1329 g of MPC (0.45 mmol), 0.855 mL of PEOMEMA solution (0.45 mmol), 2.6 mg of CTA (0.9 µmol) and 0.8 mg of ACVA (0.3 µmol) were placed in 10 mL round-bottom flask and dissolved in 5.2 mL of MeOD-*d4* and 0.97 mL of D_2O. The solution was distributed to NMR tubes equally, and each tube was purged with Ar gas for 30 min, then sealed, and the tubes were put into the oven at 70 °C. After a certain time, the tubes were taken and quenched to liquid nitrogen. The tube with the solution was analyzed by NMR, then 0.1 mL of the solution was taken and diluted to 1.5 mL by MeOH/water solution (3/1 v/v), and the diluted solution was used for SEC analysis.

To determine the reactivity ratios of MPC and PEOMEMA, copolymerization of MPC and PEOMEMA was carried out in NMR tubes. Components of the reaction mixture were dissolved previously in deuterated solvents and dosed to NMR tubes as 10% MPC solution in MeOD-*d4*, 10% CTA solution in MeOD-*d4* and 1% ACVA solution in MeOD-*d4*. For copolymerization of MPC and PEOMEMA at molar ratio 40:60, the required ingredients were dosed to NMR tube as follows: 0.1193 mL of MPC solution (32 µmol), 0.0912 mL of aqueous (50%) PEOMEMA solution (48 µmol), 2.9 µL of GPA solution (0.80 µmol), 9.4 µL of ACVA solution (0.266 µmol),

0.402 mL of MeOD-*d4* and 0.092 mL of D_2O. The tubes were purged with N_2 for 30 min, sealed and analyzed by NMR. Then the copolymerization was carried out at 70 °C for 2 hours, stopped by quenching tubes to liquid nitrogen, and the tubes with the solutions were analyzed by NMR again.

2.2.5. Synthesis of the diblock copolymers pMPC-*b*-p(PEO$_{19}$MEMA) and pMPC-*b*-p(PEO$_9$MEMA)

Diblock copolymers pMPC-*b*-p(PEO$_{19}$MEMA) were synthesized by chain extension of pMPC containing terminal trithiogroups. An example of chain extension of pMPC which acts as macroCTA by the units of PEO$_{19}$MEMA keeping the ratio $[M]_0/[pMPC]_0/[I]_0 = 120/3/1$ is presented below. 0.50 g of the dried pMPC (M_n 19 kDa according to SEC, DP 34, 0.049 mmol) were placed into a 50 mL round-bottom flask containing 22.16 mL of methanol, and the solution was stirred for an hour until full homogenization. Then 4.66 mg of the initiator ACVA (0.0166 mmol) and 3.78 g of the 50% w/w PEO$_{19}$MEMA aqueous solution (2.49 mmol) were added to the reaction mixture, followed with addition of 4.1 g of water. The solution was bubbled for 30 min with N_2 and then stirred for 24 h at 70 C. The polymerization was stopped by cooling the reaction mixture. The copolymer was purified by dialysis through a 12-14 kDa MWCO membrane against water, and separated by freeze-drying, giving the white powder (practical yield 2.18 g, 51%). Diblock copolymers pMPC-*b*-p(PEO$_9$MEMA) were synthesized by the same procedures presented above.

2.2.6. RAFT polymerization of MPC

Polymerization of 2-methacryloyloxyethyl phosphorylcholine (MPC) was carried out in a mixture MeOH:H_2O (75:25 v/v). The monomer concentration in solution was set to 20% and the initial molar ratio of CTA to the initiator was maintained constant ($[CTA]_0:[I]_0 = 3:1$) for all polymerizations. The polymerization procedure of MPC at the molar ratio to CTA equal to 40 is presented below: MPC (1.476 g, 5.0 mmol), RAFT CTA (29.1 mg, 0.01 mmol) and ACVA (9.34 mg, 3.30 µmol) were placed in 25 mL round-bottom flask and dissolved in mixture of 5.17 mL of MeOH and 1.85 mL of deionized water. The solution was bubbled for 30 min. with N_2 and then stirred for 8 hours at 70 °C. The polymerization was stopped by quenching the flask to liquid nitrogen. The polymer was precipitated by pouring the reaction mixture to 10-fold excess of acetone and purified by reprecipitation from methanol, giving the yellowish-white powder (practical yield 1.25 g, 85%).

2.2.7. RAFT polymerization of ADOPMA

Polymerization of acetonide-protected dopamine methacrylamide (ADOPMA) was carried out in DMF. The monomer concentration in solution was set to 20%, and the ratio of the monomer to CTA and initiator $[M]_0:[CTA]_0:[I]_0$ was equal to 500:5:1. The polymerization procedure of ADOPMA is as follows: ADOPMA (2.00 g, 7.65 mmol), RAFT CTA (22.3 mg, 0.077 mmol) and ACVA (4.29 mg, 0.015 mmol) were placed in 25 mL round-bottom flask and dissolved in 8.47 mL of DMF. The solution was bubbled for 30 min with N_2 and then stirred for 24 hours at 75 °C. The polymerization was stopped by quenching the flask to liquid nitrogen. The polymer was precipitated by pouring the reaction mixture to 10-fold excess of hexane:EtOAc mixture (8:2 v/v) and purified by reprecipitation from EtOAc to 9 fold excess of hexane, giving the yellowish-white powder (practical yield 1.40 g, 70%, M_n 19.1 kDa, Đ 1.15, DP 73).

2.2.8. Synthesis of the diblock copolymers pMPC-*b*-pADOPMA

Diblock copolymers pMPC-*b*-pADOPMA were synthesized by chain extension of pMPC containing terminal trithiogroups. An example of chain extension of pMPC, which acts as macroCTA by the units of ADOPMA keeping the ratio $[M]_0:[pMPC]_0:[I]_0 = 120:3:1$, is presented below. 0.50 g of the dry pMPC (M_n 19 kDa according to SEC, DP 34, 0.049 mmol) were placed into a 25 mL round-bottom flask containing 10.2 mL of methanol, and the solution was stirred for an hour until full homogenization. Then 4.66 mg of the initiator ACVA (0.0166 mmol) and 0.52 g of the monomer ADOPMA (2.0 mmol) were added to the reaction mixture. The solution was bubbled for 30 min with N_2 and then stirred for 24 hours at 75 °C. The polymerization was stopped by quenching the flask to liquid nitrogen, and the product was precipitated by pouring the reaction mixture to 10-fold excess of acetone and purified by reprecipitation from methanol to a mixture of hexane:EtOAc (9:1 v/v), giving the white powder (practical yield 0.64 g, 63%).

2.2.9. Removal of acetonide protective group

Removal of the acetonide protective groups from catechol moieties present in pADOPMA or diblock copolymers pMPC-*b*-pADOPMA was performed using TFA [179]. In a round-bottomed flask, 0.2 g of the copolymer was dissolved in 7.4 mL of dichloromethane and 0.1 mL of deionized water, and the mixture was bubbled with N_2 for 20 min. Then the mixture was cooled in

an ice bath, and 2.5 mL of TFA was added under vigorous stirring. After 30 min the solution was left stirring for 60 min at room temperature. The copolymer was purified by dialysis through 3.5 kDa MWCO regenerated cellulose membrane against water, and the solid white powder was obtained by freeze-drying (0.6 g, yield 94%).

2.3.   Analytical procedures

2.3.1. SEC measurements

The number average molecular weight (M_n) and molecular weight dispersity ($Đ = M_w/M_n$) of the synthesized polymers were determined by size exclusion chromatography (SEC) using Viscotek TDAmax (Malvern Panalytical, UK) system equipped with a triple detection array (TDA305) consisting of a refractive index detector (RI), light scattering detector (LS) simultaneously measuring the scattered light (laser 3 mW, 670 nm) at two angles – right-angle (90°) and low-angle (7°), and four-capillary bridge viscosity detector (DP) plus a Viscotek UV detector 2500 (UV). SEC measurements of pMPC, p(MPC-*grad*-PEO$_{19}$MEMA), pMPC-*b*-p(PEO$_{19}$MEMA), and pMPC-*b*-p(PEO$_9$MEMA) solutions were carried out in MeOH:H$_2$O (3:1 v/v) as an eluent at 30 °C using a constant flow rate of 0.5 mL/min and a column Viscotek A6000 M General Mixed, 300×8.0 mm. In case of MPC-PEOMEMA copolymers, the dn/dc value of each copolymer composition, essential for determination of the exact molecular weight of the copolymer, was calculated using dn/dc values of corresponding homopolymers (0.11 for pMPC and 0.132 for pPEOMEMA) determined by the method described previously.

SEC measurements of pADOPMA solutions were carried out in DMF as an eluent at 50 °C using a constant flow rate of 1.0 mL/min and a column Viscotek T6000 M General Mixed styrene-divinyl benzene type, 300×8.0 mm.

2.3.2. NMR measurements

^{1}H and ^{13}C NMR spectra of the synthesized polymers were recorded on a *Bruker 400 Ascend™* (Germany) nuclear magnetic resonance spectrometer (400 MHz) at 22 °C using D$_2$O, MeOD-*d4*, or mixture of D$_2$O/MeOD-*d4*. Chemical shifts of the signals were determined from tetramethylsilane and expressed in parts per million (ppm).

2.3.3. DLS measurements

DLS measurements of the copolymer solutions were carried out using *Zetasizer Nano ZS* (Malvern Panalytical, UK) equipped with a 4 mW HeNe laser at a wavelength of 633 nm. Measurements of the intensity of the scattered light were performed at an angle of 173°. The size distribution data were analyzed using Zetasizer software (v.7.12).

2.3.4. Surface tension measurements

The investigation of surface tension was conducted using a K100 MK2 analytical tensiometer (KRÜSS GmbH, Germany). The study employed the ring detachment method with the "KRÜSS Standard" ring (radius - 9.545 mm, wire diameter - 0.37 mm). After measurement, the ring was treated by flame. The detection sensitivity – 0.005 g, measurement sensitivity – 0.001 g, the ring immersion depth – 3 mm (10% return). The measurement was performed in a 43.5 mL volume SV10 Glass Vessel with a 50 mm measuring index. During measurement, the ring was lifted and immersed 10 times. Each sample was measured five times. Copolymer solutions were prepared by weighing 2 mg of dry copolymer on analytical scales and dissolving it in 18 mL of miliQ water. The sample was dissolved (kept in the solvent) for 24 hours. Measurements were conducted using diluted aqueous polymer solutions with various concentrations.

2.3.5. Water contact angle measurements

The hydrophilicity of the copolymers was studied by measuring water contact angle (WCA) on the copolymer layer using *Theta Lite Optical Tensiometer* from Biolin Scientific (Finland). WCA was measured in 3 different spots on the copolymer-coated gold surface. A drop of deionized water (10 µL) was applied onto the copolymer layer, and after 30 s the picture of the drop was captured and analyzed.

2.3.6. FT-IR spectroscopy

Infrared spectra of bulk compounds were collected using infrared absorption spectrometer Alpha (Bruker, Inc., Germany) equipped with a room temperature DLATGS detector and ATR accessory (Platinum ATR Diamond). Spectra were collected with 4 cm^{-1} resolution from 128 interferogram scans.

2.3.7. UV spectroscopy

UV-Vis spectra were obtained by Perkin Elmer spectrometer "Lambda 35", wavelength range of 200-700 nm. The data curation of spectra was done using Perkin Elmer "Spectrum" computer program.

2.3.8. Evaluation of lubricating properties of the copolymers of MPC and PEOMEMA

Polydimethylsiloxane (PDMS) and osteochondral probes were prepared, and PDMS-glass and cartilage-glass tribology tests were performed at the Department of Biomaterials and Biomedical Technology, University Medical Center Groningen, University of Groningen, the Netherlands (group of assoc. prof. P. Sharma).

Preparation of PDMS probe

A hemispherical PDMS probe was utilized for preliminary experiment to figure out the influence of concentration of MPC-PEOMEMA copolymers in tribology test. The PDMS mixture (monomer/ cure agent = 10:1 in volume, Sylgard-184, Dow Corning, Midland, MI, USA) was poured into a 96-well clear polystyrene (pSt) microplate (Greiner Bio-One, Frickenhausen, Germany). The plate was placed in a vacuum chamber at 80 ℃ overnight (>12 h). After curing, the probe was then pulled out of the 96-well microplate slightly. The radius and length of the PDMS probe were 3.1 and 10 mm, respectively, as same as the size of the single well of the 96-well microplate. *N*-Hexane (Sigma-Aldrich, St. Louis, MO, USA) was used to remove dust as well as fingerprints from the PDMS probe surface, and then PDMS probe was washed by Milli-Q water through sonication for 15 min. [218].

PDMS-glass tribology test

The tribology test was performed using UMT-3 (Universal Mechanical Tester, Bruker Corporation, USA) in a pin-on-plate reciprocating sliding model. The PDMS probe was mounted under the load cell (DFM-1.0, Bruker, USA) and slid against borosilicate glass (Schott BK-7, Gerhard Menzel GmbH, Germany) which was mounted on a moving stage (Figure 2.6). A normal load of 4 N and sliding velocity of 4 mm/s with a distance of ±12 mm were applied for mimicking swing face of human gait cycle [219]. 220 reciprocate cycles were chosen (back and force), corresponding to a measurement duration of 1320 s. For figuring out the influence of

concentration of MPC-PEOMEMA copolymers in tribology, 2 mg/mL solutions of various MPC-PEOMEMA copolymers in 10 mM PBS buffer were prepared in advance. During measurement, 2 mL of PBS buffer was added on the glass surface at the very beginning, and 50 μL of the copolymer solution was dosed in every 20 cycles interval until 220 cycles, giving the concentration of MPC-PEOMEMA copolymers between PDMS and glass to be 0 (1 ~ cycle 20), 0.048 mg/mL (cycle 21 ~ cycle 40), 0.096 mg/mL (cycle 41 ~ cycle 60) until 0.400 mg/mL (cycle 201 ~ cycle 220). For comparison, pure PBS buffer was used as a lubricant in whole rubbing test as control. The temperature during the measurements was hold constant at 33°C, matching the intra-articular temperature in the knee joint during mild activity [220]. Average dynamic COF during every 20 cycles corresponding to different concentrations of MPC-PEOMEMA copolymer solution was measured.
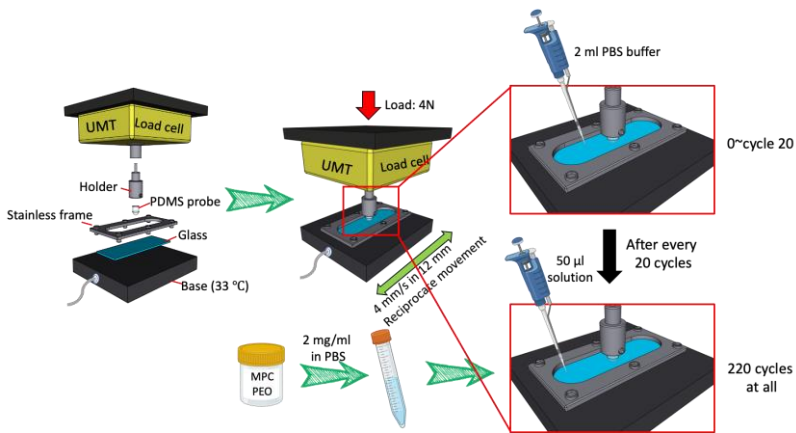
Figure 2.6. Schematic representation of the basic setup for PDMS – glass tribology measurement.

Preparation of osteochondral plug

Fresh bovine knee joints from bulls approximately two-years old were picked up from abattoir (Kroon Vlees b.v., Groningen, the Netherlands) and dissected 24 h after slaughter. Whole cartilage plug with a diameter of 12 mm drilling processing was performed at room temperature (20-24 °C) and femoral condyles of bovine knee joint was chosen (Fig. 2.7). During the drilling and cutting, the cartilage surface was under continuous wetting and cooling circumstance with PBS buffer. Extreme care was taken not to touch the osteochondral surface anytime during the plug preparation. The

osteochondral plugs were stored in PBS at 4°C before further tribological measurement and used with 24 h.
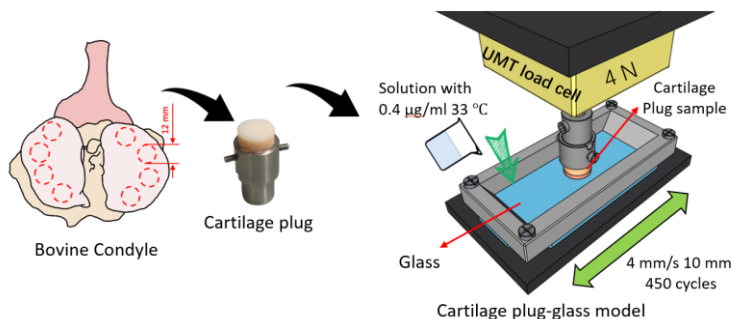
Figure 2.7. Schematic representation of the basic setup for cartilage plug – glass tribology measurement.

Cartilage-glass tribology test

Frictional experiments were performed on cartilage-borosilicate glass model which was immersed in a copolymer solution with a concentration of 0.4 mg/mL, using UMT-3 with reciprocal sliding motion ($\pm$ 10 mm with 4 mm/s under the load of 4 N). Each measurement was done at 33 °C and lasted 1 h resulting in 450 cycles. Average dynamic COF and dynamic creep in each cycle were measured. To simplify the display even further, average COF was then calculated for every 50-cycle interval until 450 cycles (i.e., cycle 0, cycle 50, cycle 100, and so on). Dynamic creep was obtained by recording the cartilage deformation using the z-position of the carriage at the start of each cycle during reciprocating sliding. These values were recorded for every 50-cycle interval until 450 cycles.

2.3.9. Evaluation of adsorption behavior of the copolymers of MPC and DOPMA on gold surface by infrared adsorption spectroscopy

Adsorption behavior of the copolymers on gold surface by the methods of Surface-enhanced infrared absorption spectroscopy (SEIRAS) and Reflection-absorption infrared spectroscopy (RAIRS) was studied in the Department of Organic Chemistry, Center for Physical Sciences and Technology, Vilnius (group of prof. G. Niaura).

Reflection-absorption infrared spectroscopy (RAIRS)

The copolymer desorption from gold surface was studied using reflection-absorption infrared spectroscopy (RAIRS). For RAIRS, microscopic 25×75 mm glass slides were coated with a 2 nm Cr adhesion layer and a 150 nm gold layer using a PVD75 (Kurt J. Lesker Co., U.S.) magnetron sputtering system. Immediately after coating, the slides were submerged in aqueous copolymer solutions (0.1 mg/mL, adjusted to pH 4 using H_2SO_4) for 85 min. In order to desorb copolymers, slides were subjected to ultrasound in a methanol solution for 15 min. RAIRS spectra were collected before and after the desorption using a Vertex 80v spectrometer (Bruker, Inc., Germany). The spectrometer was equipped with a liquid nitrogen-cooled MCT narrow band detector and horizontal RAIRS accessory reflecting p-polarized light at a grazing 80° angle. Spectra were collected with 4 cm^{-1} resolution and an aperture of 4 mm from 512 interferogram scans. The spectrometer and sample compartment were evacuated (~2 mbar) during the measurements. The spectrum of a hexadecanethiol-d$_{33}$ monolayer adsorbed on gold was used as a reference.

Surface-enhanced infrared absorption spectroscopy (SEIRAS)

SEIRAS experimental details were described elsewhere [221]. In short, the surface of mechanically polished face-angled Si crystal was subjected to 2% HF for 1 min and then coated with gold by applying a plating mixture for 4 min at room temperature. In order to increase the mechanical resistance of the gold film, the film was removed with aqua regia, and the gold film plating was repeated [222]. The gold plating solution consisted of equal volumes of (1) 0.15 M Na_2SO_3, 0.05 M $Na_2S_2O_3$, and 0.05 M NH_4Cl, (2) 20 wt% NH_4F, (3) 2 wt% HF, and (4) 0.03 M $NaAuCl_4$. After formation, the gold film was cleaned and activated by cyclic voltammetry (CV) in N_2-purged pH 5.8 sodium acetate solution (0.1 M). CV was performed using a PGSTAT101 potentiostat (Methrom, USA) starting within the 0–300 mV potential range vs. Ag/AgCl reference electrode. The upper potential limit was increased by 100 mV every three cycles until the onset of gold oxidation (at approximately 1.0 V). The CV scan speed was 20 mV/s. SEIRAS measurements were carried out using a spectrometer Vertex 80v (Bruker, Germany) equipped with a liquid-nitrogen-cooled MCT detector. The spectral resolution was 4 cm^{-1}, the aperture was 2 mm, and 50 sample scans and 100 background scans were co-added. The SEIRAS substrate was assembled into a VeeMax III accessory with a Jackfish cell J1F (Pike Technologies, USA), and the incident angle for

an ATR unit was set to 63 degrees. The spectrometer was purged with dry air for 15 hours before measurements.

2.4. Study of kinetics of the RAFT copolymerization of MPC and PEOMEMA

2.4.1. Determination of the sum monomer conversion

Overall (sum) monomer conversion (mol.%) during RAFT copolymerization was calculated by the eq. (1):

$$q^t = \frac{(\int_{5.71}^0 + \int_{6.16}^0) - (\int_{5.71}^t + \int_{6.16}^t)}{\int_{5.71}^0 + \int_{6.16}^0} \cdot 100, \quad (1)$$

where $\int_{6.16}^t$ and $\int_{5.71}^t$ are integrals of the vinyl protons shifts in ^{1}H NMR spectra of the monomers at 6.16 ppm and 5.71 ppm, respectively, after a time t of copolymerization, and $\int_{6.16}^0$ and $\int_{5.71}^0$ are the same shifts in ^{1}H NMR spectra before copolymerization.

Conversion of MPC (mol.%) was calculated by eq. (2):

$$q_{MPC}^t = \frac{\int_{3.25}^0 - \int_{3.25}^t}{\int_{3.25}^0} \cdot 100, \quad (2)$$

where $\int_{3.25}^0$ and $\int_{3.25}^t$ are integrals of the protons shifts in -N(C$\underline{H}_3$)$_3$) group of the MPC monomer in ^{1}H NMR spectra before copolymerization and after a time t of copolymerization, respectively.

Conversion of PEOMEMA (mol.%) was calculated by eq. (3):

$$q_{PEOMEMA}^t = \frac{q^t - f_{MPC}^0 \cdot q_{MPC}^t}{f_{PEOMEMA}^0} \cdot 100, \quad (3)$$

where q^t is the sum monomer conversion (eq. 1), q_{MPC}^t is the MPC conversion (eq. 2), f_{MPC}^0 and $f_{PEOMEMA}^0$ are molar fractions of MPC and PEOMEMA in the initial monomer mixture, respectively.

2.4.2. Determination of the average (cumulative) copolymer composition

The average composition of the copolymer after a specific time t of copolymerization was calculated by eq. (4):

$$F_{MPC}^t = \frac{q_{MPC}^t}{q_{MPC}^t + q_{PEOMEMA}^t}; \qquad F_{PEOMEMA}^t = \frac{q_{PEOMEMA}^t}{q_{MPC}^t + q_{PEOMEMA}^t}. \qquad (4)$$

The composition of the monomer mixture before copolymerization (eq. 5) and at a specific time t of copolymerization was calculated by eq. (6):

$$f_{MPC}^0 = \frac{\frac{1}{3}\int_{3.25}^0}{\int_{3.39}^0 + \frac{1}{3}\int_{3.25}^0}; \; f_{PEO}^0 = \frac{\int_{3.39}^0}{\int_{3.39}^0 + \frac{1}{3}\int_{3.25}^0};$$

$$f_{MPC}^0 = \frac{\int_{4.14}^0}{\int_{3.79}^0 + \int_{4.14}^0}; \; f_{PEO}^0 = \frac{\int_{3.79}^0}{\int_{3.79}^0 + \int_{4.14}^0}, \qquad (5)$$

where $\int_{3.39}^0$, $\int_{3.79}^0$ and $\int_{4.14}^0$ are integrals of the protons shifts in terminal -OCH$_3$ group in PEOMEMA, -COO-CH$_2$-C$\underline{H}_2$-O- group in PEOMEMA, and -O-CH$_2$-C$\underline{H}_2$-O-P- group in MPC, respectively;

$$f_{MPC}^t = f_{MPC}^0 - f_{MPC}^0 \cdot q_{MPC}^t;$$
$$f_{PEOMEMA}^t = f_{PEOMEMA}^0 - f_{PEOMEMA}^0 \cdot q_{PEOMEMA}^t. \qquad (6)$$

Instantaneous copolymer composition was calculated by eq. 7:

$$F_{inst.}^{MPC} = \frac{\Delta f_{MPC}^t}{\Delta f_{MPC}^t + \Delta f_{PEOMEMA}^t}. \qquad (7)$$

Theoretical (based on the terminal model of free-radical copolymerization) dependencies of instantaneous monomer feed composition and instantaneous copolymer composition on conversion were calculated by equations which are presented elsewhere [223].

2.4.3. Calculation of the reactivity ratios of the monomers in copolymerization

The reactivity ratios of MPC and PEOMEMA in RAFT copolymerization were calculated by the methods of Fineman and Ross [224], Kelen and Tüdos [225], and Meyer and Lowry [226]. The methods of Fineman and Ross, and Kelen and Tüdos are linear, which distort the error structure of the experimental data and could lead to biased and imprecise results. It was shown recently that for calculation of the reactivity ratios of the monomers in copolymerization, the methods based on non-linear least squares fitting are preferable.

Calculation according to the non-linear method of Meyer and Lowry was realized by iterative recalculation of the instantaneous copolymer composition

F_1 using initial f_0 and shifted f_1 monomer feed compositions (shifted value of f_1 depends on monomer conversion according to the equation of Meyer and Lowry). Initial (primary) values of the reactivity ratios of the monomers were calculated by the least square method, shifted value of f_1 was calculated from experimentally determined average copolymer composition at a certain monomer conversion, and the values of r_1 and r_2 together with the shifted value of f_1 were employed for calculation of F_1 by the copolymer composition equation. Iterations were made by shifting f_1 and recalculating F_1, and calculating updated values of r_1 and r_2 many times. Iterations were set until the values of r_1 and r_2 were changing insignificantly.

3. RESULTS AND DISCUSSION

3.1. Synthesis and characterization of zwitterionic copolymers containing MPC units

Biological lubrication (biolubrication) has long been a subject of scientific interest, particularly in the development of synthetic lubricants mimicking natural systems. Brush-type polymer pPEOMEMA and zwitterionic pMPC as individual polymers have been studied and applied in many biolubricating systems as promising candidates due to their similar properties, such as biocompatibility and biomimetic properties. These copolymers not only exhibit lubrication properties on various surfaces but also possess the antifouling properties, thus introducing them as highly attractive materials for biomedical applications. However, despite the individual bio-related advantages of pMPC and pPEOMEMA, the potential synergistic effects of combining these two segments remain largely unexplored. Moreover, the lack of published data on the copolymerization of MPC and PEOMEMA, whether through conventional free-radical copolymerization or RAFT copolymerization, underscores the need for further investigation. Obviously, the synthesis of copolymers incorporating both PEOMEMA and MPC segments in copolymer or diblock polymer and the producing of new properties is lacking serious investigation. In this study, a zwitterionic monomer MPC and a hydrophilic macromonomer PEOMEMA were selected to design new zwitterionic brush copolymers that have promising potential for biomedical applications.

3.1.1. Kinetics of the RAFT copolymerization of MPC and PEOMEMA

Synthetic route to the copolymers p(MPC-*co*-PEOMEMA) via RAFT copolymerization of MPC and PEOMEMA is presented in Figure 3.1a. It is well established [198,217,227] that RAFT copolymerization could give either random or gradient brush copolymer. The architecture of the brush copolymers depends on the reactivity ratios of the monomers, which could be evaluated by studying the kinetics of the copolymerization. The arrangement of PEO side chains along the backbone of the copolymers p(MPC-*co*-PEOMEMA) considerably affects the accessibility of phosphoryl choline groups and hydration of the copolymers. Kinetics of the RAFT copolymerization of MPC and PEOMEMA was studied by ^{1}H NMR spectroscopy (Fig. 3.1b) and size exclusion chromatography (SEC) using a methodology similar to that published earlier [200,217]. Copolymerization of

MPC and PEOMEMA in the mixed solvent MeOH:water = 3:1 v/v (or in MeOD-*d4*:D₂O = 3:1 v/v, if the copolymerization was carried out in NMR tubes) was carried out for a certain time, and aliquots of the reaction mixture were taken during the first 8 hours for kinetics study. The eluent for SEC analysis was identical to the solvent for copolymerization, i.e. MeOH:water = 3:1 v/v.
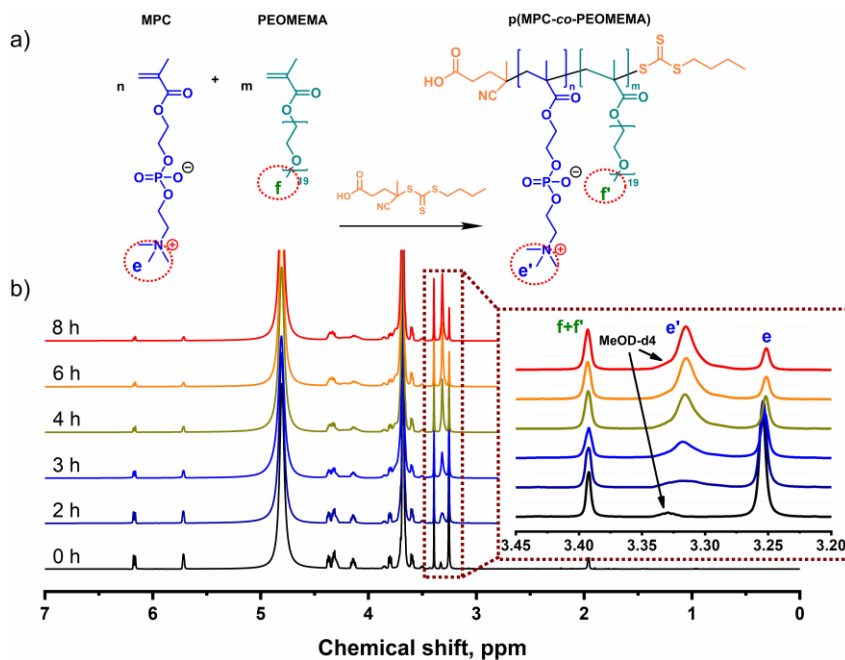
Figure 3.1. Scheme of the RAFT copolymerization of MPC and PEOMEMA with attribution protons to the chemical shifts in ^{1}H NMR spectra (a); ^{1}H NMR spectra of the reaction mixture taken during RAFT copolymerization of MPC and PEOMEMA in MeOD-*d4*:D₂O (3:1 v/v); [MPC]₀:[PEOMEMA]₀ = 53:47 mol.% (b); insert right – an expanded region of the spectra at 3.15-3.45 ppm.

First, the kinetics of the RAFT copolymerization of MPC and PEOMEMA was studied by analyzing the reaction mixtures by ^{1}H NMR spectroscopy. Changes in chemical shifts and their intensity in ^{1}H NMR spectra during copolymerization of the equimolar initial monomer mixture are presented in Fig. 3.1b. In ^{1}H NMR spectra, the shifts at 5.71 ppm, 6.16 ppm, and 6.17 ppm are attributed to the vinyl protons of the monomers. Unfortunately, the chemical shifts of the vinyl protons of the both monomers are almost at the same positions, which do not allow using them for the calculation of the consumption of the individual monomers. Nevertheless, a decrease in their intensity during copolymerization could be used to evaluate the overall

monomer conversion. The shift at 3.39 ppm is attributed to the protons of the terminal –OCH₃ group present in both the PEOMEMA monomer and PEOMEMA units in the copolymers. On the contrary, the shift of the protons attributed to the group –N(CH₃)₃ changed the position from 3.25 ppm in MPC monomer to 3.31 ppm in MPC monomeric unit in the copolymer during copolymerization. The chemical shift at 3.31 ppm is unsuitable for analytical purposes since it overlaps with the chemical shift of the deuterated methanol. Fortunately, a decrease in intensity of the shift at 3.25 ppm attributed to MPC monomer in combination with a decrease in intensity of the vinyl protons attributed to the both monomers during copolymerization allowed to calculate the consumption of the individual monomers and, at the same time, the average composition of the copolymer.

An analysis of the initial reaction mixtures with various monomer ratios by ^{1}H NMR spectroscopy revealed that the actual composition of the monomer mixtures was slightly different. For example, for the targeted equimolar monomer mixture, the actual monomer mixture was [MPC]:[PEOMEMA] = 53.6:46.4 mol.% (according to the integrated shifts at 3.25 ppm and 3.39 ppm attributed to the protons of $–N^+(CH_3)_3$ group in MPC and -O-CH₃ group in PEOMEMA, respectively), and 52.5:47.5 mol.% (according to the integrated shifts at 4.14 ppm and 3.79 ppm attributed to the protons of -O-CH₂-CH₂-O-P- group in MPC and -COO-CH₂-CH₂-O- group in PEOMEMA, respectively). Average composition of that monomer mixture was considered as [MPC]:[PEOMEMA] = 53:47 mol.%; a certain deviation from the target composition ([MPC]:[PEOMEMA] = 50:50 mol.%) was predetermined by inaccuracy in preparing small amount of the reaction mixture in NMR tube.

Copolymerization of MPC and PEOMEMA at different monomer ratios was carried out in deuterated solvents in NMR tubes to relatively low conversions (q = 3-21%); overall monomer conversions and copolymer compositions are presented in Table 3.1.

Compositions of the monomer mixtures as well as copolymer compositions at early stages of copolymerization were calculated from ^{1}H NMR spectra of the reaction mixtures. The dependence of the copolymer composition F_1 on the initial comonomer feed composition f_1 for the RAFT copolymerization of MPC (M_1) and PEOMEMA is presented in Fig. 3.2. Experimental points displayed in Fig. 3.2 evidently show that the copolymers are consistently enriched in MPC units. Reactivity ratios r_1 and r_2 for the comonomer pair MPC (M_1) and PEOMEMA (M_2) were calculated by several methods and are presented in Table 3.2. Much higher reactivity ratio of MPC compared to that of PEOMEMA implies that MPC is consumed faster during copolymerization,

which affects the comonomer feed composition and, consequently, the microstructure of the copolymers.

Table 3.1. Composition F_1 of the copolymers of MPC (M_1) and PEOMEMA (M_2) synthesized from various monomer feeds (f_1) to low conversions q and used for determination of reactivity ratios of the monomers r_1 and r_2.

f_1 (MPC)	F_1 (MPC)	Conversion, q
0.149	0.241	0.056
0.180	0.369	0.034
0.235	0.491	0.080
0.377	0.624	0.109
0.473	0.683	0.171
0.536	0.714	0.170
0.654	0.869	0.211
0.749	0.865	0.203
0.907	0.952	0.165
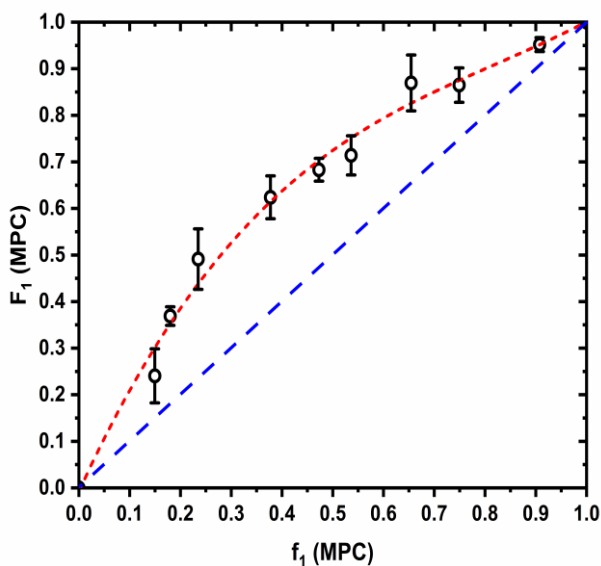
Figure 3.2. Theoretical (dashed dotted curve) and experimental (points with error bars) dependences of the copolymer composition F_1 on the initial comonomer feed composition f_1 for the RAFT copolymerization of MPC (M_1) and PEOMEMA. Theoretical dependence was calculated using reactivity ratios of the monomers $r_1 = 2.48$, $r_2 = 0.40$, determined by the method of Mayer-Lowry.

Table 3.2. Reactivity ratios of MPC (M_1) and PEOMEMA (M_2) calculated by various methods.

Method	r_1	r_2
Fineman-Ross [224]	2.10±0.28	0.32±0.08
Kelen-Tüdos [225]	2.28±0.22	0.27±0.09
Meyer-Lowry [226]	2.48±0.04	0.40±0.01

Calculation according to the method of Meyer and Lowry was realized by iterative recalculation of the copolymer composition F_1 using initial f_0 and shifted f_1 monomer feed compositions (shifted value of f_1 depends on monomer conversion according to the equation of Meyer and Lowry). Iterations were set until the values of r_1 and r_2 were changing insignificantly. Illustration of determination of the reactivity ratios of the monomers MPC (M_1) and PEOMEMA by the method of Meyer and Lowry is presented in Figure 3.3. Evidently, the monomer reactivity ratios only slightly depend on the calculation method. This is not unexpected, since overall monomer conversion was rather low (0.03 to 0.21). Nevertheless, the most accurate values of r_1 and r_2 were determined by the method of Meyer and Lowry, where the changes of the monomer feed composition with conversion were taken into account. The monomer reactivity ratios $r_1 = 2.48$ and $r_2 = 0.40$ determined by the method of Meyer and Lowry were further used for calculation of the theoretical dependences F_1 on q.
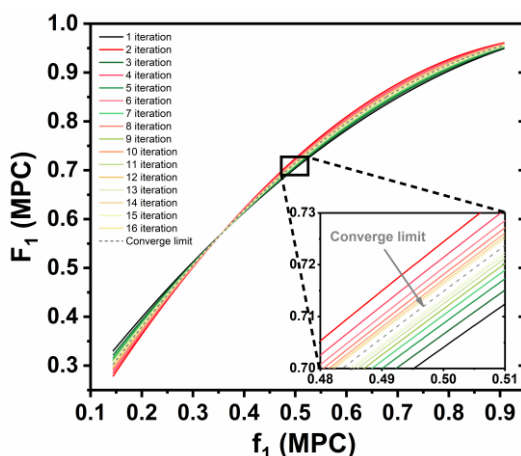
Figure 3.3. Representation of the iterative recalculations of the copolymer composition (F_1) as a function of shifted monomer feed compositions (f_1) by the method of Meyer and Lowry. The convergence limit is assigned to the ultimate values of the monomer reactivity ratios (r_1 and r_2).

SEC-RI eluograms of the aliquots taken from the reaction mixture containing excess of the monomer MPC (MPC:PEOMEMA = 77:23 mol%) are shown in Figure 3.4. Molecular weight dispersity of the copolymers containing less PEOMEMA units (lower density of PEO side chains) is low (<1.2) which is in correlation with previously published data [200].
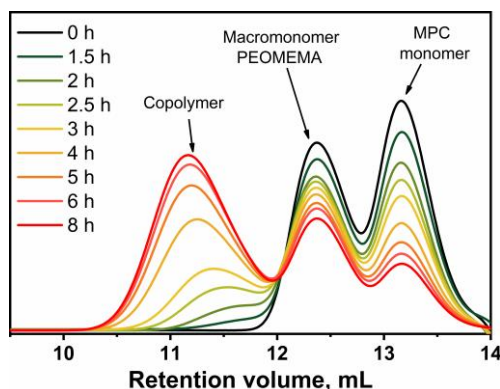
Figure 3.4. SEC-RI eluograms of the reaction mixture taken during RAFT copolymerization of MPC and PEOMEMA. Eluent MeOD-*d4*:D_2O (3:1, v/v) containing 0.1 M $NaNO_3$; $[MPC]_0$:$[PEOMEMA]_0$ = 72:28 mol. %.

It was shown earlier [200], that kinetics of copolymerization can be studied using SEC data if one of the monomers possesses relatively high molecular weight. SEC eluograms of the reaction mixtures taken during RAFT copolymerization of MPC and PEOMEMA are presented in Figure 3.5a. The RI response signals attributed to the monomer MPC, macromonomer PEOMEMA, and the copolymer are slightly overlapped. The evolution of the SEC-RI eluograms during copolymerization evidently show a decrease in intensity of the monomer and the macromonomer signals and, at the same time, an increase and a shift of the copolymer signal to lower retention volume (higher molecular weight). The signals attributed to the monomer, the macromonomer, and the copolymer were deconvoluted by the method described before [217]; deconvoluted SEC eluograms are presented in Figure 3.5b. Deconvoluted signals (their integrals) were used to calculate the overall monomer conversion, copolymerization rate, and copolymer composition [217].
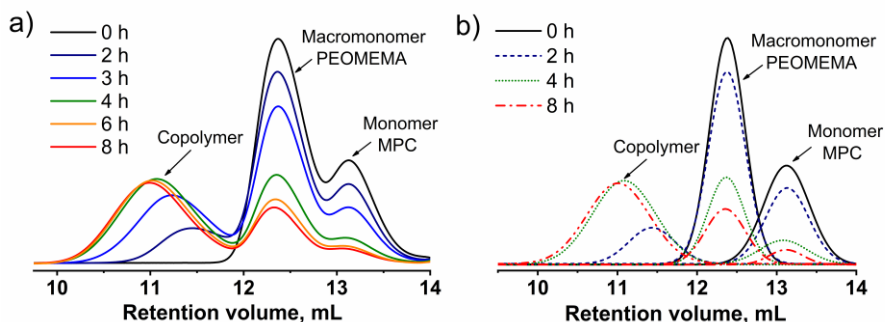
Figure 3.5. SEC-RI eluograms of the reaction mixtures (a) and evolution of deconvoluted SEC-RI eluograms (b) during RAFT copolymerization of MPC and PEOMEMA. Eluent MeOD-*d4*:D$_2$O (3:1, v/v) containing 0.1 M NaNO$_3$; [MPC]$_0$:[PEOMEMA]$_0$ = 53:47 mol.%.

An analysis of the same initial reaction mixture with equimolar monomer ratio by ^{1}H NMR spectroscopy and by SEC gave unexpected result: according to ^{1}H NMR spectroscopy, MPC content in the initial mixture was 53 mol.% while according to SEC – 69 mol.%. Such a significant difference in composition of the initial monomer mixture determined by two independent techniques cannot be explained by inaccuracy of the methods. Trying to explain the phenomenon, we made a presumption that the SEC-RI signal of the monomer MPC depends on the concentration of the monomer plus the concentration of the bound water molecules. It is well established [106,109,121] that MPC is highly hydrated, thus the phosphorylcholine side group is surrounded by water molecules and "carry" them as an integral part of the monomer. The molecular weight of the monomer MPC is 295. We theoretically tried to increase the molecular weight of the hydrated MPC by increasing the number of bound water molecules and continuing to calculate the initial monomer composition. The composition of the initial monomer mixture in SEC analysis was the same as determined by ^{1}H NMR spectroscopy ([MPC]:[PEOMEMA] = 53:47 mol.%) if the molecular weight of MPC was set to 565. These calculations led to the simple conclusion that every molecule of MPC carries about 15 molecules of water as an integral part of the monomer, at least, in methanol:water (3:1 v/v) solutions.
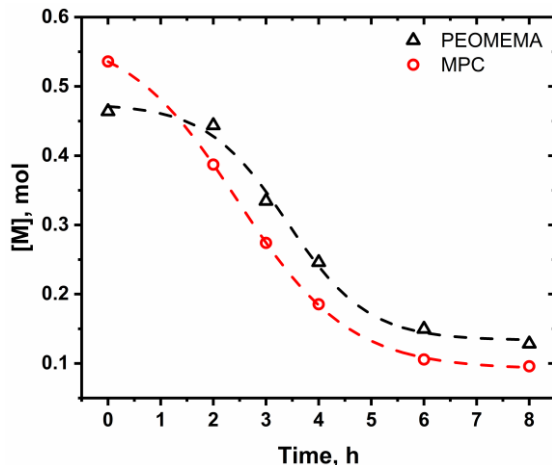
Figure 3.6. Dependencies of residual concentration of the monomers MPC and PEOMEMA on the reaction time during RAFT copolymerization of MPC and PEOMEMA in the mixture methanol:water (3:1 v/v); $[MPC]_0:[PEOMEMA]_0 = 53:47$ mol.%.

To verify the correctness of the presumption about the "increased" molecular weight of MPC shown by SEC-RI curves, we calculated average copolymer composition at various monomer conversions from ^{1}H NMR spectra of the reaction mixtures, and also from SEC data of the same mixtures using two molecular weights of MPC – 295 and 565. Changes in the average copolymer composition (amount of MPC units) with the sum conversion of the monomers are presented in Fig. 3.7a. Obviously, the curves 2 and 3 illustrating the dependences based on ^{1}H NMR spectra and SEC data with MPC of molecular weight 565 are very close. Contrarily, the curve based on SEC data with MPC of molecular weight 295 is shifted towards a very high content of MPC units in the copolymers, which is even impossible at high conversions of the monomers. Thus, our experiments prove that in the solutions of methanol and water (3:1 v/v) one molecule of the monomer MPC carries about 15 molecules of water.

Water molecules have been shown to form a cage structure around zwitterionic polymers, similar to the molecular organization of ice [124]. Water molecules are attracted to the charged functional groups of the zwitterion through ionic solvation, which forms an energy barrier which is greater than that associated with a poly(ethylene glycol) hydration shell, which is formed through hydrogen bonding. Although PEO is abundantly hydrated, such hydrates are less organized allowing the water exchange. As it was shown before [179], apparent molecular weight of PEOMEMA was not

increasing due to hydration. An increase in apparent molecular weight of MPC in methanol-water solutions we attribute to formation of clathrate cage structure of surrounding water molecules, in which water molecules are retained like in ice.

Monomer consumption curves during RAFT copolymerization of MPC and PEOMEMA in the mixed solvent of methanol and water are presented in Figure 3.6. Conversion of the monomers depends on the monomer ratio being higher at excess of MPC. Overall conversion of the monomers after 8 hours of copolymerization is moderately high, about 70-80 mol.%.

An average (cumulative) copolymer composition determined by SEC and by NMR spectroscopy is very close, and its changes with conversion are represented by the same curve (Fig. 3.7b, curve 5). Short chains of the copolymers formed at the initial stages of the copolymerization (at relatively low monomer conversions) are rich in MPC units. In contrast, long polymer chains (formed at high monomer conversions) contain nearly the same amount of MPC and PEOMEMA units. The course of the curve presenting changes in average copolymer composition, calculated theoretically according to the reactivity ratios of the monomers (Fig. 3.7b, curve 4), is different from the curve 5: theoretically calculated copolymer composition is changing much less; moreover, it is characterized by upward curvature, in contrast to the experimental curve. A comparison of these two curves suggests that experimental data are poorly described by the theoretical model based on the reactivity ratios of the monomers.

An average composition of the copolymer synthesized by RAFT copolymerization does not reflect the real composition of a chain fragment formed at a certain conversion point (at a certain chain length). Changes in copolymer composition along polymer chains are presented by the evolution of instantaneous copolymer composition during chain growth. Instantaneous copolymer composition as a function of the apparent normalized chain length calculated by derivatization of the curve presenting changes in average copolymer composition during copolymerization and calculated theoretically using experimentally determined reactivity ratios of the monomers are presented in Fig. 3.7b, curves 7 and 6, respectively. Obviously, changes in instantaneous copolymer composition along polymer chains are much larger compared to changes in average copolymer composition during copolymerization. For instance, for the copolymers synthesized by RAFT copolymerization of nearly equimolar monomer mixture to overall monomer conversion of about 80 mol.%, instantaneous copolymer composition changes along polymer chains from 75 mol.% of MPC units at the beginning to about 40 mol.% of MPC units at the end of the chains (Fig. 3.7b, curves 6 and 7).

Thus, the copolymers of MPC and PEOMEMA synthesized by RAFT copolymerization are characterized by clearly expressed gradient structure.
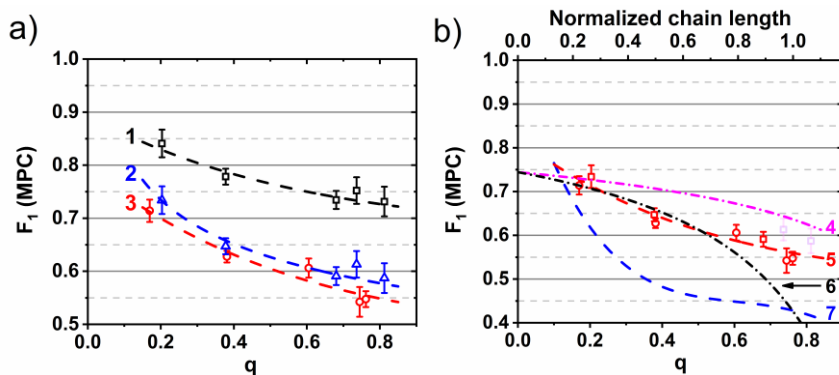
Figure 3.7. (a) Changes in average copolymer composition during RAFT copolymerization of MPC and PEOMEMA calculated from ^{1}H NMR spectra (3) and SEC-RI data (1, 2) using MPC with molecular weight 295 (1) and 565 (2); (b) changes in average copolymer composition during RAFT copolymerization of MPC and PEOMEMA calculated from experimental data (5) of SEC-RI (○) and ^{1}H NMR spectra (□) and theoretically using reactivity ratios of the monomers $r_1 = 2.48$, $r_2 = 0.40$ (4); (b) evolution of instantaneous copolymer composition formed at a certain overall monomer conversion as a function of the apparent normalized chain length calculated by derivatization of the curve 2 (7) and theoretically using reactivity ratios of the monomers $r_1 = 2.48$, $r_2 = 0.40$ (6); [MPC]$_0$:[PEOMEMA]$_0$ = 53:47 mol.%.

It is worth noting that the course of the two curves 6 and 7 (Fig. 3.7b) presenting the evolution of instantaneous copolymer composition is very different, i.e., the theoretically calculated curve is poorly coinciding with the curve obtained by derivatization of the experimental data. It means that the microstructure (changes in copolymer composition along polymer chains) of the copolymers p(MPC-*co*-PEOMEMA) synthesized by RAFT is not described (or poorly described) by the terminal model of free-radical copolymerization based on reactivity ratios of the monomers.

Although the monomer reactivity ratios in reversible deactivation radical copolymerizations are generally the same as in free-radical copolymerizations, there is a difference in the distribution of copolymer compositions for different polymer molecules [228,229]. It was shown by Matyjaszewski [230] that the differences arise not from differences in monomer reactivity ratios, but from differences in the consumption of the two

monomers. The effect is observed in the copolymerization systems where there is an intermittent activation/deactivation process between active and dormant species. Deviations are possible when two propagating species have different activation and/or deactivation rate constants. Under these conditions, one of the monomers is consumed faster compared to corresponding free-radical system, and the comonomer feed and, therefore, the copolymer composition as a function of conversion changes differently than in free-radical polymerization. The effect is generally larger when homopropagation is faster than cross-propagation (r_1, $r_2 > 1$) and at lower monomer conversion.

Likely, the above-described conditions are realized in the RAFT copolymerization of MPC and PEOMEMA (equilibrium between active and dormant species, propagating species containing a terminal unit of MPC or PEOMEMA have different activation and/or deactivation rate constants), and the monomer MPC is consumed considerably faster. This leads to a swift change in instantaneous copolymer composition during RAFT copolymerization of MPC and PEOMEMA. Consequently, even copolymers of MPC and PEOMEMA synthesized by RAFT copolymerization to medium conversion of the monomers possess clearly expressed gradient microstructure.

Fig. 3.8a demonstrates changes in molecular weight and molecular weight dispersity of the copolymers during RAFT copolymerization of MPC and PEOMEMA. Experimentally determined molecular weights correspond well with those calculated theoretically. Theoretically calculated dependence of molecular weight on monomer conversion is presented by a bent line, which is a product of uneven incorporation of the monomers into the growing polymeric chains during copolymerization (gradient distribution of the monomeric units across the polymeric chains).

Molecular weight dispersity of the copolymers Đ is not low but moderate, which is predetermined mainly by steric effects of the macromonomer PEOMEMA. At a certain point of the chain growth (q about 60%), the molecular weight dispersity Đ of the copolymers becomes almost independent of the monomer conversion (chain length). Thus, RAFT copolymerization of MPC and PEOMEMA in the presence of trithiocarbonate-type CTA proceeded in reasonably controlled manner giving well-defined gradient copolymers with predicted macromolecular parameters, i.e., molecular weight close to theoretically calculated and moderately low molecular weight dispersity (Đ below 1.3). The pseudo-first order kinetic plot for the RAFT copolymerization of MPC and PEOMEMA, plotted through experimental points obtained by ^{1}H NMR spectroscopy and by SEC, is linear (Figure 3.8b). The same linear dependence for the points obtained by two independent

methods demonstrates that SEC is a suitable method to study the kinetics of RAFT copolymerization. The copolymerization rate constant calculated from the slope of the plot is 8.46×10^{-5} s^{-1}. Thus, the rate of the RAFT copolymerization of MPC and PEOMEMA is moderately high.
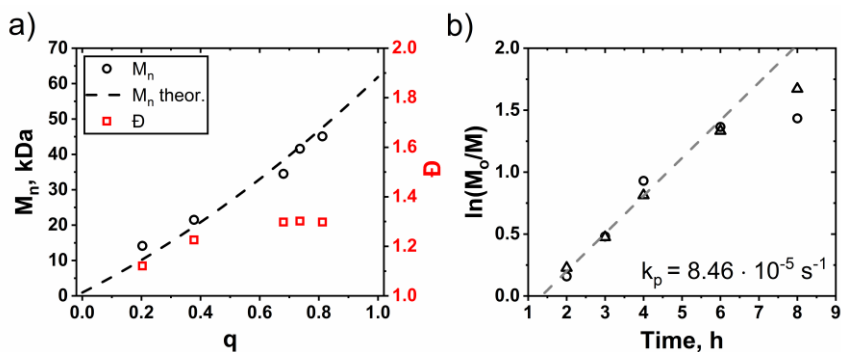
Figure 3.8. Evolution of molecular weight (○) and molecular weight dispersity (□) of the copolymers during RAFT copolymerization of MPC and PEOMEMA (a); dashed line – theoretical (calculated) dependence of the molecular weight of the copolymers on conversion; pseudo-first order kinetic plot for the RAFT copolymerization of MPC and PEOMEMA (b). Experimental points were got by SEC (△) and ^{1}H NMR spectroscopy (○). [MPC]$_0$:[PEOMEMA]$_0$ = 53:47 mol. % in MeOD-*d4*:D$_2$O (3:1 v/v)

A series of the gradient copolymers p(MPC-*grad*-PEOMEMA) with different ratio of the monomeric units were synthesized by RAFT copolymerization (Table 3.3). Copolymerization for 24 h yielded copolymers with degree of polymerization (DP) 60–70 and molecular weight dispersity Đ 1.2−1.3. The highest molecular weight dispersity (Đ 1.30) was characteristic for the brush copolymer containing high content of PEOMEMA units.

Table 3.3. Characteristics of the copolymers p(MPC-*grad*-PEOMEMA). [M]$_0$:[CTA]$_0$:[ACVA]$_0$ = 240:3:1, τ = 24 h.

Sample	[MPC]$_0$/ [PEOMEMA]$_0$	Practical yield, %	Copolymer composition, MPC mol.%	M$_n$, kDa	DP	Đ
1	25:75	51	31.9	39.4	61	1.30
2	50:50	64	59.7	34.1	65	1.25
3	75:25	70	77.4	33.7	73	1.19

3.1.2. Synthesis of hydrophilic diblock brush copolymers containing MPC and PEOMEMA units

Synthetic route to the diblock copolymers of MPC and $PEO_{19}MEMA$ is presented in Scheme 1.
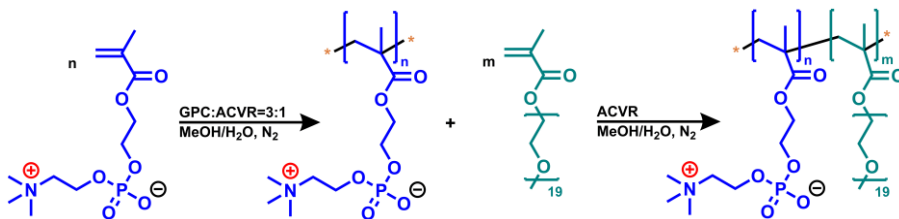
Scheme 1. Synthesis of the diblock copolymers pMPC-*b*-p(PEO_{19}MEMA).

Polymerization of MPC has been extensively studied before [71,72,106,231]. In the present study, RAFT polymerization of MPC was conducted in the mixed solvent MeOH/water = 3/1 v/v. Such a mixture of the solvents made the polymerization mixture suitable for direct SEC measurements [217]. It was shown previous section, that SEC with triple detection gave enlarged molecular weight of pMPC because of 15 molecules of water being as an integral part of the monomer. Thus, DP of pMPC was calculated assuming that molecular weight of the monomer is 565 (MPC + 15 molecules of H_2O). By changing the ratio between MPC and CTA, the monodisperse pMPC polymers with various molecular weight were successfully synthesized, and their MWD curves are presented in Figure 3.9. RAFT polymerization of MPC was well controllable giving polymers with very low molecular weight dispersity, Đ about 1.1. The average yield of MPC polymerization was 84%.

Three samples of pMPC with different chain length (DP 18, 27, and 41) were selected and used as macroCTA for the chain extension by the units of $PEO_{19}MEMA$ or PEO_9MEMA. Number average molecular weight M_n of these samples of pMPC, determined by SEC, was 10000, 15500, and 23300, respectively; molecular weight dispersity Đ of the polymers was 1.09, 1.08, and 1.10, respectively. Chain extension (formation of the second block composed by PEOMEMA units) was followed by recording SEC elution curves of the reaction mixtures.
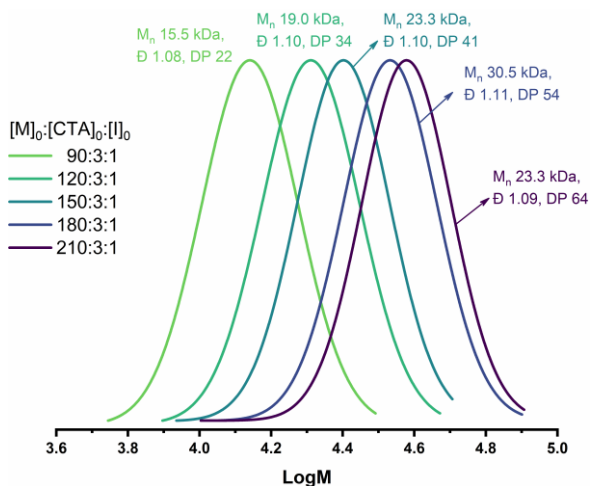
Figure 3.9. MWD curves of various pMPC samples.

SEC elution curves of the reaction mixtures taken after RAFT polymerization of MPC and chain extension of pMPC with the units of PEO_9MEMA or $PEO_{19}MEMA$ are presented in Fig. 3.10. All the elution curves contain two peaks, which are associated with the presence of a polymer (at lower retention volume) and residual monomer (at higher retention volume). It means that the monomer conversion at the moment of sampling was not very high. Residual monomer was successfully removed from pMPC by precipitation of the polymer into excess of acetone and reprecipitation from methanol, and the purified and dried pMPC was used for the chain extension. During the chain extension, the peak associated with residual monomer PEOMEMA was usually larger, i.e. conversion of PEOMEMA was lower. Nevertheless, the peaks on elution curves attributed to the block copolymer appeared unimodal and shifted towards lower retention volumes in respect to pMPC peak (Fig. 3.10). It proves formation of the block copolymers with molecular weight considerably higher than that of pMPC. Unfortunately, the peaks attributed to pMPC and the block copolymers are partially overlapped which makes the question about contamination of the block copolymers with pMPC molecules standing over. On the other hand, if present, the amount of unreacted pMPC should not be large because of absence of clearly expressed "wing" on peaks attributed to the block copolymers. Molecular weight dispersity Đ of the diblock copolymers is not low but reasonable, usually about 1.3–1.6 (Table 3.4). Such slightly increased values of Đ indirectly confirm possible presence of small amount of unreacted pMPC.

83
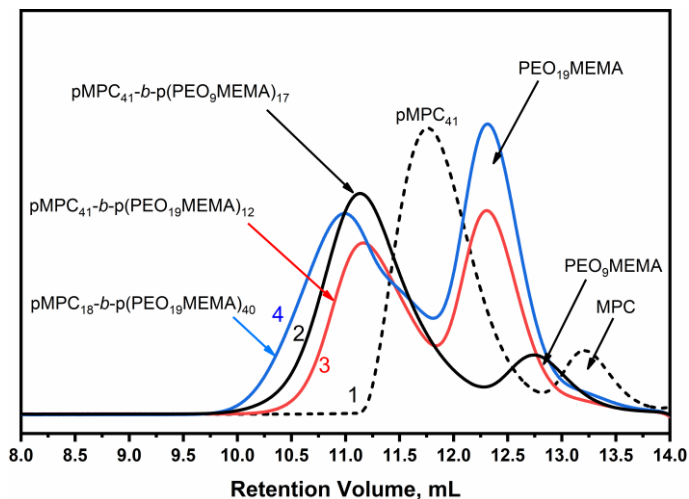
Figure 3.10. SEC-RI eluograms of the reaction mixtures taken after 8 hours of RAFT polymerization of MPC (1) and 24 hours of chain extension of pMPC with PEO$_9$MEMA (2) and PEO$_{19}$MEMA (3,4). Eluent MeOH:H$_2$O (3:1, v/v) containing 0.1 M NaNO$_3$.

Fig. 3.11 presents ^{1}H NMR spectra of pMPC and the diblock copolymers pMPC-*b*-pPEOMEMA. Characteristic chemical shifts of pMPC in MeOD-*d4* are at 4.35 ppm, 4.25 ppm, 4.10 ppm, 3.72 ppm and 3.33 ppm which are attributed to the protons in -O-C$\underline{H}_2$-CH$_2$-O-P-, P-O-C$\underline{H}_2$-CH$_2$-N-, -O-CH$_2$-C$\underline{H}_2$-O-P-, -P-O-CH$_2$-C$\underline{H}_2$-N- and -N(CH$_3$)$_3$ groups, respectively (Fig. 3.9, 1). Characteristic chemical shifts of p(PEO$_{19}$MEMA) in MeOD-*d4* are at 4.14 ppm, 3.66 ppm and 3.37 ppm which are attributed to the protons in -COO-C$\underline{H}_2$-CH$_2$-O-, -(-O-C$\underline{H}_2$-C$\underline{H}_2$-O-)$_x$- and -O-C$\underline{H}_3$ groups, respectively (Fig. 4, curves 3 and 4). In the spectra of the diblock copolymers, some chemical shifts, attributed to different monomeric units, are in close vicinity and partially overlapping (Fig. 3.11, curves 2 and 3). The most suitable for the calculation of the copolymer composition were the chemical shifts at 3.33 ppm and 3.37 ppm, which belong to MPC and PEOMEMA, respectively (Fig. 3.11, insert). Composition of the diblock copolymers calculated from ^{1}H NMR spectra is presented in Table 3.4. Length (DP) of the pPEOMEMA block was calculated by two methods – directly from the SEC data of the diblock copolymers and of pMPC, and from ^{1}H NMR spectra of the copolymers taking into account DP of the first block determined by SEC. DP of the second block calculated by the two methods was close in between with slightly higher values got by NMR. DP of the second block was not large, usually 20 to 40 (Table 3.4). Lower than expected values of DP were predetermined by

relatively low conversion of PEO$_{19}$MEMA during the chain extension, which was 50-70 mol%. This is in accord with previous publication [200] disclosing obstacled chain extension by PEOMEMA units with relatively long PEO chain. Increasing the initial ratio [PEO$_{19}$MEMA][macroCTA] led to higher DP of the second block but conversion of the macromonomer was reduced from 70 mol% to ca 50 mol%.
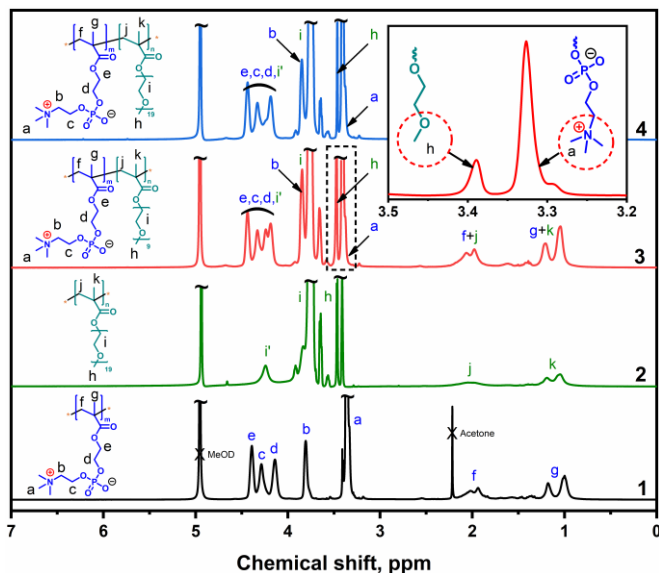
Figure 3.11. ^{1}H NMR spectra of pMPC (1), pPEO$_{19}$MEMA (2), pMPC$_{41}$-*b*-p(PEO$_9$MEMA)$_{17}$ (3) and pMPC$_{41}$-*b*-p(PEO$_{19}$MEMA)$_{12}$ in MeOD-*d4* (4). Insert top right – an expanded region of the pMPC$_{41}$-*b*-p(PEO$_9$MEMA)$_{17}$ spectrum at 3.2–3.5 ppm.

Table 3.4. Characteristics of the diblock copolymers of MPC and PEOMEMA.

Diblock copolymer	[PEO-MEMA]/ [CTA]	Composi-tion, MPC mol%	M_n, kDa	Đ	DP1, first block	DP2, second block, SEC	DP2, second block, NMR
pMPC-*b*-p(PEO$_{19}$MEMA)	100	34.6	64.0	1.55	27	51	56
	60	31.0	47.6	1.57	18	40	43
	50	51.9	39.3	1.53	27	25	23
	40	54.0	36.9	1.41	27	23	26
	20	77.4	31.8	1.33	41	12	14
pMPC-*b*-p(PEO$_9$MEMA)	60	12.2	75.1	1.43	18	72	67
	40	40.9	34.8	1.53	27	39	43
	20	70.7	31.5	1.38	41	17	25

Chain extension of pMPC with the units of PEO$_9$MEMA was going easier and resulted in the diblock copolymers in which DP of the second block was close to that predicted by the initial ratio [PEO$_{19}$MEMA][macroCTA] (Table 3.4). Conversion of the macromonomer was higher in that case (usually, about 90 mol%) but molecular weight dispersity Ð of the diblock copolymers pMPC-*b*-p(PEO$_9$MEMA) was not low, comparable with that of the diblock copolymers pMPC-*b*-p(PEO$_{19}$MEMA). These data suggest that the synthesis of the diblock copolymers containing a brush-type block by the RAFT method is complicated irrespective of the macromonomer size.

3.1.3. Synthesis of amphiphilic diblock copolymers of MPC and DOPMA

Synthetic route to the diblock copolymers with acetonide-protected catechol groups pMPC-*b*-pADOPMA and their counterparts with unprotected catechol groups pMPC-*b*-pDOPMA are presented in Scheme 2.
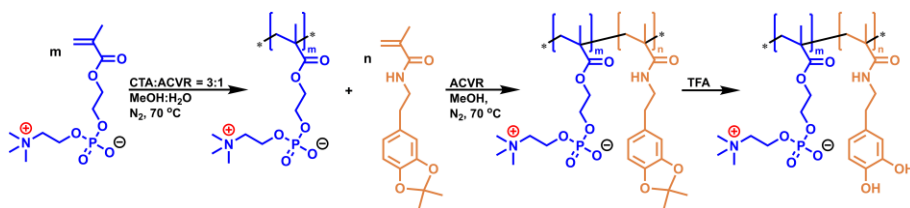
Scheme 2. Synthesis of the diblock copolymers pMPC-*b*-pDOPMA.

For the synthesis of the diblock copolymers, low molecular weight dispersity pMPC (Ð = 1.10) was used as the first block (macro-CTA), and the ratio of [ADOPMA]:[macroCTA] was kept constant 40:1. The ratio of [macroCTA]:[ACVA] remained the same – 3:1. In previous studies, many amphiphilic diblock copolymers were synthesized starting from pMPC block [50,51,98,232,233]. Several solvents were used for the chain extension reaction, including methanol [50], ethanol [233], and some of organic mixtures such as ethanol:chloroform (3:7 v/v) [51], methanol:DMSO (1:1 v/v) [232], and ethanol:THF (1:1 or 3:1 v/v) [6]. In the present study, chain extension by the units of ADOPMA from pMPC was done in MeOH, EtOH and several mixtures of these alcohols with DMF and CHCl$_3$ (Table 3.5).

Table 3.5. Characteristics of the diblock copolymers pMPC-*b*-pADOPMA.

Entry	Solvent	Copolymer composition, MPC mol%	DP1, first block (SEC)	DP2, second block (NMR)	M_n, kDa
1	MeOH	72.0	22	9	8.7
2	MeOH:DMF (1:2 v/v)	67.9		10	9.2
3	EtOH	85.0		6	11.6
4	EtOH:CHCl$_3$ (3:7 v/v)	82.7	34	7	11.9
5		83.5		7	11.8
6	MeOH	75.9	41	13	15.3
7		85.6	54	9	18.3
8		86.3	64	10	21.5

In all the cases, pADOPMA block was short, DP not more than 13. The use of cosolvents DMF and CHCl$_3$ was not justified since these solvents do not solubilize pMPC, especially with higher DP. Methanol proved out as the most suitable solvent well solubilizing pMPC block and partially solubilizing pADOPMA. It was shown by DLS analysis (Figure 3.12) that at concentration 1 mg/mL the diblock copolymers are well soluble in methanol but form aggregates at concentration 50 mg/mL which is similar to that in the reaction mixture during chain extension. We suppose that insufficient solubilization of pADOPMA block by MeOH was the main reason impeding receiving that block with higher DP.
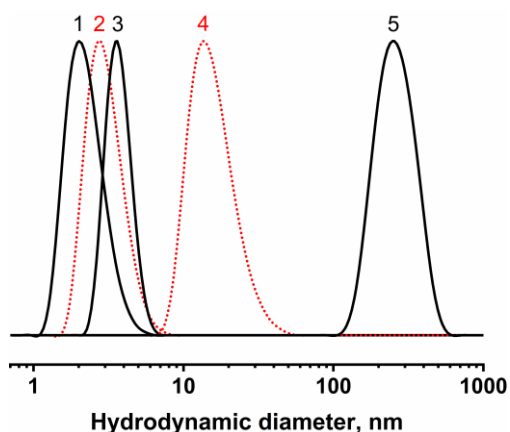
Figure 3.12. Particle distribution curves of pMPC (1, 2) and of the acetonide-protected copolymer pMPC-*b*-pADOPMA (3-5) in methanol (1, 3, 5) and

water (2, 4) at 25 °C. Copolymer concentration in methanol is 1 mg/mL (3) and 50 mg/mL (5).

Usually, chain extension by units of another monomer during synthesis of diblock copolymers is evaluated by SEC analysis. Unfortunately, we had no possibility to study the diblock copolymers of pMPC and pADOPMA by SEC because of absence of an eluent dissolving both blocks of a very different nature. The only common solvent for the both hydrophilic pMPC block and hydrophobic pADOPMA block was methanol, which is not compatible with the known SEC columns. Composition of the diblock copolymers and DP of the second block were calculated from ^{1}H NMR spectra of the copolymers taking into account DP of the first block determined by SEC.
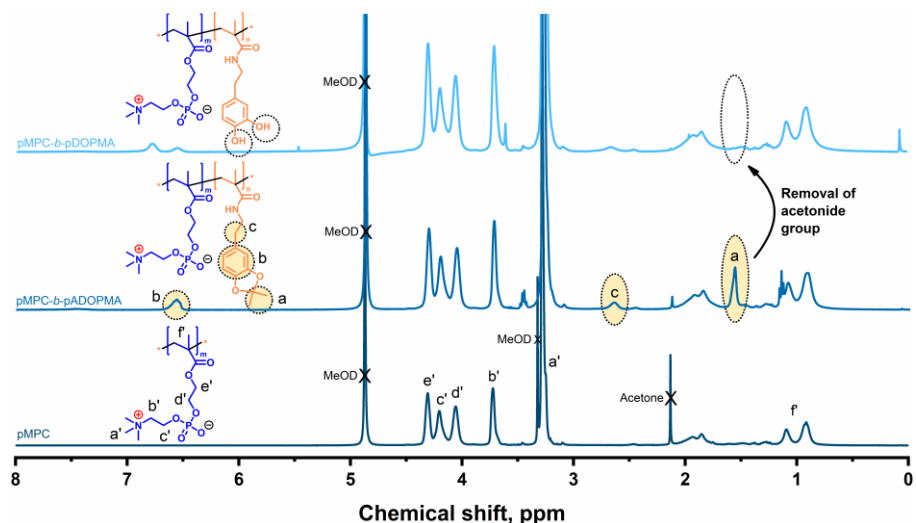
Figure 3.13. ^{1}H NMR spectra of pMPC, diblock copolymer with acetonide-protected catechol groups pMPC-*b*-pADOPMA and diblock copolymer with unprotected catechol groups pMPC-*b*-pDOPMA in MeOD-*d4*.

^{1}H NMR spectra of pMPC and of the diblock copolymers pMPC-*b*-pADOPMA and pMPC-*b*-pDOPMA are presented in Figure 3.13. In the spectrum of pMPC, chemical shifts at 3.25 ppm, 3.75 ppm, 4.05 ppm, 4.19 ppm and 4.30 ppm are attributed to the protons in -N$^+$(C$\underline{H}_3$)$_3$, -N-C$\underline{H}_2$-, -O-C$\underline{H}_2$-C$\underline{H}_2$-O-P-, -N$^+$-C$\underline{H}_2$-C$\underline{H}_2$-, and -COO-C$\underline{H}_2$-C$\underline{H}_2$- groups, respectively. In the spectrum of the diblock copolymer with protected catechol groups, there are three additional chemical shifts at 1.56 ppm, 2.61 ppm and 6.50 ppm

(marked yellow), which are assigned to acetonide group -C(C$\underline{H}_3$)$_2$, methylene group -NH-CH$_2$-C$\underline{H}_2$-, and benzene ring (3H), respectively.

Copolymer composition was calculated by comparing intensity of the chemical shifts of -N-C$\underline{H}_2$-(2H, 3.72 ppm) and O-C$\underline{H}_2$-C$\underline{H}_2$-O-P-C$\underline{H}_2$- (6H, 4.6–4.0 ppm) groups of pMPC, and intensity of the chemical shifts of acetonide (6H, 1.56 ppm) and -NH-CH$_2$-C$\underline{H}_2$- (2H, 2.61 ppm) groups of ADOPMA. Strong chemical shift at 3.25 ppm attributed to the protons in -N$^+$(C$\underline{H}_3$)$_3$ group of MPC was superimposed by two chemical shifts of MeOD-*d4* and ADOPMA (-NH-C$\underline{H}_2$-), and was not useful for quantification. Chemical shift at 6.5 ppm attributed to the aromatic protons of ADOPMA was not used for the calculation of the copolymer composition since integral area of that chemical shift was reduced compared to other chemical shifts of ADOPMA. This could be due to partial masking of the catechol group because of insufficient solvation by methanol. Chemical composition of the diblock copolymers determined by ^{1}H NMR spectroscopy was verified by independent method based on UV-VIS adsorption spectra of the copolymer solutions in methanol (Figure 3.14 and 3.15). Calculations based on NMR spectra and UV-VIS spectra of the copolymer solutions gave close results (deviation less than 1%) (Tables 3.6 and 3.7). Composition of the diblock copolymers served for calculation of DP of the second block of the copolymers (Table 3.7).

Table 3.6. Calculation of the copolymer composition from the data of UV-Vis spectroscopy.

Copolymer	Concen-tration, mg/mL	Absorbance at 289 nm, a.u.	Corrected absorbance, a.u.	ADOPMA in copolymer, mg	Copolymer composition, ADOPMA mol%
pMPC-*b*-pADOPMA	0.25	0.64	0.57	0.037	16.4
	0.5	1.25	1.07	0.074	16.4
	1	2.44	2.05	0.147	16.3
pMPC	0.25	0.08			
	0.5	0.18			
	1	0.39			

Table 3.7. Composition of the diblock copolymers calculated from ^{1}H NMR and UV-VIS spectra.

Diblock polymer	Monome-ric unit	Attributed functional group	Chemi-cal shift, ppm	Inte-gral area	Integral area per proton	Molar fraction by NMR, %	Molar fraction by UV-VIS, %	DP in polymeric block
pMPC-*b*-pADOPMA	MPC	-N(C$\underline{H}_3$)$_3$	3.27	49.98	5.554	83.5	83.6 ± 0.1	34*
		-PO$_4$-CH$_2$-C$\underline{H}_2$-N-	3.72	10.14	5.068			
		-C$\underline{H}_2$-C$\underline{H}_2$-PO$_4$-C$\underline{H}_2$-	4.3-4.0	29.69	4.948			
	ADOPMA	-C(C$\underline{H}_3$)$_2$	1.56	6.000	1.000	16.5	16.4 ± 0.1	7
		-NH-CH$_2$-C$\underline{H}_2$-	2.61	2.040	1.021			
		Benzene ring (3H)	6.50	2.659	0.886			

* DP calculated from SEC analysis.

A series of pADOPMA absorption spectra in methanol showed typical benzene ring absorption peak at 289 nm (Figures 3.14 and 3.15). Solutions of pMPC showed wide but weaker than pADOPMA absorption peak ranging from 270 nm to 350 nm (maximum at 310 nm). Intensity of pADOPMA peak was corrected by subtracting intensity of pMPC absorption at 289 nm. The calibration graph absorption of ADOPMA versus concentration was used for determination of the amount of monomeric units carrying benzene ring in the copolymers pMPC-*b*-pADOPMA (Figure 3.16). Results of determination are summarized in Table 3.7.
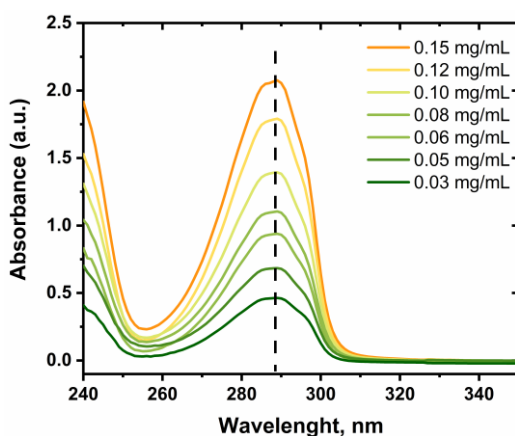
Figure 3.14. UV-VIS spectra of pADOPMA in MeOH. The data of polymer absorbance at 289 nm is used for calibration graph.
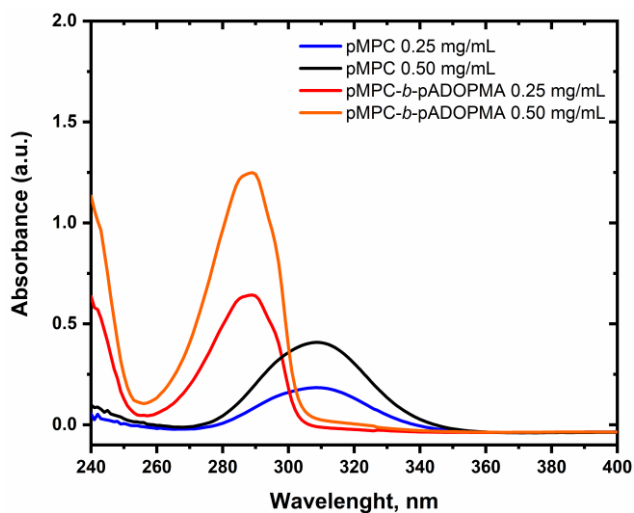
Figure 3.15. UV-Vis spectra of pMPC and pMPC-*b*-pADOPMA in MeOH.
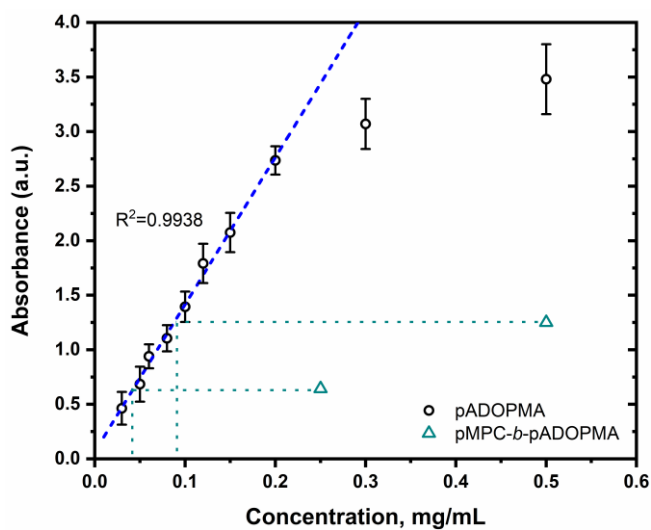
Figure 3.16. Calibration graph Absorbance versus concentration of ADOPMA; experimental points Δ – absorbance of pMPC-*b*-pADOPMA at 289 nm.
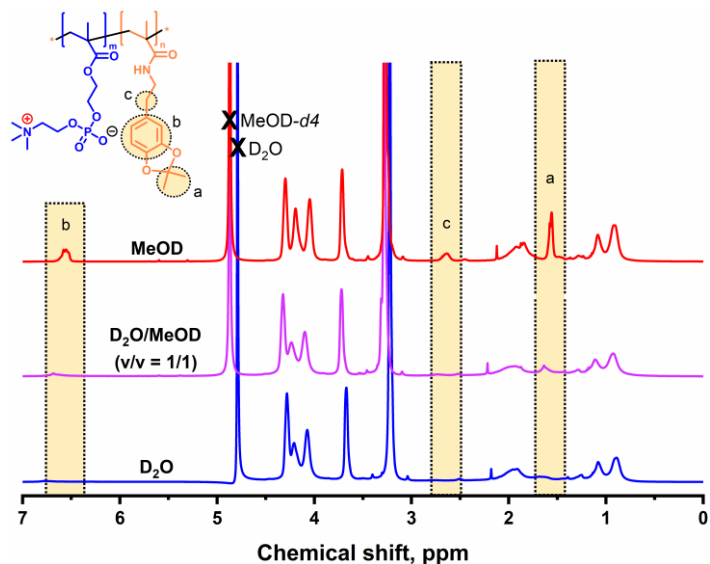
Figure 3.17. ^{1}H NMR spectra of the diblock copolymer pMPC-*b*-pADOPMA in D₂O, MeOD-*d4*/D₂O mixture and MeOD-*d4*. The appearance of chemical shifts characteristic for pADOPMA block (marked in yellow) in MeOD-*d4* containing solutions proved diblock structure of the copolymer.

Trying to substantiate the presence of diblock copolymers, ^{1}H NMR and ^{13}C NMR spectra of the diblock copolymers pMPC-*b*-pADOPMA were recorded in D₂O, MeOD-*d4* and the mixture of these solvents MeOD-*d4*:D₂O (1:1 v/v) (Figure 3.17 and 3.18). Chemical shifts typical for ADOPMA were hardly visible in D₂O, while they appeared in the solvent mixture and had maximal intensity in MeOD-*d4*. Such behavior is characteristic for amphiphilic diblock copolymers in solutions with preferential solvation of one block [234,235].
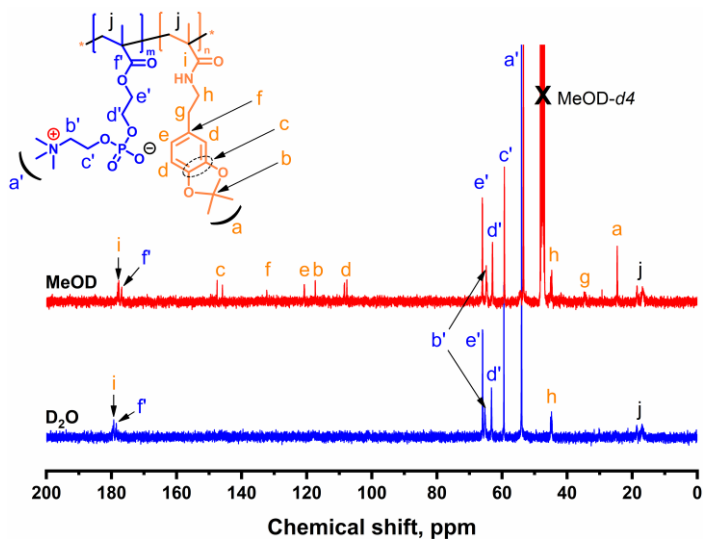
Figure 3.18. ^{13}C NMR spectra of the diblock copolymer pMPC-*b*-pADOPMA in D$_2$O and MeOD-*d4*.

To ascertain possible micellization of the diblock copolymers in aqueous solutions, ^{1}H NMR spectra of the diblock copolymers in D$_2$O solutions at various concentrations were recorded (Figure 3.19). These spectra were then used to calculate the DOPMA (ADOPMA) content in the copolymers (Table 3.8). It was found that the DOPMA (ADOPMA) content calculated from the spectra at concentration of 10 mg/mL of the copolymers was approximately half as much as that calculated from the spectra at concentration of 0.1 mg/mL of the copolymers. Moreover, the calculated ADOPMA content was 3-4 times lower compared to DOPMA content. It is evident that at higher concentration of the copolymers, a significant part of the catechol groups is hindered, as the monomeric units containing catechol groups are situated in the core part of the micelles. The tendency for micellization is much higher for the copolymers with acetonide-protected catechol groups. The extent of micellization of the copolymer with unprotected catechol groups, pMPC-*b*-pDOPMA, at low concentration (0.1 mg/mL) is low, since DOPMA content calculated from ^{1}H NMR spectrum in D$_2$O differ only slightly from that calculated from ^{1}H NMR spectrum in MeOD-*d4*, where the copolymer is fully solubilized (Table 3.8).
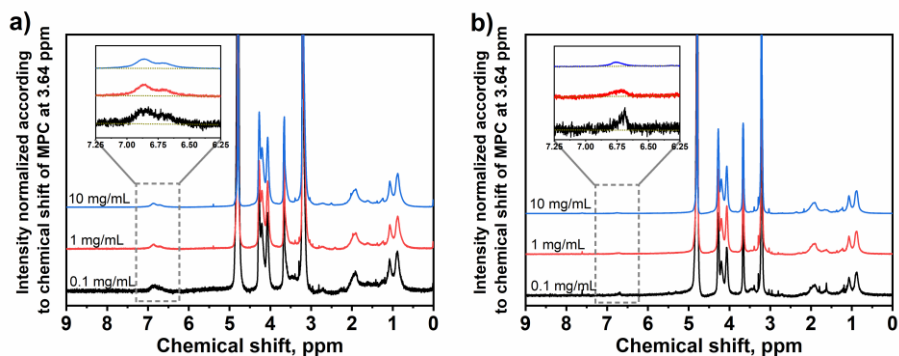
Figure 3.19. ^{1}H NMR spectra of the diblock copolymers with unprotected catechol groups pMPC-*b*-pDOPMA (A) and with acetonide-protected catechol groups pMPC-*b*-pADOPMA (B) in D_2O at various concentrations of the copolymers.

Table 3.8. DOPMA (ADOPMA) content in the copolymers pMPC-*b*-pDOPMA and pMPC-*b*-pADOPMA determined from ^{1}H NMR spectra of the copolymers in D_2O solutions of various concentrations.

Copolymer	Deuterated solvent	Concentration, mg/mL	DOPMA (ADOPMA) content, mol%
pMPC-*b*-pDOPMA	MeOD-*d4*	10	24.1
	D_2O	10	12.6
		1	13.7
		0.1	20.7
pMPC-*b*-pADOPMA	MeOD-*d4*	10	24.1
	D_2O	10	3.1
		1	5.1
		0.1	6.4

Formation of the diblock copolymer with no residual (unreacted) pMPC and side product pADOPMA were confirmed also by particle size distribution (PSD) curves of these polymers in water and methanol (Figure 3.12). pMPC is fully soluble in water and in methanol with particle size less than 5 nanometers. pADOPMA is not soluble in water and only partially soluble in methanol (short length polymers only, not shown in Figure 3.12). Particle size of the diblock copolymer in water is much larger with an average value of about 20 nm, moreover, aqueous solution of the diblock copolymer does not contain any traces of the particles with diameter

less than 5 nm. The diblock copolymer was soluble in methanol but an average value of the particle diameter was evidently larger compared to that of pMPC.

Diblock copolymers with unprotected catechol groups pMPC-*b*-pDOPMA were obtained by removal of acetonide protective groups. ^{1}H NMR spectra confirmed full deprotection of catechol moieties with no side products (Figure 3.12, the disappearance of the acetonide -C(C$\underline{H}_3$)$_2$ signal at 1.5 ppm).

3.2. Properties of zwitterionic copolymers containing MPC units

3.2.1. Hydrophilicity of gradient and diblock copolymers of MPC

It is well known that pMPC is superhydrophilic material with a water contact angle (WCA) of less than 20° [114,236,237]. pPEOMEMA is also hydrophilic and like pMPC is capable of holding water molecules. The hydrophilicity of the copolymers p(MPC-*grad*-PEOMEMA) containing a small and large amount of MPC units was evaluated by measuring WCA on the adsorbed copolymer layers formed on glass slides when these slides were kept immersed in dilute copolymer solutions, then pulled out and dried. The WCA of the bare glass surface is ≈30° [238]. Coating of the glass surface with the copolymers p(MPC-*grad*-PEOMEMA) increases the hydrophilicity shifting WCA of the surface from 35° to as low as 7° (Fig. 3.20). It is worth to mention that the WCA of the copolymers does not depend on copolymer composition and is very low, which means that the copolymers p(MPC-*grad*-PEOMEMA) are superhydrophilic. A comparison of WCA values for pMPC and the copolymers p(MPC-*grad*-PEOMEMA) shows the dominant role of MPC units in determining the hydrophilicity of the copolymers.

Wetting behavior of the adsorbed diblock copolymers of MPC and DOPMA with protected and unprotected catechol groups on gold surface was investigated. The film of the diblock copolymer pMPC-*b*-pDOPMA exhibited a more strongly pronounced hydrophilicity with a contact angle of sessile drop equal to 29°, compared to 54° of the acetonide-protected copolymer pMPC-*b*-pADOPMA (Figure 3.21). After ultrasonic treatment, the wetting angles decreased by nearly 20° of the both copolymers, indicating an additional increase in hydrophilicity. Several processes may explain the observed changes, such as mechanical removal of polymer ad-layers and weakly adsorbed polymer molecules, and reorientation of the adsorbed polymer chains exposing hydrophilic phosphorylcholine head groups to ambient environment.
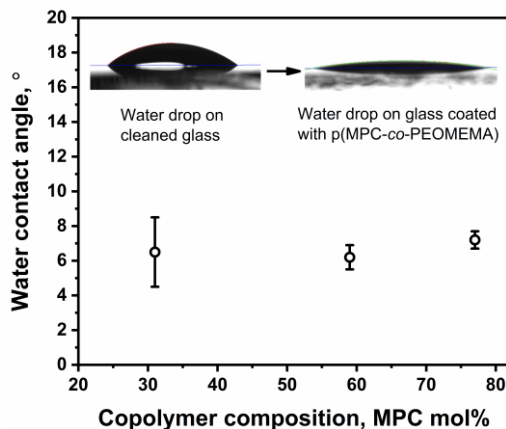
Figure 3.20. Water contact angle of the copolymers p(MPC-*grad*-PEOMEMA). Insert – visualization of the determination of WCA.
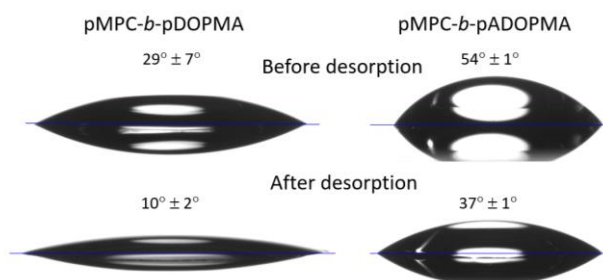
Figure 3.21. Wetting angles of the diblock copolymers of MPC and DOPMA adsorbed on flat gold film before and after desorption with ultrasound in methanol for 15 min.

3.2.2. Surface activity of diblock copolymers of MPC

In order to elucidate the potential surface activity of the diblock copolymers of MPC, surface tension of aqueous solutions of the diblock copolymers of MPC with PEOMEMA and with DOPMA were investigated. The dependence of the surface tension of aqueous solution of the diblock copolymer pMPC-*b*-pADOPMA on the copolymer concentration is presented in Figure 3.22. It was shown that surface tension of the copolymer solution did not change in the concentration range of 0.001 to 0.1 mg/mL, i.e., it remained similar to that characteristic of water. The surface tension started to decrease only at higher copolymer concentrations (0.5-1.0 mg/mL). Thus, it

can be stated that diblock copolymers of MPC and ADOPMA exhibit very weak surface activity. pMPC showed no surface activity which is in accord with previous published data [239,240].
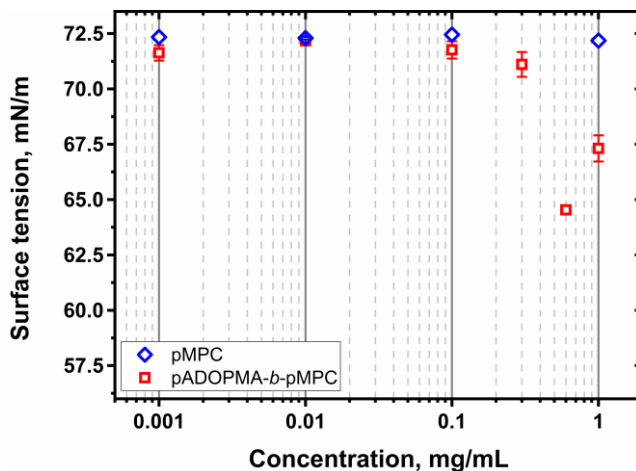
Figure 3.22. Dependence of the surface tension of aqueous solutions of the diblock polymer pMPC-*b*-pADOPMA on copolymer concentration (25 °C).
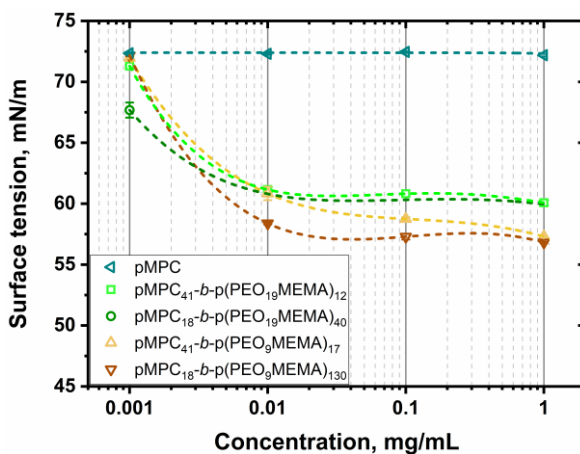
Figure 3.23. Dependence of the surface tension of aqueous solutions of the diblock copolymers pMPC-*b*-pPEOMEMA on copolymer concentration.

The dependence of the surface tension of aqueous solutions of the diblock copolymers pMPC-*b*-pPEOMEMA on copolymer concentration is presented in Fig. 3.23. Upon increasing copolymer concentration from 0.001 to 0.01 mg/mL, surface tension of the copolymer solutions was reduced from 72

mN/m to 58-60 mN/m. Further increase in concentration up to 1 mg/mL yielded negligible alterations in surface tension. A course of the dependences indicated that critical micelle concentration in aqueous solutions of these diblock copolymers is attained at approx. 0.01 mg/mL. Surface tension of the solutions remained almost unaffected by the length of the copolymer blocks, but exhibited a modest dependency on the length of the PEO chain: a more pronounced reduction in surface tension occurred in the solutions of the diblock copolymer with shorter PEO chains (9 monomeric units).

3.2.3. Cononsolvency of the gradient copolymers of MPC and PEOMEMA

It is well known that pMPC exhibits so called cononsolvency, i.e., it is soluble both in water and ethanol, but is insoluble in the mixtures of the above solvents containing 60–92 vol% of ethanol [106,241]. Cononsolvency of pMPC is explained by competitive hydrogen bonding of the solvent and cosolvent with the polymer: in this hydrogen bond competition pMPC side groups prefer water rather than ethanol since water molecules form an ice-like clathrate structure around phosphoryl groups of MPC facilitating the formation of the inner salt [106]. Cononsolvency of the copolymers p(MPC-*grad*-PEOMEMA) was studied by DLS. The solubility of the copolymers was evaluated by measuring the hydrodynamic diameter (D_h) of the particles formed in water, ethanol, and their mixtures. DLS measurements were carried out at various temperatures, which made it possible to evaluate the effect of two factors (solvent and temperature) on solubility, macromolecular size, and aggregation of the copolymers.

Particle size distribution (PSD) curves of the copolymers p(MPC-*grad*-PEOMEMA) containing 32 mol.% and 77 mol.% of MPC units in water and ethanol are presented in Fig. 3.24. Obviously, water and ethanol are good solvents for the copolymers p(MPC-*grad*-PEOMEMA), irrespective of their composition, since the copolymers are at the molecular level with a hydrodynamic diameter of the particles less than 10 nm. Elevation of temperature did not affect the particle size of the copolymers dissolved in pure water, e.g., the particle size of the copolymer p(MPC-*grad*-PEOMEMA) containing 77 mol.% of MPC units remained almost the same: 6.4 ±2.1 nm at 25 °C and 5.7 ±1.3 nm at 65 °C (Figure 3.24). In contrast, the diameter of the particles of the same copolymer dissolved in ethanol was reduced almost twice by increasing the temperature from 25°C (d = 4.3 ±1.2 nm) to 65 °C (d = 2.3 ±0.59 nm). Compactization of the particles at higher temperature indicates that solubilizing power of ethanol is becoming worse under these conditions;

nevertheless, the copolymers are still soluble in ethanol at 65 °C. Solvation of the copolymers p(MPC-*grad*-PEOMEMA) by water is very good and does not depend on temperature.
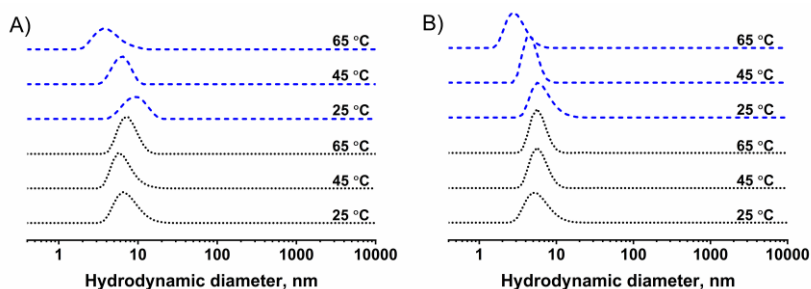
Figure 3.24. PSD curves (by volume) of the copolymers p(MPC-*grad*-PEOMEMA) containing 32 mol% (A) and 77 mol% (B) of MPC units in water (black) and ethanol (blue) at various temperatures.

Solubility of the copolymers in the mixed solvent of water and ethanol with an ethanol content of 20 vol% and 40 vol% was also good, with the particle size diameter of less than 10 nm (Fig. 3.24). Addition of ethanol reduced the hydrodynamic diameter of the particles to 2–4 nm, which evidently shows worse solvating conditions in ethanol-containing solutions. This is in accord with the explanations of the cononsolvency of pMPC based on relatively worse solvating of the polymer by ethanol [106].
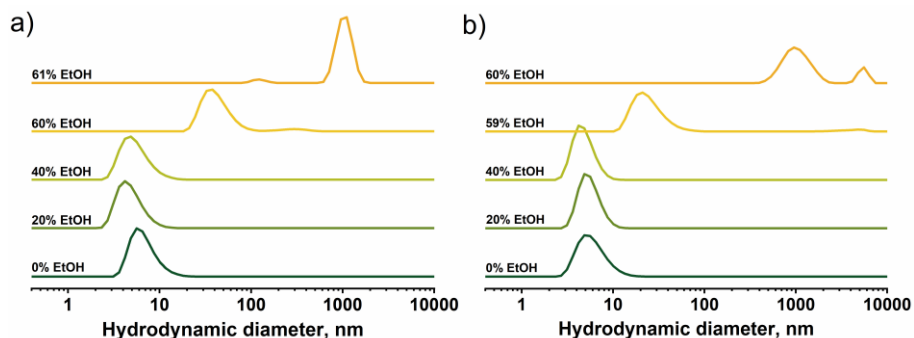
Figure 3.25. PSD curves (by volume) of the copolymer p(MPC-*grad*-PEOMEMA) containing 32 mol.% (a) and 77 mol.% (b) of MPC units in water and water-ethanol mixtures.
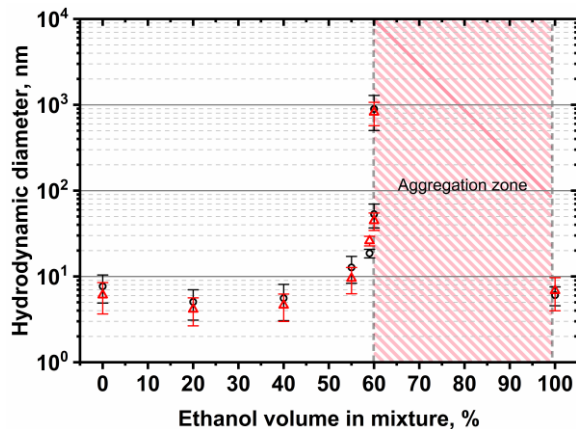
Figure 3.26. Cononsolvency of the copolymers p(MPC-*grad*-PEOMEMA) containing 32 mol.% (○) and 77 mol.% (△) of MPC units in mixtures of water and ethanol.

In the mixed solutions containing about 60 vol% of ethanol, aggregation of the copolymers p(MPC-*grad*-PEOMEMA) occurs, which is reflected in a sharp increase in particle size (Fig. 3.25). In this case, there is a slight difference between the copolymers, containing large (77 mol.%) and small (32 mol.%) amount of MPC units: the copolymers with a large amount of MPC units begin to aggregate when ethanol content in the mixed solvent is 59 vol%, while the copolymers with small amount of MPC units – when ethanol content is 60 vol%. At such compositions of the mixed solvent, small but stable (micellar?) aggregates are formed (d = 20-40 nm), which are converted to large aggregates (d > 800 nm) at higher content of ethanol in the mixed solvent. The summary of cononsolvency and aggregation zone is demonstrated in Figure 3.26.

3.2.4. Solubility and aggregation of the diblock copolymers of MPC

PSD curves of the diblock copolymers of MPC and DOPMA with acetonide-protected and deprotected catechol groups PMA in water and methanol are presented in Figure 3.27. The diblock copolymer pMPC-*b*-pADOPMA was completely soluble in methanol (d = 4-5 nm), partially soluble in methanol-water mixture, and a formed of micellar aggregates in water (10-40 nm). The profile of particle size did not significantly change upon increasing the temperature up to 65 °C. The diblock copolymer with unprotected catechol groups pMPC-*b*-pDOPMA, despite its higher hydrophilicity, formed aggregates (30-200 nm) in methanol, water and

mixtures of methanol and water. Interestingly, increasing the temperature made this copolymer soluble in water. Likely, aggregates formed through interactions of catechol hydroxyl groups, were disrupted at elevated temperatures.
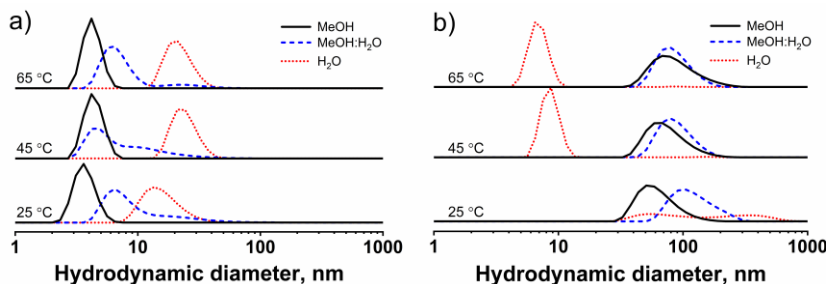
Figure 3.27. PSD curves of the diblock copolymers pMPC-*b*-pADOPMA (a) and pMPC-*b*-pDOPMA (b) in methanol, methanol-water mixture and water.

Figure 3.28 presents PSD curves of gradient and diblock copolymers of MPC and PEOMEMA. These copolymers were fully soluble in water and ethanol. An increase in temperature did not affect solubility of the copolymers in water but made copolymer coils more compact in ethanol indicating worse solubilizing conditions. Good solubility of the diblock copolymers of MPC and PEOMEMA in water and ethanol means that solvation of the both blocks are similar which impedes formation of larger aggregates.
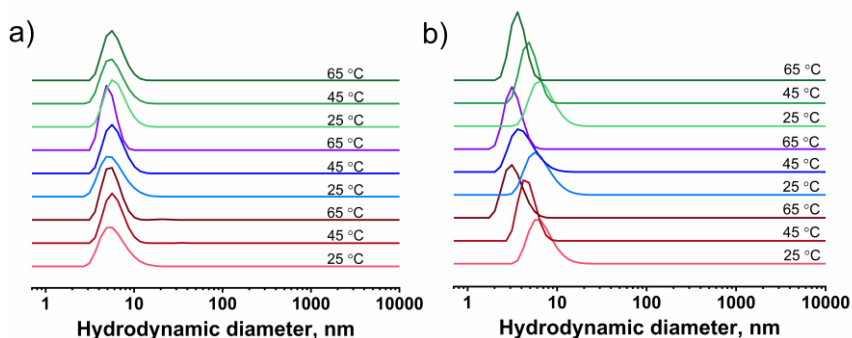
Figure 3.28. PSD curves of the copolymers p(MPC-*grad*-pPEOMEMA) (red palette), pMPC-*b*-pPEO$_{19}$MEMA (blue palette) and pMPC-*b*-pPEO$_9$MEMA (green palette) in water (a) and ethanol (b) at different temperatures.

3.3. Aqueous lubrication by diblock and gradient copolymers of MPC and PEOMEMA

Characteristics of the (co)polymers used in tribology tests are presented in Table 3.9. In short, the set of polymers includes homopolymers pMPC and p(PEO$_{19}$MEMA), two block copolymers containing p(PEO$_{19}$MEMA) block – one with relatively long pMPC block pMPC-*b*-p(PEO$_{19}$MEMA)-1 and another with relatively short pMPC block pMPC-*b*-p(PEO$_{19}$MEMA)-2, block copolymer pMPC-*b*-p(PEO$_9$MEMA) with relatively long pMPC block, and gradient copolymer pMPC-*grad*-p(PEO$_{19}$MEMA).

Table 3.9. Characteristics of the (co)polymers of MPC and PEOMEMA used in tribology tests.

(Co)polymer	Copolymer composition, MPC mol%	M_n from SEC, kDa	Đ	DP (first block DP + second block DP
pMPC	100	23.3	1.10	41
p(PEO$_{19}$MEMA)	0	59.1	1.37	62
pMPC-*b*-p(PEO$_{19}$MEMA)-1	77.4	31.8	1.33	41 + 12
pMPC-*b*-p(PEO$_{19}$MEMA)-2	31.0	47.6	1.57	18 + 40
pMPC-*b*-p(PEO$_9$MEMA)	70.7	31.5	1.38	41 + 17
pMPC-*grad*-p(PEO$_{19}$MEMA)	59.8	49.9	1.41	69

For determination of the proper concentration of the copolymers of MPC and PEOMEMA for articular cartilage lubrication, the PDMS-glass tribological tests were performed before cartilage plug-glass tribological measurements. Figure 3.29 presents the results of PDMS-glass system which is placed in PBS solutions of the copolymers of MPC and PEOMEMA.

Figure 3.29a presents the dependence of the dynamic COF on concentration of various MPC-PEOMEMA copolymers, and Figure 3.29b compares the values of COF obtained at the copolymer concentration 0.4 mg/mL. All solutions except pure PBS (control) gave rise to the reduction of COF while increasing the concentration up to 0.4 mg/mL. PBS was not able to lubricate the PDMS and glass interface; COF of the PBS solution was rather stable and was around 0.413 ± 0.067 (Figure 3.29b). The best lubrication was provided by the copolymer of gradient structure p(MPC-*grad*-PEO$_{19}$MEMA); COF at concentration of the copolymer 0.4 mg/mL was lowered by 100 folds to 0.004 ± 0.002. Slightly higher value of COF (0.007 ± 0.002) was observed

for the diblock copolymer with relatively long pMPC block pMPC-*b*-(PEO$_{19}$MEMA)-1.
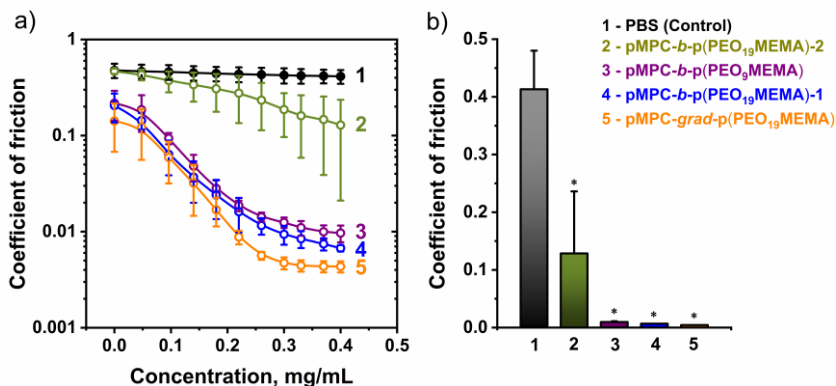
Figure 3.29. Dynamic COF of PDMS-glass in PBS solutions of MPC and PEOMEMA copolymers; (a) COF as a function of the copolymer concentration; (b) COF at the copolymer concentration in PBS solution 0.4 mg/mL. The error bars show the standard deviation (n = 3); $^*p < 0.5$ compared with control group.

Lubricating effect of the diblock copolymer with relatively short pMPC block pMPC-*b*-(PEO$_{19}$MEMA)-2 was significantly lower expressed by much higher value of COF (0.088 ± 0.125). Length of PEO chain had little effect on lubricating properties of the copolymers: replacement of the diblock copolymer pMPC-*b*-(PEO$_{19}$MEMA)-1 by the diblock copolymer of similar structure but with shorter PEO chain pMPC-*b*-(PEO$_9$MEMA) gave rise COF value from 0.007± 0.002 to 0.010 ± 0.006. Thus, all tested copolymers of MPC and PEOMEMA possessed good anti-friction properties but the best lubrication was provided by the copolymers containing large amount of MPC units. At concentrations of the copolymers higher than 0.4 mg/mL, a decrease of COF was slow and negligible. We chose 0.4 mg/mL as the optimal copolymer concentration for the following osteochondral plug lubricating measurement.

Figure 3.30 presents results of dynamic COF at the cartilage plug – glass interface. COF for all the samples showed an increasing trend over time (Figure 3.30a), especially for the control (PBS). This is in accordance with interstitial fluid pressurization and weeping (IFPW) mechanism of cartilage [206,242,243], the experimental proof of which was provided by Ateshian et al [244]. In the presence of PBS (control), the COF after 450 cycles was observed to be 0.480 ± 0.048.
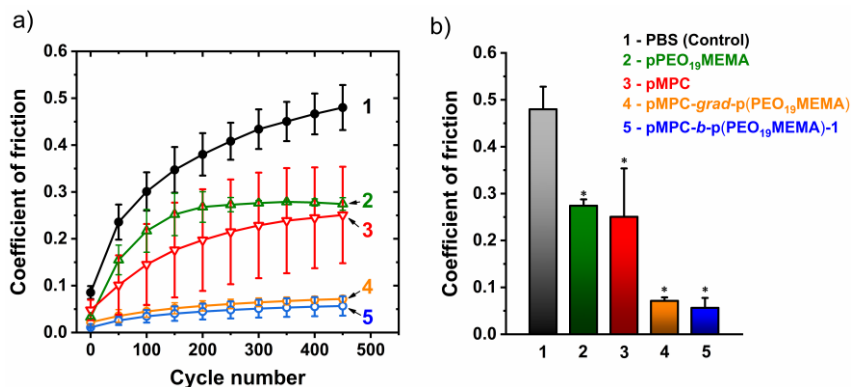
Figure 3.30. Dynamic COF of cartilage-glass in PBS solutions of pMPC, p(PEO$_{19}$MEMA) and MPC-PEOMEMA copolymers at the concentration 0.4 mg/mL: (a) COF as a function of the cycle number; (b) COF at the cycle number 450. The error bars show the standard deviation (n = 3); $^*p < 0.5$ compared with control group.

pMPC, pPEOMEMA and the copolymers used in this study are expected neither to interfere with the fluid pressurization in the cartilage nor with the weeping of the fluid from the cartilage. Since all of these are surface active molecules, we can expect them to show an effect when there is substantial solid-solid contact between cartilage and glass, i.e. in the later period of sliding. COF values of pMPC and p(PEO$_{19}$MEMA) after 450 cycles were 0.251 ± 0.103 and 0.274 ± 0.014, respectively, which is almost half as compare to the control situation (PBS). Rather high COF value of p(PEO$_{19}$MEMA) is in accord with previous observations [118] that neutral brushes of poly(ethylene oxide) in aqueous media provide rather weak lubrication. pMPC being attached to surfaces usually provides excellent lubrication (is characterized by very low COF value) [126]. On the other hand, pMPC homopolymer, dissolved in water and in aqueous PBS or NaCl solutions, even at high polymer concentration, demonstrates satisfactory but not nearly good lubrication [245]. Exclusively good lubrication of cartilage was provided by the copolymers p(MPC-*grad*-PEO$_{19}$MEMA) and pMPC-*b*-p(PEO$_{19}$MEMA)-1; no increase in COF was observed after 450 cycles as COF at the end increased only to 0.072 ± 0.007 and 0.057 ± 0.021, respectively, which was 7 to 8 folds lower than that in the control test (PBS, 0.480 ± 0.048). Thus, a clear synergistic lubrication effect of MPC and PEO segments in the copolymers is demonstrated.

The best lubrication, both between PDMS–glass and cartilage–glass, was provided by the diblock copolymer pMPC-*b*-p(PEO$_{19}$MEMA)-1 and gradient

copolymer p(MPC-*grad*-PEO$_{19}$MEMA). Both copolymers are rich in MPC units and contain long PEO side chains. One should note that the copolymer p(MPC-*grad*-PEO$_{19}$MEMA) possess strongly expressed gradient microstructure which means that at one end polymer molecules are rich in MPC units and at another end in PEO$_{19}$MEMA units. In other words, microstructure of the copolymer p(MPC-*grad*-PEO$_{19}$MEMA) somewhat resembles to that of the diblock copolymer pMPC-*b*-p(PEO$_{19}$MEMA). We suppose, exclusively good lubricating behaviour of these two copolymers depends on several factors including sufficient amount of MPC units and similar microstructure of the macromolecules.

Trying to answer the question, why lubricating effect of the diblock and gradient copolymers of MPC and PEO$_{19}$MEMA is significantly larger compared to that of the corresponding homopolymers pMPC and p(PEO$_{19}$MEMA), we should refer to the lubrication mechanisms of these polymers and possibilities to adsorb on contacting surfaces. Excellent lubricating properties of MPC polymers are explained by hydration lubrication according to which water molecules within hydration shells surrounding zwitterionic groups are firmly attached but are at the same time very fluid, thus serving as efficient lubricating layers [118]. One should note that excellent lubrication is provided by pMPC brushes [114,126] but not by pMPC homopolymer [245]. pMPC molecules are neutral (phosphate and ammonium groups form inner salt [106]) and likely have small affinity to negatively charged glass surface. Such presumption is based on recent findings that internal phosphoryl groups of pMPC are partially (ca 10 %) protonated [246]. Lubrication by PEOMEMA brush polymers, usually called boundary lubrication [205], is due to the effect of the steric repulsive forces between the polymer chains and water molecules that maintain a thin lubricating fluid layer at the interfacial region between the sliding surfaces. It is known [247] that pPEOMEMA homopolymer has the ability to attach to silica surface through the side chain segments forming hydrogen bonds. Stronger adsorption of the bottle-brush polymer compared to PEO homopolymer was explained by higher surface affinity and smaller loss in conformational entropy upon adsorption.

Based on information presented above we propose hypothesis explaining very good lubrication in the solutions of diblock and gradient copolymers of MPC and PEO$_{19}$MEMA. Likely, diblock copolymers initially adsorb preferentially parallel to the surface with both the pMPC block and the bottle-brush p(PEO$_{19}$MEMA) block in contact with the surface. This idea is borrowed from studies presenting adsorption of the diblock copolymers consisting of a cationic block and non-ionic bottle-brush block [213], and

diblock copolymers consisting of a pDOPMA block and pMPC block. However, as adsorption proceeds, because of higher surface affinity, PEO$_{19}$MEMA segments are replacing MPC segments at the surface, and this results in a transformation of the layer structure. During this transformation, the PEO chains are accumulated at the surface and the pMPC chains are extended away from the surface. Thus, it is expected, that brush-like layers of pMPC are formed on glass surfaces providing hydration lubrication.

3.4. Adsorption dynamics of diblock copolymers pMPC-*b*-pADOPMA and pMPC-*b*-pDOPMA on gold surface

Diblock copolymers pMPC-*b*-pADOPMA and pMPC-*b*-pDOPMA with DP of pMPC block 41 and DP of pADOPMA (pDOPMA) block 13 were used for adsorption on gold surface. The adsorption behavior of the diblock copolymers on gold surface was investigated using various infrared spectroscopy techniques, namely, attenuated total reflection (ATR) FTIR, surface-enhanced infrared absorption spectroscopy (SEIRAS), and reflection absorption infrared spectroscopy (RAIRS). Vibrational marker bands specific to acetonide-protected and deprotected dopamine methacrylamide were determined using ATR-FTIR of the methanol-dissolved homopolymers pDOPMA and pADOPMA (Figure 3.31). The assignment is based on literature [248–257], the H/D exchange experiment, and DFT calculations [258].
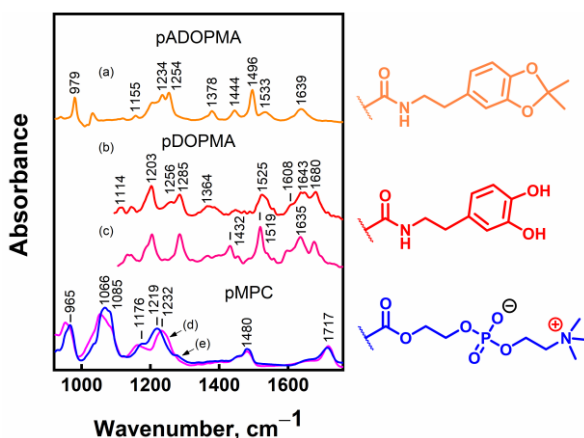
Figure 3.31. ATR-FTIR spectra of pADOPMA (M$_n$ 19.1 kDa, Đ 1.15, DP 73) dissolved in CH$_3$OH (a), pDOPMA in CH$_3$OH (b) and MeOD-*d4* (c), powder pMPC (M$_n$ 23300, Đ 1.10, DP 41) (d), and pMPC dissolved in water (e). The solvent spectra are subtracted. At right, top to bottom, fragments of acetonide-

protected dopamine in pADOPMA, dopamine in pDOPMA, and phosphorylcholine in pMPC.

The pMPC unit comprises a phosphorylcholine head group, whose characteristic spectral bands at 1080 and 1230 cm^{-1} are assigned to symmetric and asymmetric phosphate group stretching, respectively. The asymmetric stretching $\nu_{as}(PO_2)$ is highly sensitive to hydration level and may vary as much as 30 cm^{-1} in frequency (Figure 3.31d and e) [251,252].

Figure 3.31 shows the spectral developments in the 1200–1600 cm^{-1} range associated with adsorption of the copolymers on the gold surface. Given the 3.5:1 molar ratio between the units of MPC and DOPMA in the copolymers, the SEIRAS spectra should predominantly feature MPC bands, specifically, $\nu_{as}(PO_2)$ near 1230 cm^{-1} and C–H deformation motion near 1480 cm^{-1}. However, that is not the case as the spectra are populated with DOPMA-specific bands near 1255, 1284, 1369, and 1529 cm^{-1}, indicating that interaction between the copolymer and gold primarily ensues through the catechol –OH groups and not phosphorylcholine. In fact, the phosphate spectral mode is vanishingly weak, and thus the PO$_2$ groups are likely to be positioned at a distance from the surface. Time-resolved SEIRAS spectra indicate that the main adsorption and molecular reorientation occur approximately for the first 10 minutes, followed by modest intensity gain and slight wavenumbers shift. A clearer picture emerges from the difference spectrum of 60 min minus 1 min, which shows a concurrent intensity increase of DOPMA-related 1280 cm^{-1} and a decrease of MPC-related C–H deformation at 1481 cm^{-1}. Spectral data indicate that at the first adsorption stage (first 1 min), zwitterionic pMPC units are predominantly located near the gold surface; at the second adsorption stage (2–16 min), reorientation of the diblock copolymers proceeds at the surface resulting in positioning the pDOPMA block directly to the surface. A shift of $\delta(COH)$ from 1380 cm^{-1} at 4 min to 1369 cm^{-1} at 60 min suggests establishing stronger catechol hydrogen-bond interaction with the gold surface.
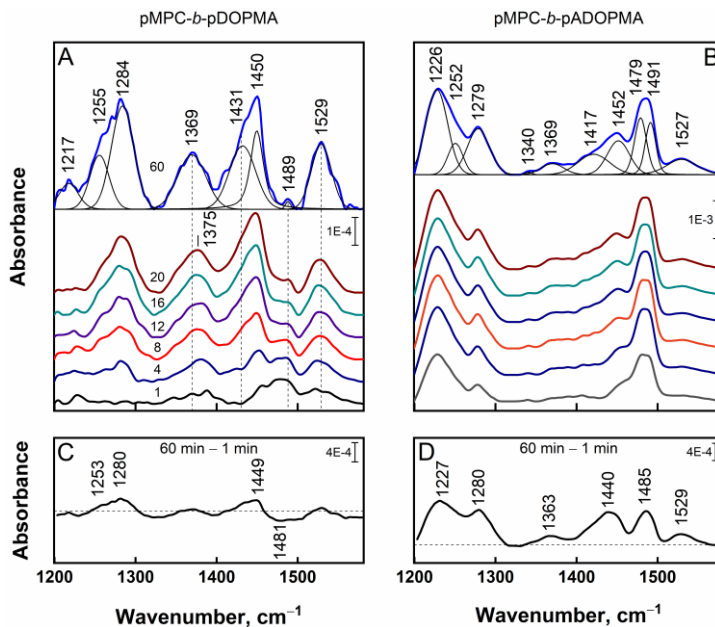
Figure 3.32. (A, B) Time-dependent SEIRAS spectra of the diblock copolymers pMPC-*b*-pDOPMA and pMPC-*b*-pADOPMA adsorbed to gold surface in H_2O. Incubation time in minutes is indicated above the corresponding spectrum. 60-min spectra are deconvoluted using Gaussian-Lorentzian shape components. (C, D) Difference spectra of 60-min minus 1-min.

Figure 3.32 B, D presents time-resolved spectra related to surface-adsorption of acetonide-protected diblock copolymers pMPC-*b*-pADOPMA. Here the PO_2-related spectral mode appears as a strong feature near 1226 cm^{-1} and indicates phosphorylcholine's close proximity to the gold surface and possible bonding. The pADOPMA could be recognized from 1252, 1491, and 1527 cm^{-1} peaks. These modes remain intense and show minimal time-dependent variability. Notable is a medium intensity feature near 1279 cm^{-1} characteristic for the catechol group without acetonide protection. Its intensity tends to increase with time, evidenced by the positive feature in the difference spectrum. We interpret this mode as evidence of the spontaneous deprotection of some pADOPMA units when they come into contact with a pristine nanostructured gold surface.

The catechol state in the copolymer, either acetonide-protected or deprotected, strongly affects adsorption dynamic. Figure 3.33 shows the spectral modes' intensity evolutions and fitted Langmuir-Freundlich isotherm.

Notably, the intensity evolution is much faster for the acetonide-protected copolymer. The strongest surface-affinity of the diblock copolymer pMPC-*b*-pADOPMA is recognized of PO_2 (1226 cm^{-1}) and protected catechol group (1485 cm^{-1}). The diblock copolymer with unprotected catechol groups pMPC-*b*-pDOPMA, on the other hand, adsorbed with less acceleration. Interestingly, the 1370 cm^{-1} (COH deformation) mode's intensity starts to decline following 50 minutes of incubation. We presume the cleavage of the CO–H bond and subsequent covalent bonding to gold (Au–O). Furthermore, the pMPC block associated-1489 cm^{-1} mode, initially dominant, diminishes during the first 20 minutes. Surprisingly, no modes associated with PO_2 vibrations – a component of the pMPC block – are detected at any given time during adsorption. Such complex behavior might illustrate reorientation and competing interactions between pMPC and pDOPMA blocks for the possible adsorption on gold and perhaps unfavored orientation for SEIRAS of some polymer moieties.
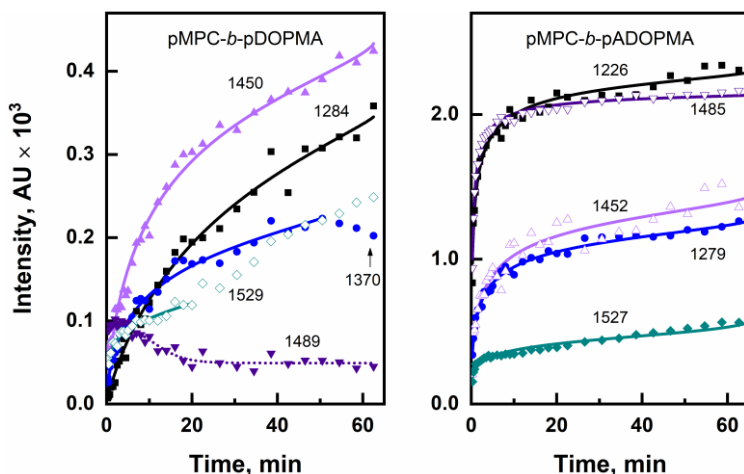
Figure 3.33. Temporal evolution of selected SEIRAS spectral band intensities of the diblock copolymers pMPC-*b*-pDOPMA and pMPC-*b*-pADOPMA. Experimental data are approximated with modified Langmuir-Freundlich isotherm (solid lines).

Desorption of the diblock copolymers pMPC-*b*-pDOPMA and pMPC-*b*-pADOPMA from a 150-nm magnetron sputtered gold film was performed in an ultrasonic bath in methanol for 15 min, followed by thorough rinsing. Reflection absorption infrared spectroscopy (RAIRS) data were recorded before and after the desorption (Figure 3.34). Both aspects – removal and reorientation of molecules – may contribute to the RAIRS spectra, because

intensity of the RAIRS signal depends on the amount of material and surface selection rule (dipole orientation with respect to surface determines spectral mode intensity). We found 66% reduction in the area under the curve within the 750–1800 cm^{-1} range for the acetonide-protected copolymer and only a 29% reduction for the copolymer with unprotected catechol groups. Thus, less material was removed from the surface for the copolymer with unprotected catechol groups as it has higher extent of surface-active sites (catechol group and phosphorylcholine head group).
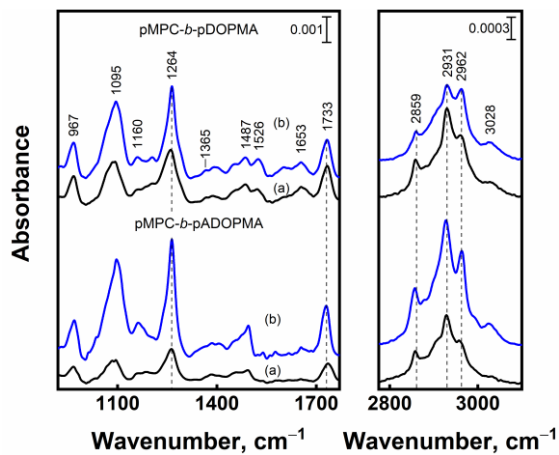
Figure 3.34. RAIRS spectra of the gold surface with adsorbed diblock copolymers before (b) and after (a) ultrasonication in methanol for 15 min.

The intensity of ν(=C–H) mode at 3028 cm^{-1} is sensitive to benzene ring orientation. The integral intensity decrease (with respect to integral intensity of the 2750–3200 cm^{-1} range) was only 15% for the copolymer pMPC-*b*-pDOPMA and 45% for the copolymer pMPC-*b*-pADOPMA. This observation attests the maintained orientation of unprotected catechol on a gold surface, and more flexible orientation of the protected catechol. The relative intensity of ν_s(CH$_2$) and ν_{as}(CH$_2$) bands at 2859 and 2931 cm^{-1}, respectively, increases after ultrasonication procedure; while the relative intensity of ν_{as}(CH$_3$) and ring ν(=C–H) modes at 2962 and 3028 cm^{-1}, respectively, decreases after sonication, indicating preservation of more flat orientation of ring group at the surface for the adsorbed copolymer pMPC-*b*-pDOPMA. In the case of the copolymer with acetonide-protected catechol groups pMPC-*b*-pADOPMA, all the bands in high frequency spectral region (2800–3100 cm^{-1}) considerably decrease in intensity indicating different adsorption state of the copolymer.

Wetting properties of the diblock copolymer pMPC-*b*-pDOPMA adsorbed on nanostructured gold and its acetonide-protected counterpart were studied using SEIRAS under an external electric potential. Figure 3.35 shows the dependency of spectral intensity of O–H stretching vibrational mode of the polymer-proximal water in the two cycles of potential cycling. Over the whole potential window, the copolymer with unprotected catechol groups shows the capacity to attract water molecules with the extent far greater compared to the copolymer pMPC-*b*-pADOPMA. Such an observation aligns with temporal SEIRAS evolution and contact angle measurements that suggested exposure of phosphorylcholine groups to the environment. Water near the copolymer pMPC-*b*-pADOPMA, on the other hand, shows little sensitivity to potential and is distanced from the surface at mostly all potentials tested. For pMPC-*b*-pADOPMA, a frequency upshift of 40–50 cm^{-1} was observed for water band components at –0.4 V, suggesting the potential-induced withdrawal of water molecules engaged in weaker hydrogen bonding [259,260].
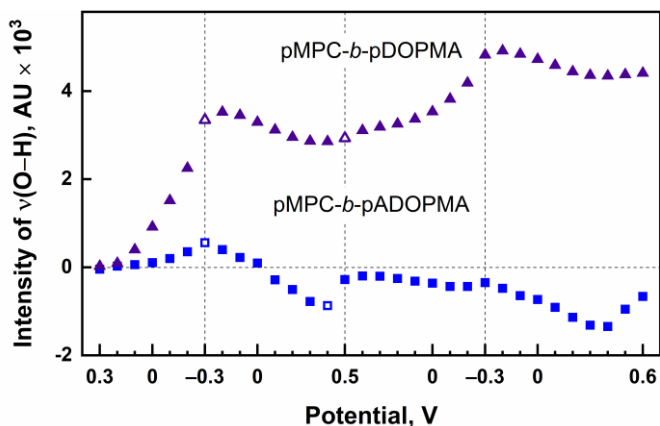
Figure 3.35. Dependence of ν(O–H) integral intensity of water on electric potential with respect to Ag/AgCl reference electrode for the gold surface with adsorbed diblock copolymers pMPC-*b*-pDOPMA and pMPC-*b*-pADOPMA. Potential limits are marked by dashed vertical lines.

In conclusion, SEIRAS and contact angle measurements demonstrate that, under varying external electric potentials, the copolymer with unprotected catechol groups pMPC-*b*-pDOPMA significantly outperforms its acetonide-protected counterpart in attracting water molecules, likely due to the exposed phosphorylcholine groups.
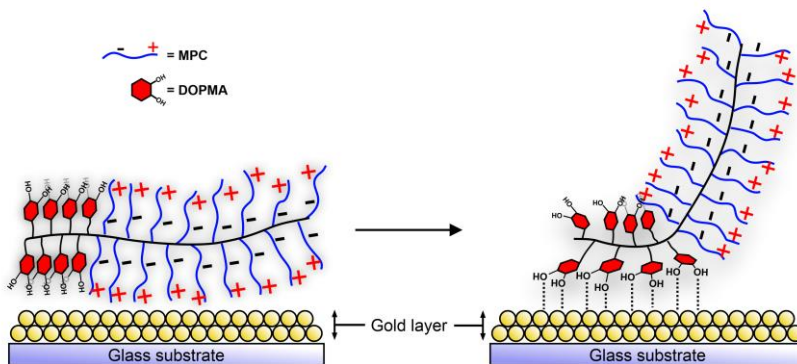
Figure 3.36. Schematic illustration of the time evolution of structure of the block copolymers pMPC-*b*-pDOPMA on the gold surface during the adsorption process.

By combining ATR-FTIR, SEIRAS and RAIRS spectroscopy, it was demonstrated that the adsorption of the diblock copolymers pMPC-*b*-pDOPMA on gold surface is a prolonged process. At the first adsorption stage, zwitterionic phosphorylcholine groups are predominantly located near the gold surface but later reorientation of the diblock copolymers proceeds at the surface resulting in positioning the pDOPMA block directly to the surface. These data indirectly indicate that in adsorbed layers of the diblock copolymers pMPC-*b*-pDOPMA, the block of pMPC is likely extended into the bulk forming highly hydrated layer (Figure 3.36). Such vision is in accord with previous studies showing excellent swelling of surface-anchored pMPC chains, which was demonstrated by increased root-mean-square roughness of the coated surface upon pre-wetting with pure water immersion [98]. It was confirmed by AFM examination, that surface hydrophilicity was enhanced by orientation of zwitterionic units of the pMPC block towards the aqueous phase [98].

Conclusions

1. Kinetics of the RAFT copolymerization of the zwitterionic monomer 2-methacryloyloxyethyl phosphorylcholine (MPC, M_1) with the macromonomer PEO methacrylate with medium-length PEO chain (PEOMEMA, M_2) was studied by ^{1}H NMR spectroscopy and size exclusion chromatography (SEC). The dependences of average (cumulative) copolymer composition on conversion of the monomers differed significantly from that calculated by the terminal model of free-radical copolymerization based on reactivity ratios of the monomers determined experimentally $r_1 = 2.48$ and $r_2 = 0.40$. The copolymers p(MPC-*grad*-PEOMEMA) possessed strongly expressed gradient microstructure, even those synthesized up to medium conversion of the monomers. Despite gradient microstructure, molecular weight dispersity of the copolymers was moderately low (Đ < 1.3), and molecular weight was close to that predicted theoretically.

2. Hydrophilic diblock brush copolymers containing both phosphorylcholine groups and PEO side chains were synthesized by successive RAFT polymerization of the zwitterionic monomer MPC and PEO-containing macromonomer PEOMEMA. The first block of pMPC was characterized by very low molecular weight dispersity (Đ ≤ 1.1) while molecular weight dispersity of the diblock copolymers was not low but reasonable, usually about 1.3–1.6. Degree of polymerization of the second block was controllable and varied between 10 and 70.

3. Amphiphilic diblock copolymers pMPC-*b*-pDOPMA containing a block of pMPC with unique properties to prevent nonspecific protein adsorption and enhance lubrication in aqueous media, and a block of pDOPMA distinguished by excellent adhesion performance were synthesized by RAFT polymerization. The DOPMA monomer with acetonide-protected catechol group (ADOPMA) was used for the synthesis, allowing the prevention of undesirable side reactions during polymerization and preserving the synthesized copolymers from oxidation during storage. The diblock structure of the copolymers was substantiated by ^{1}H NMR and ^{13}C NMR spectra as well as by DLS particle size distribution curves of the copolymers with protected and unprotected catechol groups in various solvents.

4. In mixed solutions of ethanol and water, the phenomenon of cononsolvency is observed for hydrophilic gradient and diblock copolymers of MPC and PEOMEMA. Gradient copolymers p(MPC-*grad*-PEOMEMA), irrespective of composition, show evident superhydrophilicity with a water contact angle

about 7°, while diblock copolymers pMPC-*b*-pPEOMEMA exhibit surface activity in aqueous solutions with critical micellization concentration 0.01 mg/mL. Amphiphilic diblock copolymers of MPC and DOPMA are soluble in methanol but undergo micellization in aqueous solutions.

5. Lubricating effect of the diblock and gradient copolymers of MPC and PEOMEMA was evaluated by tribological measurements in the systems PDMS–glass and cartilage–glass. The best lubrication was provided by the copolymers with relatively large amount of MPC units. Average dynamic coefficient of friction (COF) in the system PDMS–glass at concentration of the copolymers 0.4 mg/mL was only 0.004–0.007, while COF values of the copolymers in the system cartilage-glass after 450 cycles of sliding 0.06–0.07. Excellent lubricating effect of the diblock and gradient copolymers of MPC and PEOMEMA was explained by preferential adsorption of PEOMEMA segments resulting in brush-like layers of pMPC on glass surfaces providing hydration lubrication.

6. Adsorption behavior of the diblock copolymers pMPC-*b*-pADOPMA and pMPC-*b*-pDOPMA on gold surfaces was investigated using various infrared spectroscopy techniques, namely, ATR-FTIR, SEIRAS, and RAIRS. The copolymer with acetonide-protected catechol groups pMPC-*b*-pADOPMA exhibited rapid and intense physisorption with significant ultrasound-induced desorption. In contrast, the copolymer with unprotected catechol groups pMPC-*b*-pDOPMA exhibited chemical adsorption characteristics, evidenced by slower adsorption dynamics, stronger interaction during desorption, and notable spectral shifts.

7. Spectral data indicate that at the first adsorption stage, zwitterionic phosphorylcholine groups are predominantly located near the gold surface, but later the reorientation of the diblock copolymers proceeds at the surface, resulting in positioning the pDOPMA block directly to the surface. SEIRAS measurements under varying electric potentials and water contact angle analysis revealed abundant exposure of phosphorylcholine groups, indicating superior hydrophilicity and water molecule attraction. These findings indirectly indicate that in adsorbed layers of the diblock copolymers pMPC-*b*-pDOPMA, the block of pMPC is likely extended into the bulk, forming a highly hydrated layer.

REFERENCES

[1] J.H. Quastel, Membrane Structure and Function, Science (80). 158 (1967) 146–161. https://doi.org/10.1126/science.158.3797.146.

[2] K. Ishihara, Successful Development of Biocompatible Polymers Designed by Natures Original Inspiration, Procedia Chem. 4 (2012) 34–38. https://doi.org/10.1016/j.proche.2012.06.005.

[3] X. Yu, Z. Liu, J. Janzen, I. Chafeeva, S. Horte, W. Chen, R.K. Kainthan, J.N. Kizhakkedathu, D.E. Brooks, Polyvalent choline phosphate as a universal biomembrane adhesive, Nat. Mater. 11 (2012) 468–476. https://doi.org/10.1038/nmat3272.

[4] K. Ishihara, W. Chen, Y. Liu, Y. Tsukamoto, Y. Inoue, Cytocompatible and multifunctional polymeric nanoparticles for transportation of bioactive molecules into and within cells, Sci. Technol. Adv. Mater. 17 (2016) 300–312. https://doi.org/10.1080/14686996.2016.1190257.

[5] J. Liu, J.C. Conboy, Structure of a Gel Phase Lipid Bilayer Prepared by the Langmuir−Blodgett/Langmuir-Schaefer Method Characterized by Sum-Frequency Vibrational Spectroscopy, Langmuir. 21 (2005) 9091–9097. https://doi.org/10.1021/la051500e.

[6] M. Mukai, D. Ihara, C.-W. Chu, C.-H. Cheng, A. Takahara, Synthesis and Hydration Behavior of a Hydrolysis-Resistant Quasi-Choline Phosphate Zwitterionic Polymer, Biomacromolecules. 21 (2020) 2125–2131. https://doi.org/10.1021/acs.biomac.0c00120.

[7] T. Goda, K. Ishihara, Y. Miyahara, Critical update on 2-methacryloyloxyethyl phosphorylcholine (MPC) polymer science, J. Appl. Polym. Sci. 132 (2015) 41766.
https://doi.org/10.1002/APP.41766.

[8] A.L. Lewis, Z.L. Cumming, H.H. Goreish, L.C. Kirkwood, L.A. Tolhurst, P.W. Stratford, Crosslinkable coatings from phosphorylcholine-based polymers, Biomaterials. 22 (2001) 99–111. https://doi.org/https://doi.org/10.1016/S0142-9612(00)00083-1.

[9] M. Singh, N. Tarannum, Polyzwitterions, in: Eng. Biomater. Drug Deliv. Syst., Elsevier, 2018: pp. 69–101. https://doi.org/10.1016/B978-0-08-101750-0.00004-0.

[10] Q. Shao, S. Jiang, Molecular Understanding and Design of Zwitterionic Materials, Adv. Mater. 27 (2015) 15–26.
https://doi.org/10.1002/adma.201404059.

[11] E. Campaigne, The contributions of Fritz Arndt to resonance theory, J. Chem. Educ. 36 (1959) 336. https://doi.org/10.1021/ed036p336.

[12] T. Alfrey, H. Morawetz, E.B. Fitzgerald, R.M. Fuoss, Syhthetic electrical analog of proteins, J. Am. Chem. Soc. 72 (1950) 1864–1864. https://doi.org/10.1021/ja01160a532.

[13] Y. Itoh, K. Abe, S. Senoh, Solution and membrane properties of zwitterionic polymers, Die Makromol. Chemie. 187 (1986) 1691–1697. https://doi.org/10.1002/macp.1986.021870713.

[14] J.A. Hayward, D. Chapman, Biomembrane surfaces as models for polymer design: the potential for haemocompatibility, Biomaterials. 5 (1984) 135–142. https://doi.org/10.1016/0142-9612(84)90047-4.

[15] K. Ishihara, R. Aragaki, T. Ueda, A. Watenabe, N. Nakabayashi, Reduced thrombogenicity of polymers having phospholipid polar groups, J. Biomed. Mater. Res. 24 (1990) 1069–1077. https://doi.org/10.1002/jbm.820240809.

[16] E. Schönemann, J. Koc, J.F. Karthäuser, O. Özcan, D. Schanzenbach, L. Schardt, A. Rosenhahn, A. Laschewsky, Sulfobetaine Methacrylate Polymers of Unconventional Polyzwitterion Architecture and Their Antifouling Properties, Biomacromolecules. 22 (2021) 1494–1508. https://doi.org/10.1021/acs.biomac.0c01705.

[17] K. Ishihara, Blood-Compatible Surfaces with Phosphorylcholine-Based Polymers for Cardiovascular Medical Devices, Langmuir. 35 (2019) 1778–1787. https://doi.org/10.1021/acs.langmuir.8b01565.

[18] A.L. Lewis, P.D. Hughes, L.C. Kirkwood, S.W. Leppard, R.P. Redman, L.A. Tolhurst, P.W. Stratford, Synthesis and characterisation of phosphorylcholine-based polymers useful for coating blood filtration devices, Biomaterials. 21 (2000) 1847–1859.

https://doi.org/10.1016/S0142-9612(00)00055-7.

[19] T. Ueda, H. Oshida, K. Kurita, K. Ishihara, N. Nakabayashi, Preparation of 2-Methacryloyloxyethyl Phosphorylcholine Copolymers with Alkyl Methacrylates and Their Blood Compatibility, Polym. J. 24 (1992) 1259–1269. https://doi.org/10.1295/polymj.24.1259.

[20] Y. Iwasaki, K. Kurita, K. Ishihara, N. Nakabayashi, Effect of methylene chain length in phospholipid moiety on blood compatibility of phospholipid polymers, J. Biomater. Sci. Polym. Ed. 6 (1995) 447–461. https://doi.org/10.1163/156856294X00437.

[21] K. Ishihara, A. Fujiike, Y. Iwasaki, K. Kurita, N. Nakabayashi, Synthesis of polymers having a phospholipid polar group connected to a poly(oxyethylene) chain and their protein adsorption-resistance properties, J. Polym. Sci. Part A Polym. Chem. 34 (1996) 199–205. https://doi.org/10.1002/(SICI)1099-0518(19960130)34:2<199::AID-POLA6>3.0.CO;2-P.

[22] K. Sugiyama, K. Ohga, H. Aoki, Emulsion copolymerization of 2-(acryloyloxy)ethylphosphoryl-choline with vinyl monomers and protein adsorption at resultant copolymer microspheres, Macromol. Chem. Phys. 196 (1995) 1907–1916.

https://doi.org/10.1002/macp.1995.021960610.

[23] T. Oishi, H. Uchiyama, K. Onimura, H. Tsutsumi, Synthesis and

Properties of Poly(methacrylate) Bearing a Phosphorylcholine Analogous Group, Polym. J. 30 (1998) 17–22. https://doi.org/10.1295/polymj.30.17.

[24] K. Sugiyama, K. Ohga, Surface modified poly(methyl methacrylate) with 1-methyl- 2-methacrylamidoethyl phosphorylcholine moiety, Macromol. Chem. Phys. 200 (1999) 1439–1445. https://doi.org/10.1002/(SICI)1521-3935(19990601)200:6<1439::AID-MACP1439>3.0.CO;2-B.

[25] Y. Iwasaki, K. Ishihara, Phosphorylcholine-containing polymers for biomedical applications, Anal. Bioanal. Chem. 381 (2005) 534–546. https://doi.org/10.1007/s00216-004-2805-9.

[26] J. Koc, E. Schönemann, A. Amuthalingam, J. Clarke, J.A. Finlay, A.S. Clare, A. Laschewsky, A. Rosenhahn, Low-Fouling Thin Hydrogel Coatings Made of Photo-Cross-Linked Polyzwitterions, Langmuir. 35 (2019) 1552–1562. https://doi.org/10.1021/acs.langmuir.8b02799.

[27] A. Laschewsky, A. Rosenhahn, Molecular Design of Zwitterionic Polymer Interfaces: Searching for the Difference, Langmuir. 35 (2019) 1056–1071. https://doi.org/10.1021/acs.langmuir.8b01789.

[28] K. Ishihara, T. Ueda, N. Nakabayashi, Preparation of Phospholipid Polymers and Their Properties as Polymer Hydrogel Membranes, Polym. J. 22 (1990) 355–360. https://doi.org/10.1295/polymj.22.355.

[29] M. Yaseen, J.R. Lu, J.R.P. Webster, J. Penfold, The Structure of Zwitterionic Phosphocholine Surfactant Monolayers, Langmuir. 22 (2006) 5825–5832. https://doi.org/10.1021/la053316z.

[30] S. Chen, L. Li, C. Zhao, J. Zheng, Surface hydration: Principles and applications toward low-fouling/nonfouling biomaterials, Polymer (Guildf). 51 (2010) 5283–5293. https://doi.org/10.1016/j.polymer.2010.08.022.

[31] A. Dėdinaitė, Biomimetic lubrication, Soft Matter. 8 (2012) 273–284. https://doi.org/10.1039/C1SM06335A.

[32] B. Li, P. Jain, J. Ma, J.K. Smith, Z. Yuan, H.-C. Hung, Y. He, X. Lin, K. Wu, J. Pfaendtner, S. Jiang, Trimethylamine N-oxide–derived zwitterionic polymers: A new class of ultralow fouling bioinspired materials, Sci. Adv. 5 (2024) 9562. https://doi.org/10.1126/sciadv.aaw9562.

[33] S.T. Ahmed, D.E. Leckband, Protein Adsorption on Grafted Zwitterionic Polymers Depends on Chain Density and Molecular Weight, Adv. Funct. Mater. 30 (2020) 2000757. https://doi.org/10.1002/adfm.202000757.

[34] K. Ishihara, Revolutionary advances in 2-methacryloyloxyethyl phosphorylcholine polymers as biomaterials, J. Biomed. Mater. Res. Part A. 107 (2019) 933–943. https://doi.org/10.1002/jbm.a.36635.

[35] Y. Iwasaki, K. Ishihara, Cell membrane-inspired phospholipid polymers for developing medical devices with excellent biointerfaces, Sci. Technol. Adv. Mater. 13 (2012) 64101. https://doi.org/10.1088/1468-6996/13/6/064101.

[36] K. Ishihara, Phospholipid Polymers, in: Encycl. Polym. Sci. Technol., 2012. https://doi.org/https://doi.org/10.1002/0471440264.pst574.

[37] S. Meng, Z. Liu, W. Zhong, Q. Wang, Q. Du, Phosphorylcholine modified chitosan: Appetent and safe material for cells, Carbohydr. Polym. 70 (2007) 82–88.

https://doi.org/10.1016/j.carbpol.2007.03.006.

[38] F. Nederberg, T. Bowden, J. Hilborn, Synthesis, Characterization, and Properties of Phosphoryl Choline Functionalized Poly ε-caprolactone and Charged Phospholipid Analogues, Macromolecules. 37 (2004) 954–965. https://doi.org/10.1021/ma035433b.

[39] T. Zhang, Z. Song, H. Chen, X. Yu, Z. Jiang, Synthesis and characterization of phosphoryl-choline-capped poly(ε-caprolactone)-poly(ethylene oxide) di-block co-polymers and its surface modification on polyurethanes, J. Biomater. Sci. Polym. Ed. 19 (2008) 509–524. https://doi.org/10.1163/156856208783719464.

[40] Y. Zheng, Y. Yan, W. Zhao, H. Wang, Y. Sun, J. Han, H. Zhang, Self-Assembled Nanospheres with Enhanced Interfacial Lubrication for the Treatment of Osteoarthritis, ACS Appl. Mater. Interfaces. 14 (2022) 21773–21786. https://doi.org/10.1021/acsami.1c19853.

[41] Y. Zheng, J. Yang, J. Liang, X. Xu, W. Cui, L. Deng, H. Zhang, Bioinspired Hyaluronic Acid/Phosphorylcholine Polymer with Enhanced Lubrication and Anti-Inflammation, Biomacromolecules. 20 (2019) 4135–4142. https://doi.org/10.1021/acs.biomac.9b00964.

[42] L. Wang, Y. Wang, Q. Jin, F. Jia, H. Wang, J. Ji, Biomimic pH/reduction dual-sensitive reversibly cross-linked hyaluronic acid prodrug micelles for targeted intracellular drug delivery, Polymer (Guildf). 76 (2015) 237–244. https://doi.org/10.1016/j.polymer.2015.09.003.

[43] Y. Kadoma, Synthesis and Hemolysis Test of the Polymer Containing Phosphorylcholine Groups, Koubunshi Ronbunshu. 35 (1978) 423–427. https://cir.nii.ac.jp/crid/1574231873997381504.

[44] S. Monge, G. David, Phosphorus-Based Polymers, Royal Society of Chemistry, Cambridge, 2014.

https://doi.org/10.1039/9781782624523.

[45] T. Umeda, T. Nakaya, M. Imoto, Polymeric phospholipid analogues, 14. The convenient preparation of a vinyl monomer containing a phospholipid analogue, Die Makromol. Chemie, Rapid Commun. 3 (1982) 457–459. https://doi.org/10.1002/marc.1982.030030701.

[46] H. Wang, A. Miyamoto, T. Hirano, M. Seno, T. Sato, Radical

polymerization of 2-methacryloyloxyethyl phosphorylcholine in water: kinetics and salt effects, Eur. Polym. J. 40 (2004) 2287–2290. https://doi.org/10.1016/j.eurpolymj.2004.06.012.

[47] I.Y. Ma, E.J. Lobb, N.C. Billingham, S.P. Armes, A.L. Lewis, A.W. Lloyd, J. Salvage, Synthesis of Biocompatible Polymers. 1. Homopolymerization of 2-Methacryloyloxyethyl Phosphorylcholine via ATRP in Protic Solvents: An Optimization Study, Macromolecules. 35 (2002) 9306–9314.

https://doi.org/10.1021/ma0210325.

[48] M. Mu, T. Konno, Y. Inoue, K. Ishihara, Solubilization of poorly water-soluble compounds using amphiphilic phospholipid polymers with different molecular architectures, Colloids Surfaces B Biointerfaces. 158 (2017) 249–256. https://doi.org/10.1016/j.colsurfb.2017.06.040.

[49] K. Sugiyama, H. Aoki, Surface Modified Polymer Microspheres Obtained by the Emulsion Copolymerization of 2-Methacryloyloxyethyl Phosphorylcholine with Various Vinyl Monomers, Polym. J. 26 (1994) 561–569. https://doi.org/10.1295/polymj.26.561.

[50] S. Yusa, K. Fukuda, T. Yamamoto, K. Ishihara, Y. Morishima, Synthesis of Well-Defined Amphiphilic Block Copolymers Having Phospholipid Polymer Sequences as a Novel Biocompatible Polymer Micelle Reagent, Biomacromolecules. 6 (2005) 663–670. https://doi.org/10.1021/bm0495553.

[51] C. Kojima, R. Katayama, T. Lien Nguyen, Y. Oki, A. Tsujimoto, S. Yusa, K. Shiraishi, A. Matsumoto, Different antifouling effects of random and block copolymers comprising 2-methacryloyloxyethyl phosphorylcholine and dodecyl methacrylate, Eur. Polym. J. 136 (2020) 109932. https://doi.org/10.1016/j.eurpolymj.2020.109932.

[52] M. Ayaki, A. Iwasawa, Y. Niwano, Cytotoxicity assays of new artificial tears containing 2-methacryloyloxyethyl phosphorylcholine polymer for ocular surface cells, Jpn. J. Ophthalmol. 55 (2011) 541–546. https://doi.org/10.1007/s10384-011-0073-8.

[53] T.L. Nguyen, Y. Kawata, K. Ishihara, S. Yusa, Synthesis of Amphiphilic Statistical Copolymers Bearing Methoxyethyl and Phosphorylcholine Groups and Their Self-Association Behavior in Water, Polymers (Basel). 12 (2020) 1808. https://doi.org/10.3390/polym12081808.

[54] O. Nazarova, E. Chernova, A. Dobrodumov, Y. Zolotova, M. Bezrukova, T. Nekrasova, E. Vlasova, E. Panarin, New water-soluble copolymers of 2-methacryloyloxyethyl phosphorylcholine for surface modification, J. Appl. Polym. Sci. 138 (2021) 50272. https://doi.org/10.1002/app.50272.

[55] T. Sato, T. Miyoshi, M. Seno, Kinetic study on the radical polymerization of 2-methacryloyloxyethyl phosphorylcholine, J.

Polym. Sci. Part A Polym. Chem. 38 (2000) 509–515. https://doi.org/10.1002/(SICI)1099-0518(20000201)38:3<509::AID-POLA17>3.0.CO;2-M.

[56] C.M. Gardner, C.E. Brown, H.D.H. Stöver, Synthesis and properties of water-soluble azlactone copolymers, J. Polym. Sci. Part A Polym. Chem. 50 (2012) 4674–4685. https://doi.org/10.1002/pola.26281.

[57] K. Ishihara, Y. Iwasaki, Reduced protein adsorption on novel phospholipid polymers., J. Biomater. Appl. 13 (1998) 111–127. https://doi.org/10.1177/088532829801300203.

[58] W. Lin, N. Kampf, J. Klein, Designer Nanoparticles as Robust Superlubrication Vectors, ACS Nano. 14 (2020) 7008–7017. https://doi.org/10.1021/acsnano.0c01559.

[59] S.-I. Sawada, Y. Iwasaki, N. Nakabayashi, K. Ishihara, Stress response of adherent cells on a polymer blend surface composed of a segmented polyurethane and MPC copolymers, J. Biomed. Mater. Res. Part A. 79A (2006) 476–484. https://doi.org/10.1002/jbm.a.30820.

[60] A.L. Lewis, Phosphorylcholine-based polymers and their use in the prevention of biofouling, Colloids Surfaces B Biointerfaces. 18 (2000) 261–275. https://doi.org/10.1016/S0927-7765(99)00152-6.

[61] X. Lin, K. Fukazawa, K. Ishihara, Photoreactive Polymers Bearing a Zwitterionic Phosphorylcholine Group for Surface Modification of Biomaterials, ACS Appl. Mater. Interfaces. 7 (2015) 17489–17498. https://doi.org/10.1021/acsami.5b05193.

[62] K. Matyjaszewski, Overview: Fundamentals of Controlled/Living Radical Polymerization, in: Control. Radic. Polym., American Chemical Society, 1998: pp. 2–30. https://doi.org/10.1021/bk-1998-0685.ch001.

[63] W.A. Braunecker, K. Matyjaszewski, Controlled/living radical polymerization: Features, developments, and perspectives, Prog. Polym. Sci. 32 (2007) 93–146.

https://doi.org/https://doi.org/10.1016/j.progpolymsci.2006.11.002.

[64] D. Zhou, L.-W. Zhu, B.-H. Wu, Z.-K. Xu, L.-S. Wan, End-functionalized polymers by controlled/living radical polymerizations: synthesis and applications, Polym. Chem. 13 (2022) 300–358. https://doi.org/10.1039/D1PY01252E.

[65] E.J. Lobb, I. Ma, N.C. Billingham, S.P. Armes, A.L. Lewis, Facile Synthesis of Well-Defined, Biocompatible Phosphorylcholine-Based Methacrylate Copolymers via Atom Transfer Radical Polymerization at 20 °C, J. Am. Chem. Soc. 123 (2001) 7913–7914. https://doi.org/10.1021/ja003906d.

[66] Y. Liu, L. Mao, S. Yang, M. Liu, H. Huang, Y. Wen, F. Deng, Y. Li, X. Zhang, Y. Wei, Synthesis and biological imaging of fluorescent polymeric nanoparticles with AIE feature via the combination of

RAFT polymerization and post-polymerization modification, Dye. Pigment. 158 (2018) 79–87.

https://doi.org/10.1016/j.dyepig.2018.05.032.

[67] G. Moad, E. Rizzardo, S.H. Thang, RAFT Polymerization and Some of its Applications, Chem. – An Asian J. 8 (2013) 1634–1644. https://doi.org/10.1002/asia.201300262.

[68] D.J. Keddie, G. Moad, E. Rizzardo, S.H. Thang, RAFT Agent Design and Synthesis, Macromolecules. 45 (2012) 5321–5342. https://doi.org/10.1021/ma300410v.

[69] G. Moad, E. Rizzardo, S.H. Thang, Radical addition–fragmentation chemistry in polymer synthesis, Polymer (Guildf). 49 (2008) 1079–1131. https://doi.org/10.1016/j.polymer.2007.11.020.

[70] K. Ishihara, T. Tsuji, T. Kurosaki, N. Nakabayashi, Hemocompatibility on graft copolymers composed of poly(2-methacryloyloxyethyl phosphorylcholine) side chain and poly(n -butyl methacrylate) backbone, J. Biomed. Mater. Res. 28 (1994) 225–232. https://doi.org/10.1002/jbm.820280213.

[71] N. Bhuchar, Z. Deng, K. Ishihara, R. Narain, Detailed study of the reversible addition–fragmentation chain transfer polymerization and co-polymerization of 2-methacryloyloxyethyl phosphorylcholine, Polym. Chem. 2 (2011) 632–639.

https://doi.org/10.1039/C0PY00300J.

[72] Y. Liu, Y. Inoue, S. Sakata, S. Kakinoki, T. Yamaoka, K. Ishihara, Effects of molecular architecture of phospholipid polymers on surface modification of segmented polyurethanes., J. Biomater. Sci. Polym. Ed. 25 (2014) 474–486.

https://doi.org/10.1080/09205063.2013.873282.

[73] E.S. Read, K.L. Thompson, S.P. Armes, Synthesis of well-defined primary amine-based homopolymers and block copolymers and their Michael addition reactions with acrylates and acrylamides, Polym. Chem. 1 (2010) 221–230. https://doi.org/10.1039/B9PY00320G.

[74] B. Yuan, Q. Chen, W.-Q. Ding, P.-S. Liu, S.-S. Wu, S.-C. Lin, J. Shen, Y. Gai, Copolymer Coatings Consisting of 2-Methacryloyloxyethyl Phosphorylcholine and 3-Methacryloxypropyl Trimethoxysilane via ATRP To Improve Cellulose Biocompatibility, ACS Appl. Mater. Interfaces. 4 (2012) 4031–4039. https://doi.org/10.1021/am3008399.

[75] Y. Ma, Y. Tang, N.C. Billingham, S.P. Armes, A.L. Lewis, A.W. Lloyd, J.P. Salvage, Well-Defined Biocompatible Block Copolymers via Atom Transfer Radical Polymerization of 2-Methacryloyloxyethyl Phosphorylcholine in Protic Media, Macromolecules. 36 (2003) 3475–3484. https://doi.org/10.1021/ma021762c.

[76] S. Yusa, D. Oka, Y. Iwasaki, K. Ishihara, pH-Responsive Association

Behavior of Biocompatible Random Copolymers Containing Pendent Phosphorylcholine and Fatty Acid, Langmuir. 38 (2022) 5119–5127. https://doi.org/10.1021/acs.langmuir.1c02200.

[77] P. Sae-ung, K.W. Kolewe, Y. Bai, E.W. Rice, J.D. Schiffman, T. Emrick, V.P. Hoven, Antifouling Stripes Prepared from Clickable Zwitterionic Copolymers, Langmuir. 33 (2017) 7028–7035. https://doi.org/10.1021/acs.langmuir.7b01431.

[78] N. Shahkaramipour, C.K. Lai, S.R. Venna, H. Sun, C. Cheng, H. Lin, Membrane Surface Modification Using Thiol-Containing Zwitterionic Polymers via Bioadhesive Polydopamine, Ind. Eng. Chem. Res. 57 (2018) 2336–2345. https://doi.org/10.1021/acs.iecr.7b05025.

[79] S. McRae Page, M. Martorella, S. Parelkar, I. Kosif, T. Emrick, Disulfide Cross-Linked Phosphorylcholine Micelles for Triggered Release of Camptothecin, Mol. Pharm. 10 (2013) 2684–2692. https://doi.org/10.1021/mp400114n.

[80] J.-M. Noy, C. Cao, M. Stenzel, Length of the Stabilizing Zwitterionic Poly(2-methacryloyloxyethyl phosphorycholine) Block Influences the Activity of the Conjugated Arsenic Drug in Drug-Directed Polymerization-Induced Self-Assembly Particles, ACS Macro Lett. 8 (2019) 57–63. https://doi.org/10.1021/acsmacrolett.8b00853.

[81] R. Kojima, M.C.Z. Kasuya, K. Ishihara, K. Hatanaka, Synthesis of Amphiphilic Copolymers by Soap-free Interface-Mediated Polymerization, Polym. J. 41 (2009) 370–373. https://doi.org/10.1295/polymj.PJ2008322.

[82] S.K. Yoon, D.J. Chung, Development of Blood Compatible Composite Using MPC Copolymer and Polyolefin for Non-PVC Blood Bag Application, Macromol. Res. 28 (2020) 319–326. https://doi.org/10.1007/s13233-020-8047-7.

[83] J. Ci, H. Kang, C. Liu, A. He, R. Liu, Thermal sensitivity and protein anti-adsorption of hydroxypropyl cellulose-g- poly(2-(methacryloyloxy) ethyl phosphorylcholine), Carbohydr. Polym. 157 (2017) 757–765. https://doi.org/10.1016/j.carbpol.2016.10.051.

[84] L. Yan, K. Ishihara, Graft copolymerization of 2-methacryloyloxyethyl phosphorylcholine to cellulose in homogeneous media using atom transfer radical polymerization for providing new hemocompatible coating materials, J. Polym. Sci. Part A Polym. Chem. 46 (2008) 3306–3313. https://doi.org/10.1002/pola.22670.

[85] S. Kalasin, R.A. Letteri, T. Emrick, M.M. Santore, Adsorbed Polyzwitterion Copolymer Layers Designed for Protein Repellency and Interfacial Retention, Langmuir. 33 (2017) 13708–13717. https://doi.org/10.1021/acs.langmuir.7b03391.

[86] S.G. Roy, S. Banerjee, P. De, Cationic Polymerization of Nonpolar Vinyl Monomers for Producing High Performance Polymers, in: Ref.

Modul. Mater. Sci. Mater. Eng., Elsevier, 2016. https://doi.org/10.1016/B978-0-12-803581-8.01357-6.

[87] S. Chatterjee, M. Ohshio, S. Yusa, T. Ooya, Controlled Micelle Formation and Stable Capture of Hydrophobic Drug by Alkylated POSS Methacrylate Block Copolymers, ACS Appl. Polym. Mater. 1 (2019) 2108–2119. https://doi.org/10.1021/acsapm.9b00412.

[88] W. Feng, S. Zhu, K. Ishihara, J.L. Brash, Adsorption of Fibrinogen and Lysozyme on Silicon Grafted with Poly(2-methacryloyloxyethyl Phosphorylcholine) via Surface-Initiated Atom Transfer Radical Polymerization, Langmuir. 21 (2005) 5980–5987. https://doi.org/10.1021/la050277i.

[89] S. Sakata, Y. Inoue, K. Ishihara, Molecular Interaction Forces Generated during Protein Adsorption to Well-Defined Polymer Brush Surfaces, Langmuir. 31 (2015) 3108–3114.

https://doi.org/10.1021/acs.langmuir.5b00351.

[90] T. Goda, T. Konno, M. Takai, T. Moro, K. Ishihara, Biomimetic phosphorylcholine polymer grafting from polydimethylsiloxane surface using photo-induced polymerization, Biomaterials. 27 (2006) 5151–5160. https://doi.org/10.1016/j.biomaterials.2006.05.046.

[91] M. Tizzotti, A. Charlot, E. Fleury, M. Stenzel, J. Bernard, Modification of Polysaccharides Through Controlled/Living Radical Polymerization Grafting—Towards the Generation of High Performance Hybrids, Macromol. Rapid Commun. 31 (2010) 1751–1772. https://doi.org/10.1002/marc.201000072.

[92] C. Bartholome, E. Beyou, E. Bourgeat-Lami, P. Chaumont, N. Zydowicz, Nitroxide-Mediated Polymerizations from Silica Nanoparticle Surfaces: "Graft from" Polymerization of Styrene Using a Triethoxysilyl-Terminated Alkoxyamine Initiator, Macromolecules. 36 (2003) 7946–7952. https://doi.org/10.1021/ma034491u.

[93] K. Fukazawa, A. Nakao, M. Maeda, K. Ishihara, Photoreactive Initiator for Surface-Initiated ATRP on Versatile Polymeric Substrates, ACS Appl. Mater. Interfaces. 8 (2016) 24994–24998. https://doi.org/10.1021/acsami.6b07145.

[94] M. Kyomoto, T. Moro, Y. Takatori, H. Kawaguchi, K. Nakamura, K. Ishihara, Self-initiated surface grafting with poly(2-methacryloyloxyethyl phosphorylcholine) on poly(ether-ether-ketone), Biomaterials. 31 (2010) 1017–1024. https://doi.org/10.1016/j.biomaterials.2009.10.055.

[95] M. Kyomoto, K. Ishihara, Self-Initiated Surface Graft Polymerization of 2-Methacryloyloxyethyl Phosphorylcholine on Poly(ether ether ketone) by Photoirradiation, ACS Appl. Mater. Interfaces. 1 (2009) 537–542. https://doi.org/10.1021/am800260t.

[96] D. Pranantyo, L.Q. Xu, K.-G. Neoh, E.-T. Kang, Y.X. Ng, S.L.-M. Teo,

Tea Stains-Inspired Initiator Primer for Surface Grafting of Antifouling and Antimicrobial Polymer Brush Coatings, Biomacromolecules. 16 (2015) 723–732.

https://doi.org/10.1021/bm501623c.

[97] Y. Uyama, K. Kato, Y. Ikada, Surface Modification of Polymers by Grafting, in: H. Galina, Y. Ikada, K. Kato, R. Kitamaru, J. Lechowicz, Y. Uyama, C. Wu (Eds.), Grafting/Characterization Tech. Model., Springer Berlin Heidelberg, Berlin, Heidelberg, 1998: pp. 1–39. https://doi.org/10.1007/3-540-69685-7_1.

[98] S.-H. Chen, Y. Chang, K. Ishihara, Reduced Blood Cell Adhesion on Polypropylene Substrates through a Simple Surface Zwitterionization, Langmuir. 33 (2017) 611–621.

https://doi.org/10.1021/acs.langmuir.6b03295.

[99] A.B. Asha, Y. Chen, H. Zhang, S. Ghaemi, K. Ishihara, Y. Liu, R. Narain, Rapid Mussel-Inspired Surface Zwitteration for Enhanced Antifouling and Antibacterial Properties, Langmuir. 35 (2019) 1621–1630. https://doi.org/10.1021/acs.langmuir.8b03810.

[100] J.L. Dalsin, B.-H. Hu, B.P. Lee, P.B. Messersmith, Mussel Adhesive Protein Mimetic Polymers for the Preparation of Nonfouling Surfaces, J. Am. Chem. Soc. 125 (2003) 4253–4258. https://doi.org/10.1021/ja0284963.

[101] Q. Guo, J. Chen, J. Wang, H. Zeng, J. Yu, Recent progress in synthesis and application of mussel-inspired adhesives, Nanoscale. 12 (2020) 1307–1324. https://doi.org/10.1039/C9NR09780E.

[102] N. Patil, C. Falentin-Daudré, C. Jérôme, C. Detrembleur, Mussel-inspired protein-repelling ambivalent block copolymers: controlled synthesis and characterization, Polym. Chem. 6 (2015) 2919–2933. https://doi.org/10.1039/C5PY00127G.

[103] L. Han, L. Xiang, J. Zhang, J. Chen, J. Liu, B. Yan, H. Zeng, Biomimetic Lubrication and Surface Interactions of Dopamine-Assisted Zwitterionic Polyelectrolyte Coatings, Langmuir. 34 (2018) 11593–11601. https://doi.org/10.1021/acs.langmuir.8b02473.

[104] K. Shibata, T. Tanigawa, H. Ito, T. Kubo, K. Hosoya, Effect of Solvents on the Surface Modification of Hydrophilic Macro-Porous Particles with an Ion-Exchange Monomer Having Both Anion and Cation Exchange Groups, Chromatography. 37 (2016) 99–104. https://doi.org/10.15583/jpchrom.2016.004.

[105] Y. Oshiba, Y. Harada, T. Yamaguchi, Precise surface modification of porous membranes with well-defined zwitterionic polymer for antifouling applications, J. Memb. Sci. 619 (2021) 118772. https://doi.org/10.1016/j.memsci.2020.118772.

[106] K. Ishihara, M. Mu, T. Konno, Y. Inoue, K. Fukazawa, The unique hydration state of poly(2-methacryloyloxyethyl phosphorylcholine), J.

Biomater. Sci. Polym. Ed. 28 (2017) 884–899. https://doi.org/10.1080/09205063.2017.1298278.

[107] T. Goda, J. Watanabe, M. Takai, K. Ishihara, Water structure and improved mechanical properties of phospholipid polymer hydrogel with phosphorylcholine centered intermolecular cross-linker, Polymer (Guildf). 47 (2006) 1390–1396.

https://doi.org/10.1016/j.polymer.2005.12.043.

[108] H. Kitano, K. Takaha, M. Gemmei-Ide, Raman spectroscopic study of the structure of water in aqueous solutions of amphoteric polymers, Phys. Chem. Chem. Phys. 8 (2006) 1178–1185. https://doi.org/10.1039/B513601F.

[109] T. Morisaku, J. Watanabe, T. Konno, M. Takai, K. Ishihara, Hydration of phosphorylcholine groups attached to highly swollen polymer hydrogels studied by thermal analysis, Polymer (Guildf). 49 (2008) 4652–4657. https://doi.org/10.1016/j.polymer.2008.08.025.

[110] T.L. Nguyen, M. Mukai, D. Ihara, A. Takahara, S. Yusa, Association Behavior of a Homopolymer Containing Choline Phosphonate Groups in Aqueous Solutions, Chem. Lett. 51 (2021) 103–106. https://doi.org/10.1246/cl.210601.

[111] J. Liu, J. Wang, Y. Xue, T. Chen, D. Huang, Y. Wang, K. Ren, Y. Wang, G. Fu, J. Ji, Biodegradable phosphorylcholine copolymer for cardiovascular stent coating, J. Mater. Chem. B. 8 (2020) 5361–5368. https://doi.org/10.1039/D0TB00813C.

[112] A.L. Lewis, L.A. Tolhurst, P.W. Stratford, Analysis of a phosphorylcholine-based polymer coating on a coronary stent pre- and post-implantation, Biomaterials. 23 (2002) 1697–1706. https://doi.org/10.1016/S0142-9612(01)00297-6.

[113] T. Goda, T. Konno, M. Takai, K. Ishihara, Photoinduced phospholipid polymer grafting on Parylene film: Advanced lubrication and antibiofouling properties, Colloids Surfaces B Biointerfaces. 54 (2007) 67–73. https://doi.org/10.1016/j.colsurfb.2006.09.006.

[114] M. Kobayashi, Y. Terayama, N. Hosaka, M. Kaido, A. Suzuki, N. Yamada, N. Torikai, K. Ishihara, A. Takahara, Friction behavior of high-density poly(2-methacryloyloxyethyl phosphorylcholine) brush in aqueous media, Soft Matter. 3 (2007) 740–746. https://doi.org/10.1039/B615780G.

[115] T. Moro, Y. Takatori, K. Ishihara, T. Konno, Y. Takigawa, T. Matsushita, U. Chung, K. Nakamura, H. Kawaguchi, Surface grafting of artificial joints with a biocompatible polymer for preventing periprosthetic osteolysis, Nat. Mater. 3 (2004) 829–836. https://doi.org/10.1038/nmat1233.

[116] U. Raviv, S. Giasson, N. Kampf, J.-F. Gohy, R. Jéröme, J. Klein, Lubrication by charged polymers, Nature. 425 (2003) 163–165.

https://doi.org/10.1038/nature01970.

[117] U. Raviv, S. Perkin, P. Laurat, J. Klein, Fluidity of Water Confined Down to Subnanometer Films, Langmuir. 20 (2004) 5322–5332. https://doi.org/10.1021/la030419d.

[118] J. Klein, Hydration lubrication, Friction. 1 (2013) 1–23. https://doi.org/10.1007/s40544-013-0001-7.

[119] J. Klein, Repair or Replacement--A Joint Perspective, Science (80-.). 323 (2009) 47–48. https://doi.org/10.1126/science.1166753.

[120] D. Fu, Y. Lu, Z. Peng, W. Zhong, A zwitterionic hydrogel with a surprising function of increasing the ionic conductivity of alkali metal chloride or sulfuric acid water-soluble electrolyte, J. Mater. Chem. A. 11 (2023) 13543–13551. https://doi.org/10.1039/D3TA02104A.

[121] K. Ishihara, H. Nomura, T. Mihara, K. Kurita, Y. Iwasaki, N. Nakabayashi, Why do phospholipid polymers reduce protein adsorption?, J. Biomed. Mater. Res. 39 (1998) 323–330. https://doi.org/10.1002/(SICI)1097-4636(199802)39:2<323::AID-JBM21>3.0.CO;2-C.

[122] L. Ma, A. Gaisinskaya-Kipnis, N. Kampf, J. Klein, Origins of hydration lubrication, Nat. Commun. 6 (2015) 6060. https://doi.org/10.1038/ncomms7060.

[123] T. Hatakeyama, M. Tanaka, H. Hatakeyama, Studies on bound water restrained by poly(2-methacryloyloxyethyl phosphorylcholine): Comparison with polysaccharide–water systems, Acta Biomater. 6 (2010) 2077–2082. https://doi.org/10.1016/j.actbio.2009.12.018.

[124] S. Shiomoto, K. Inoue, H. Higuchi, S. Nishimura, H. Takaba, M. Tanaka, M. Kobayashi, Characterization of Hydration Water Bound to Choline Phosphate-Containing Polymers, Biomacromolecules. 23 (2022) 2999–3008. https://doi.org/10.1021/acs.biomac.2c00484.

[125] W. Lin, J. Klein, Hydration Lubrication in Biomedical Applications: From Cartilage to Hydrogels, Accounts Mater. Res. 3 (2022) 213–223. https://doi.org/10.1021/accountsmr.1c00219.

[126] M. Chen, W.H. Briscoe, S.P. Armes, H. Cohen, J. Klein, Polyzwitterionic brushes: Extreme lubrication by design, Eur. Polym. J. 47 (2011) 511–523.

https://doi.org/10.1016/j.eurpolymj.2010.10.007.

[127] L. Yang, X. Zhao, X. Liao, R. Wang, Z. Fan, S. Ma, F. Zhou, Biomimetic chitosan-derived bifunctional lubricant with superior antibacterial and hydration lubrication performances, J. Colloid Interface Sci. 629 (2023) 859–870. https://doi.org/10.1016/j.jcis.2022.09.098.

[128] A. Fakhari, C. Berkland, Applications and emerging trends of hyaluronic acid in tissue engineering, as a dermal filler and in

osteoarthritis treatment, Acta Biomater. 9 (2013) 7081–7092. https://doi.org/10.1016/j.actbio.2013.03.005.

[129] W. Lin, R. Mashiah, J. Seror, A. Kadar, O. Dolkart, T. Pritsch, R. Goldberg, J. Klein, Lipid-hyaluronan synergy strongly reduces intrasynovial tissue boundary friction, Acta Biomater. 83 (2019) 314–321. https://doi.org/10.1016/j.actbio.2018.11.015.

[130] W. Zhao, H. Wang, Y. Han, H. Wang, Y. Sun, H. Zhang, Dopamine/Phosphorylcholine Copolymer as an Efficient Joint Lubricant and ROS Scavenger for the Treatment of Osteoarthritis, ACS Appl. Mater. Interfaces. 12 (2020) 51236–51248. https://doi.org/10.1021/acsami.0c14805.

[131] K. Zhang, J. Yang, Y. Sun, M. He, J. Liang, J. Luo, W. Cui, L. Deng, X. Xu, B. Wang, H. Zhang, Thermo-Sensitive Dual-Functional Nanospheres with Enhanced Lubrication and Drug Delivery for the Treatment of Osteoarthritis, Chem. – A Eur. J. 26 (2020) 10564–10574. https://doi.org/10.1002/chem.202001372.

[132] H. Chen, T. Sun, Y. Yan, X. Ji, Y. Sun, X. Zhao, J. Qi, W. Cui, L. Deng, H. Zhang, Cartilage matrix-inspired biomimetic superlubricated nanospheres for treatment of osteoarthritis, Biomaterials. 242 (2020) 119931. https://doi.org/10.1016/j.biomaterials.2020.119931.

[133] Y. Wang, L. Wan, Y. Sun, H. Zhang, Synthesis of articular cartilage-inspired branched polyelectrolyte polymer for enhanced lubrication, Biosurface and Biotribology. 6 (2020) 82–86. https://doi.org/10.1049/bsbt.2020.0004.

[134] R.E. Holmlin, X. Chen, R.G. Chapman, S. Takayama, G.M. Whitesides, Zwitterionic SAMs that Resist Nonspecific Adsorption of Protein from Aqueous Buffer, Langmuir. 17 (2001) 2841–2850. https://doi.org/10.1021/la0015258.

[135] K. Ishihara, Biomimetic materials based on zwitterionic polymers toward human-friendly medical devices, Sci. Technol. Adv. Mater. 23 (2022) 498–524. https://doi.org/10.1080/14686996.2022.2119883.

[136] P.-S. Liu, Q. Chen, S.-S. Wu, J. Shen, S.-C. Lin, Surface modification of cellulose membranes with zwitterionic polymers for resistance to protein adsorption and platelet adhesion, J. Memb. Sci. 350 (2010) 387–394. https://doi.org/10.1016/j.memsci.2010.01.015.

[137] D.R. Lu, S.J. Lee, K. Park, Calculation of solvation interaction energies for protein adsorption on polymer surfaces, J. Biomater. Sci. Polym. Ed. 3 (1992) 127–147. https://doi.org/10.1163/156856291X00232.

[138] Y. Higuchi, Y. Asano, T. Kuwahara, M. Hishida, Rotational Dynamics of Water at the Phospholipid Bilayer Depending on the Head Groups Studied by Molecular Dynamics Simulations, Langmuir. 37 (2021) 5329–5338. https://doi.org/10.1021/acs.langmuir.1c00417.

[139] Y.-H. Zhao, X.-Y. Zhu, K.-H. Wee, R. Bai, Achieving Highly Effective

Non-biofouling Performance for Polypropylene Membranes Modified by UV-Induced Surface Graft Polymerization of Two Oppositely Charged Monomers, J. Phys. Chem. B. 114 (2010) 2422–2429. https://doi.org/10.1021/jp908194g.

[140] Y. Yu, J. Wang, C. Liu, B. Zhang, H. Chen, H. Guo, G. Zhong, W. Qu, S. Jiang, H. Huang, Evaluation of inherent toxicology and biocompatibility of magnesium phosphate bone cement, Colloids Surfaces B Biointerfaces. 76 (2010) 496–504. https://doi.org/10.1016/j.colsurfb.2009.12.010.

[141] M. Ayaki, A. Iwasawa, Y. Niwano, Cytotoxicity assays of new artificial tears containing 2-methacryloyloxyethyl phosphorylcholine polymer for ocular surface cells, Jpn. J. Ophthalmol. 55 (2011) 541–546. https://doi.org/10.1007/s10384-011-0073-8.

[142] X. Niu, D. Li, Y. Chen, F. Ran, Modification of a polyethersulfone membrane with a block copolymer brush of poly(2-methacryloyloxyethyl phosphorylcholine- co -glycidyl methacrylate) and a branched polypeptide chain of Arg–Glu–Asp–Val, RSC Adv. 9 (2019) 25274–25284. https://doi.org/10.1039/C9RA04234B.

[143] W. Lin, J. Klein, Recent Progress in Cartilage Lubrication, Adv. Mater. 33 (2021) 2005513. https://doi.org/10.1002/adma.202005513.

[144] J. Katta, Z. Jin, E. Ingham, J. Fisher, Effect of nominal stress on the long term friction, deformation and wear of native and glycosaminoglycan deficient articular cartilage, Osteoarthr. Cartil. 17 (2009) 662–668. https://doi.org/10.1016/j.joca.2008.10.008.

[145] J.W. Liew, L.K. King, A. Mahmoudian, Q. Wang, H.F. Atkinson, D.B. Flynn, C.T. Appleton, M. Englund, I.K. Haugen, L.S. Lohmander, J. Runhaar, T. Neogi, G. Hawker, A scoping review of how early-stage knee osteoarthritis has been defined, Osteoarthr. Cartil. (2023). https://doi.org/10.1016/j.joca.2023.04.015.

[146] T. Vos, S.S. Lim, C. Abbafati, K.M. Abbas, Global burden of 369 diseases and injuries in 204 countries and territories, 1990–2019: a systematic analysis for the Global Burden of Disease Study 2019, Lancet. 396 (2020) 1204–1222. https://doi.org/10.1016/S0140-6736(20)30925-9.

[147] H. Sato, T. Takahashi, H. Ide, T. Fukushima, M. Tabata, F. Sekine, K. Kobayashi, M. Negishi, Y. Niwa, Antioxidant activity of synovial fluid, hyaluronic acid, and two subcomponents of hyaluronic acid. synovial fluid scavenging effect is enhanced in rheumatoid arthritis patients, Arthritis Rheum. 31 (1988) 63–71.

https://doi.org/10.1002/art.1780310110.

[148] J.D. Evanich, C.J. Evanich, M.B. Wright, J.A. Rydlewicz, Efficacy of Intraarticular Hyaluronic Acid Injections in Knee Osteoarthritis, Clin. Orthop. Relat. Res. 390 (2001) 173–181.

https://doi.org/10.1097/00003086-200109000-00020.

[149] G.H. Lo, M. LaValley, T. McAlindon, D.T. Felson, Intra-articular Hyaluronic Acid in Treatment of Knee OsteoarthritisA Meta-analysis, JAMA. 290 (2003) 3115–3121.

https://doi.org/10.1001/jama.290.23.3115.

[150] T. Goda, Y. Miyahara, K. Ishihara, Phospholipid-mimicking cell-penetrating polymers: principles and applications, J. Mater. Chem. B. 8 (2020) 7633–7641. https://doi.org/10.1039/D0TB01520B.

[151] T. Moro, Y. Takatori, M. Kyomoto, K. Ishihara, K. Saiga, K. Nakamura, H. Kawaguchi, Surface grafting of biocompatible phospholipid polymer MPC provides wear resistance of tibial polyethylene insert in artificial knee joints, Osteoarthr. Cartil. 18 (2010) 1174–1182. https://doi.org/10.1016/j.joca.2010.05.019.

[152] G. Liu, Y. Feng, N. Zhao, Z. Chen, J. Shi, F. Zhou, Polymer-based lubricating materials for functional hydration lubrication, Chem. Eng. J. 429 (2022) 132324. https://doi.org/10.1016/j.cej.2021.132324.

[153] R. Iwata, P. Suk-In, V.P. Hoven, A. Takahara, K. Akiyoshi, Y. Iwasaki, Control of Nanobiointerfaces Generated from Well-Defined Biomimetic Polymer Brushes for Protein and Cell Manipulations, Biomacromolecules. 5 (2004) 2308–2314.

https://doi.org/10.1021/bm049613k.

[154] M. Kyomoto, T. Moro, K. Saiga, M. Hashimoto, H. Ito, H. Kawaguchi, Y. Takatori, K. Ishihara, Biomimetic hydration lubrication with various polyelectrolyte layers on cross-linked polyethylene orthopedic bearing materials, Biomaterials. 33 (2012) 4451–4459. https://doi.org/10.1016/j.biomaterials.2012.03.028.

[155] O. Tairy, N. Kampf, M. Driver, S. Armes, J. Klein, Dense, Highly Hydrated Polymer Brushes via Modified Atom-Transfer-Radical-Polymerization: Structure, Surface Interactions, and Frictional Dissipation, Macromolecules. 48 (2015) 140–151. https://doi.org/10.1021/ma5019439.

[156] Y. Iwasaki, M. Takamiya, R. Iwata, S. Yusa, K. Akiyoshi, Surface modification with well-defined biocompatible triblock copolymers, Colloids Surfaces B Biointerfaces. 57 (2007) 226–236. https://doi.org/10.1016/j.colsurfb.2007.02.007.

[157] K. Ishihara, M. Mu, T. Konno, Water-soluble and amphiphilic phospholipid copolymers having 2-methacryloyloxyethyl phosphorylcholine units for the solubilization of bioactive compounds, J. Biomater. Sci. Polym. Ed. 29 (2018) 844–862. https://doi.org/10.1080/09205063.2017.1377023.

[158] J. Zhao, Y.-D. Chai, J. Zhang, P.-F. Huang, K. Nakashima, Y.-K. Gong, Long circulating micelles of an amphiphilic random copolymer bearing cell outer membrane phosphorylcholine zwitterions, Acta

Biomater. 16 (2015) 94–102.

https://doi.org/10.1016/j.actbio.2015.01.019.

[159] S. Chantasirichot, Y. Inoue, K. Ishihara, Amphiphilic Triblock Phospholipid Copolymers Bearing Phenylboronic Acid Groups for Spontaneous Formation of Hydrogels with Tunable Mechanical Properties, Macromolecules. 47 (2014) 3128–3135. https://doi.org/10.1021/ma5006099.

[160] S. Liu, Q. Zhang, Y. Han, Y. Sun, Y. Zhang, H. Zhang, Bioinspired Surface Functionalization of Titanium Alloy for Enhanced Lubrication and Bacterial Resistance, Langmuir. 35 (2019) 13189–13195. https://doi.org/10.1021/acs.langmuir.9b02263.

[161] G.-Y. Liu, L.-P. Lv, C.-J. Chen, X.-S. Liu, X.-F. Hu, J. Ji, Biocompatible and biodegradable polymersomes for pH-triggered drug release, Soft Matter. 7 (2011) 6629–6636. https://doi.org/10.1039/C1SM05308F.

[162] L. Wang, W. Dai, M. Yang, X. Wei, K. Ma, B. Song, P. Jia, Y. Gong, J. Yang, J. Zhao, Cell membrane mimetic copolymer coated polydopamine nanoparticles for combined pH-sensitive drug release and near-infrared photothermal therapeutic, Colloids Surfaces B Biointerfaces. 176 (2019) 1–8.

https://doi.org/10.1016/j.colsurfb.2018.12.057.

[163] R. Xie, Y. Tian, S. Peng, L. Zhang, Y. Men, W. Yang, Poly(2-methacryloyloxyethyl phosphorylcholine)-based biodegradable nanogels for controlled drug release, Polym. Chem. 9 (2018) 4556–4565. https://doi.org/10.1039/C8PY00948A.

[164] H. Hu, J.C. Dyke, B.A. Bowman, C.-C. Ko, W. You, Investigation of Dopamine Analogues: Synthesis, Mechanistic Understanding, and Structure–Property Relationship, Langmuir. 32 (2016) 9873–9882. https://doi.org/10.1021/acs.langmuir.6b02141.

[165] S. Moulay, Dopa/Catechol-Tethered Polymers: Bioadhesives and Biomimetic Adhesive Materials, Polym. Rev. 54 (2014). https://doi.org/10.1080/15583724.2014.881373.

[166] Q. Ye, F. Zhou, W. Liu, Bioinspired catecholic chemistry for surface modification, Chem. Soc. Rev. 40 (2011) 4244–4258. https://doi.org/10.1039/C1CS15026J.

[167] M.A. North, C.A. Del Grosso, J.J. Wilker, High Strength Underwater Bonding with Polymer Mimics of Mussel Adhesive Proteins, ACS Appl. Mater. Interfaces. 9 (2017) 7866–7872. https://doi.org/10.1021/acsami.7b00270.

[168] P. Kord Forooshani, B.P. Lee, Recent approaches in designing bioadhesive materials inspired by mussel adhesive protein, J. Polym. Sci. Part A Polym. Chem. 55 (2017) 9–33. https://doi.org/10.1002/pola.28368.

[169] B.P. Lee, P.B. Messersmith, J.N. Israelachvili, J.H. Waite, Mussel-Inspired Adhesives and Coatings, Annu. Rev. Mater. Res. 41 (2011) 99–132. https://doi.org/10.1146/annurev-matsci-062910-100429.

[170] R. Guo, Q. Su, J. Zhang, A. Dong, C. Lin, J. Zhang, Facile Access to Multisensitive and Self-Healing Hydrogels with Reversible and Dynamic Boronic Ester and Disulfide Linkages, Biomacromolecules. 18 (2017) 1356–1364. https://doi.org/10.1021/acs.biomac.7b00089.

[171] H.N. Nguyen, E.T. Nadres, B.G. Alamani, D.F. Rodrigues, Designing polymeric adhesives for antimicrobial materials: Poly(ethylene imine) polymer, graphene, graphene oxide and molybdenum trioxide-a biomimetic approach, J. Mater. Chem. B. 5 (2017) 6616–6628. https://doi.org/10.1039/c7tb00722a.

[172] J. Chen, Q. Su, R. Guo, J. Zhang, A. Dong, C. Lin, J. Zhang, A Multitasking Hydrogel Based on Double Dynamic Network with Quadruple-Stimuli Sensitiveness, Autonomic Self-Healing Property, and Biomimetic Adhesion Ability, Macromol. Chem. Phys. 218 (2017) 1–9. https://doi.org/10.1002/macp.201700166.

[173] J. Ko, Y.J. Kim, Y.S. Kim, Self-Healing Polymer Dielectric for a High Capacitance Gate Insulator, ACS Appl. Mater. Interfaces. 8 (2016) 23854–23861. https://doi.org/10.1021/acsami.6b08220.

[174] H. Satoh, Y. Saito, H. Yabu, Robust platforms for creating organic–inorganic nanocomposite microspheres: decorating polymer microspheres containing mussel-inspired adhesion layers with inorganic nanoparticles, Chem. Commun. 50 (2014) 14786–14789. https://doi.org/10.1039/C4CC05433D.

[175] Y. Saito, M. Shimomura, H. Yabu, Breath Figures of Nanoscale Bricks: A Universal Method for Creating Hierarchic Porous Materials from Inorganic Nanoparticles Stabilized with Mussel-Inspired Copolymers, Macromol. Rapid Commun. 35 (2014) 1763–1769. https://doi.org/10.1002/marc.201400363.

[176] H. Yabu, H. Ohshima, Y. Saito, Double-phase-functionalized magnetic janus polymer microparticles containing TiO_2 and Fe_2O_3 nanoparticles encapsulated in mussel-inspired amphiphilic polymers, ACS Appl. Mater. Interfaces. 6 (2014) 18122–18128. https://doi.org/10.1021/am506530s.

[177] H.J. Meredith, J.J. Wilker, The Interplay of Modulus, Strength, and Ductility in Adhesive Design Using Biomimetic Polymer Chemistry, Adv. Funct. Mater. 25 (2015) 5057–5065.

https://doi.org/10.1002/adfm.201501880.

[178] L. Li, B. Yan, L. Zhang, Y. Tian, H. Zeng, Mussel-inspired antifouling coatings bearing polymer loops, Chem. Commun. 51 (2015) 15780–15783. https://doi.org/10.1039/c5cc06852e.

[179] M. Steponaviciute, V. Klimkevicius, R. Makuska, Synthesis and

stability against oxidation of random brush copolymers carrying PEO side chains and catechol moieties, Mater. Today Commun. 25 (2020) 101262. https://doi.org/10.1016/j.mtcomm.2020.101262.

[180] I. Dobryden, M. Steponavičiūtė, V. Klimkevičius, R. Makuška, A. Dėdinaitė, X. Liu, R.W. Corkery, P.M. Claesson, Bioinspired Adhesion Polymers: Wear Resistance of Adsorption Layers, Langmuir. 35 (2019) 15515–15525.

https://doi.org/10.1021/acs.langmuir.9b01818.

[181] M. Šetka, F.A. Bahos, D. Matatagui, M. Potoček, Z. Kral, J. Drbohlavová, I. Gràcia, S. Vallejos, Love wave sensors based on gold nanoparticle-modified polypyrrole and their properties to ammonia and ethylene, Sensors Actuators B Chem. (2019) 127337. https://doi.org/10.1016/j.snb.2019.127337.

[182] Y. Han, J. Yang, W. Zhao, H. Wang, Y. Sun, Y. Chen, J. Luo, L. Deng, X. Xu, W. Cui, H. Zhang, Biomimetic injectable hydrogel microspheres with enhanced lubrication and controllable drug release for the treatment of osteoarthritis, Bioact. Mater. 6 (2021) 3596–3607. https://doi.org/10.1016/j.bioactmat.2021.03.022.

[183] X. Mao, K. Chen, Y. Zhao, C. Xiong, J. Luo, Y. Wang, B. Wang, H. Zhang, Bioinspired surface functionalization of biodegradable mesoporous silica nanoparticles for enhanced lubrication and drug release, Friction. 11 (2023) 1194–1211.

https://doi.org/10.1007/s40544-022-0648-z.

[184] J. Niu, H. Wang, J. Chen, X. Chen, X. Han, H. Liu, Bio-inspired zwitterionic copolymers for antifouling surface and oil-water separation, Colloids Surfaces A Physicochem. Eng. Asp. 626 (2021) 127016. https://doi.org/10.1016/j.colsurfa.2021.127016.

[185] A.A. D'souza, R. Shegokar, Polyethylene glycol (PEG): a versatile polymer for pharmaceutical applications, Expert Opin. Drug Deliv. 13 (2016) 1257–1275. https://doi.org/10.1080/17425247.2016.1182485.

[186] A. Kolate, D. Baradia, S. Patil, I. Vhora, G. Kore, A. Misra, PEG — A versatile conjugating ligand for drugs and drug delivery systems, J. Control. Release. 192 (2014) 67–81.

https://doi.org/10.1016/j.jconrel.2014.06.046.

[187] J.-F. Lutz, Polymerization of oligo(ethylene glycol) (meth)acrylates: Toward new generations of smart biocompatible materials, J. Polym. Sci. Part A Polym. Chem. 46 (2008) 3459–3470. https://doi.org/10.1002/pola.22706.

[188] S.B. Tiwari, J. DiNunzio, A. Rajabi-Siahboomi, Drug–Polymer Matrices for Extended Release, in: C.G. Wilson, P.J. Crowley (Eds.), Control. Release Oral Drug Deliv., Springer US, Boston, MA, 2011: pp. 131–159. https://doi.org/10.1007/978-1-4614-1004-1_7.

[189] A. Abuchowski, J.R. McCoy, N.C. Palczuk, T. van Es, F.F. Davis, Effect of covalent attachment of polyethylene glycol on immunogenicity and circulating life of bovine liver catalase., J. Biol. Chem. 252 (1977) 3582–3586. https://doi.org/10.1016/S0021-9258(17)40292-4.

[190] S.Y. Fam, C.F. Chee, C.Y. Yong, K.L. Ho, A.R. Mariatulqabtiah, W.S. Tan, Stealth Coating of Nanoparticles in Drug-Delivery Systems, Nanomaterials. 10 (2020) 787. https://doi.org/10.3390/nano10040787.

[191] V. Klimkevicius, E. Voronovic, G. Jarockyte, A. Skripka, F. Vetrone, R. Rotomskis, A. Katelnikovas, V. Karabanovas, Polymer brush coated upconverting nanoparticles with improved colloidal stability and cellular labeling, J. Mater. Chem. B. 10 (2022) 625–636. https://doi.org/10.1039/D1TB01644J.

[192] X. Zhang, Y. Dai, Recent development of brush polymers via polymerization of poly(ethylene glycol)-based macromonomers, Polym. Chem. 10 (2019) 2212–2222.

https://doi.org/10.1039/C9PY00104B.

[193] X. Lu, K. Zhang, PEGylation of therapeutic oligonucletides: From linear to highly branched PEG architectures, Nano Res. 11 (2018) 5519–5534. https://doi.org/10.1007/s12274-018-2131-8.

[194] Á. Szabó, I. Szanka, G. Tolnai, G. Szarka, B. Iván, LCST-type thermoresponsive behaviour of interpolymer complexes of well-defined poly(poly(ethylene glycol) methacrylate)s and poly(acrylic acid) synthesized by ATRP, Polymer (Guildf). 111 (2017) 61–66. https://doi.org/10.1016/j.polymer.2017.01.018.

[195] G. Vancoillie, D. Frank, R. Hoogenboom, Thermoresponsive poly(oligo ethylene glycol acrylates), Prog. Polym. Sci. 39 (2014) 1074–1095. https://doi.org/10.1016/j.progpolymsci.2014.02.005.

[196] I. Capek, Surface active properties of polyoxyethylene macromonomers and their role in radical polymerization in disperse systems, Adv. Colloid Interface Sci. 88 (2000) 295–357.

https://doi.org/10.1016/S0001-8686(99)00025-1.

[197] S. Shahalom, T. Tong, S. Emmett, B.R. Saunders, Poly(DEAEMa-co-PEGMa): A New pH-Responsive Comb Copolymer Stabilizer for Emulsions and Dispersions, Langmuir. 22 (2006) 8311–8317. https://doi.org/10.1021/la061229g.

[198] M. Steponaviciute, V. Klimkevicius, R. Makuska, Synthesis and Properties of Cationic Gradient Brush Copolymers Carrying PEO Side Chains and Catechol Moieties, Macromol. Chem. Phys. 222 (2021) 2000364. https://doi.org/10.1002/macp.202000364.

[199] M. Kavaliauskaite, M. Steponaviciute, J. Kievisaite, A. Katelnikovas, V. Klimkevicius, Synthesis and Study of Thermoresponsive Amphiphilic Copolymers via RAFT Polymerization, Polymers

(Basel). 14 (2022). https://doi.org/10.3390/polym14020229.

[200] V. Klimkevicius, R. Makuska, Successive RAFT polymerization of poly(ethylene oxide) methyl ether methacrylates with different length of PEO chains giving diblock brush copolymers, Eur. Polym. J. 86 (2017) 94–105. https://doi.org/10.1016/j.eurpolymj.2016.11.026.

[201] S. Lowe, N.M. O'Brien-Simpson, L.A. Connal, Antibiofouling polymer interfaces: poly(ethylene glycol) and other promising candidates, Polym. Chem. 6 (2015) 198–212.

https://doi.org/10.1039/C4PY01356E.

[202] B. Xu, C. Feng, J. Hu, P. Shi, G. Gu, L. Wang, X. Huang, Spin-Casting Polymer Brush Films for Stimuli-Responsive and Anti-Fouling Surfaces, ACS Appl. Mater. Interfaces. 8 (2016) 6685–6692. https://doi.org/10.1021/acsami.5b12820.

[203] J. Iruthayaraj, E. Poptoshev, A. Vareikis, R. Makuška, A. van der Wal, P.M. Claesson, Adsorption of Low Charge Density Polyelectrolyte Containing Poly(ethylene oxide) Side Chains on Silica: Effects of Ionic Strength and pH, Macromolecules. 38 (2005) 6152–6160. https://doi.org/10.1021/ma050851x.

[204] P. Linse, P.M. Claesson, Modeling of Bottle-Brush Polymer Adsorption onto Mica and Silica Surfaces: Effect of Side-Chain Length, Macromolecules. 43 (2010) 2076–2083.

https://doi.org/10.1021/ma902577m.

[205] M. Müller, S. Lee, H.A. Spikes, N.D. Spencer, The Influence of Molecular Architecture on the Macroscopic Lubrication Properties of the Brush-Like Co-polyelectrolyte Poly(L-lysine)- g -poly(ethylene glycol) (PLL- g -PEG) Adsorbed on Oxide Surfaces, Tribol. Lett. 15 (2003) 395–405.

https://doi.org/10.1023/B:TRIL.0000003063.98583.bb.

[206] J. Katta, Z. Jin, E. Ingham, J. Fisher, Biotribology of articular cartilage- A review of the recent advances, Med. Eng. Phys. 30 (2008) 1349–1363. https://doi.org/10.1016/j.medengphy.2008.09.004.

[207] T. Pettersson, A. Naderi, R. Makuška, P.M. Claesson, Lubrication Properties of Bottle-Brush Polyelectrolytes: An AFM Study on the Effect of Side Chain and Charge Density, Langmuir. 24 (2008) 3336–3347. https://doi.org/10.1021/la703229n.

[208] J. Iruthayaraj, G. Olanya, P.M. Claesson, Viscoelastic Properties of Adsorbed Bottle-brush Polymer Layers Studied by Quartz Crystal Microbalance — Dissipation Measurements, J. Phys. Chem. C. 112 (2008) 15028–15036. https://doi.org/10.1021/jp804395f.

[209] A. Naderi, G. Olanya, R. Makuška, P.M. Claesson, Desorption of bottle-brush polyelectrolytes from silica by addition of linear polyelectrolytes studied by QCM-D and reflectometry, J. Colloid Interface Sci. 323

(2008) 223–228. https://doi.org/https://doi.org/10.1016/j.jcis.2008.04.022.

[210] A. Naderi, J. Iruthayaraj, A. Vareikis, R. Makuška, P.M. Claesson, Surface Properties of Bottle-Brush Polyelectrolytes on Mica: Effects of Side Chain and Charge Densities, Langmuir. 23 (2007) 12222–12232. https://doi.org/10.1021/la701716t.

[211] G. Olanya, J. Iruthayaraj, E. Poptoshev, R. Makuska, A. Vareikis, P.M. Claesson, Adsorption Characteristics of Bottle-Brush Polymers on Silica: Effect of Side Chain and Charge Density, Langmuir. 24 (2008) 5341–5349. https://doi.org/10.1021/la703739v.

[212] G. Bijelic, A. Shovsky, I. Varga, R. Makuska, P.M. Claesson, Adsorption characteristics of brush polyelectrolytes on silicon oxynitride revealed by dual polarization interferometry, J. Colloid Interface Sci. 348 (2010) 189–197. https://doi.org/https://doi.org/10.1016/j.jcis.2010.03.067.

[213] X. Liu, A. Dedinaite, M. Rutland, E. Thormann, C. Visnevskij, R. Makuska, P.M. Claesson, Electrostatically Anchored Branched Brush Layers, Langmuir. 28 (2012) 15537–15547. https://doi.org/10.1021/la3028989.

[214] G. Heydari, E. Tyrode, C. Visnevskij, R. Makuska, P.M. Claesson, Temperature-Dependent Deicing Properties of Electrostatically Anchored Branched Brush Layers of Poly(ethylene oxide), Langmuir. 32 (2016) 4194–4202. https://doi.org/10.1021/acs.langmuir.6b00671.

[215] X. Liu, E. Thormann, A. Dedinaite, M. Rutland, C. Visnevskij, R. Makuska, P.M. Claesson, Low friction and high load bearing capacity layers formed by cationic-block-non-ionic bottle-brush copolymers in aqueous media, Soft Matter. 9 (2013) 5361–5371. https://doi.org/10.1039/C3SM27862J.

[216] G. Olanya, E. Thormann, I. Varga, R. Makuška, P.M. Claesson, Protein interactions with bottle-brush polymer layers: Effect of side chain and charge density ratio probed by QCM-D and AFM, J. Colloid Interface Sci. 349 (2010) 265–274. https://doi.org/https://doi.org/10.1016/j.jcis.2010.05.061.

[217] V. Klimkevicius, M. Steponaviciute, R. Makuska, Kinetics of RAFT polymerization and copolymerization of vinyl monomers by size exclusion chromatography, Eur. Polym. J. 122 (2020) 109356. https://doi.org/10.1016/J.EURPOLYMJ.2019.109356.

[218] Y. Xi, C.H. Choi, R. Chang, H.J. Kaper, P.K. Sharma, Tribology of Pore-Textured Hard Surfaces under Physiological Conditions: Effects of Texture Scales, Langmuir. 39 (2023) 6657–6665. https://doi.org/10.1021/acs.langmuir.2c03377.

[219] K. Ren, M.A. Reina Mahecha, M. Hübner, Z. Cui, H.J. Kaper, H.C. van

der Veen, P.K. Sharma, Tribology of enzymatically degraded cartilage mimicking early osteoarthritis, Friction. 11 (2023) 1724–1740. https://doi.org/10.1007/s40544-022-0701-y.

[220] K. Ren, H. Wan, H.J. Kaper, P.K. Sharma, Dopamine-conjugated hyaluronic acid delivered via intra-articular injection provides articular cartilage lubrication and protection, J. Colloid Interface Sci. 619 (2022) 207–218. https://doi.org/10.1016/j.jcis.2022.03.119.

[221] V. Pudžaitis, M. Talaikis, R. Sadzevičienė, L. Labanauskas, G. Niaura, Electrochemical SEIRAS Analysis of Imidazole-Ring-Functionalized Self-Assembled Monolayers, Materials (Basel). 15 (2022) 7221. https://doi.org/10.3390/ma15207221.

[222] M. Yaguchi, T. Uchida, K. Motobayashi, M. Osawa, Speciation of Adsorbed Phosphate at Gold Electrodes: A Combined Surface-Enhanced Infrared Absorption Spectroscopy and DFT Study, J. Phys. Chem. Lett. 7 (2016) 3097–3102.

https://doi.org/10.1021/acs.jpclett.6b01342.

[223] G. Odian, Principles of Polymerization, Wiley, 2004. https://doi.org/10.1002/047147875X.

[224] M. Fineman, S.D. Ross, Linear method for determining monomer reactivity ratios in copolymerization, J. Polym. Sci. 5 (1950) 259–262. https://doi.org/10.1002/pol.1950.120050210.

[225] F. Tüdos, T. Kelen, T. Földes-berezsnich, B. Turcsányi, Analysis of Linear Methods for Determining Copolymerization Reactivity Ratios. III. Linear Graphic Method for Evaluating Data Obtained at High Conversion Levels, J. Macromol. Sci. Part A - Chem. 10 (1976) 1513–1540. https://doi.org/10.1080/00222337608060768.

[226] V.E. Meyer, G.G. Lowry, Integral and differential binary copolymerization equations, J. Polym. Sci. Part A Gen. Pap. 3 (1965) 2843–2851. https://doi.org/10.1002/pol.1965.100030811.

[227] N. Roka, M. Pitsikalis, Statistical copolymers of N-vinylpyrrolidone and benzyl methacrylate via RAFT: Monomer reactivity ratios, thermal properties and kinetics of thermal decomposition, J. Macromol. Sci. Part A. 55 (2018) 222–230.

https://doi.org/10.1080/10601325.2017.1403858.

[228] C.J. Hawker, A.W. Bosman, E. Harth, New Polymer Synthesis by Nitroxide Mediated Living Radical Polymerizations, Chem. Rev. 101 (2001) 3661–3688. https://doi.org/10.1021/cr990119u.

[229] K. Matyjaszewski, J. Xia, Atom Transfer Radical Polymerization, Chem. Rev. 101 (2001) 2921–2990.

https://doi.org/10.1021/cr940534g.

[230] K. Matyjaszewski, Factors Affecting Rates of Comonomer Consumption in Copolymerization Processes with Intermittent

Activation, Macromolecules. 35 (2002) 6773–6781. https://doi.org/10.1021/ma0208180.

[231] R. Mao, M.B. Huglin, A new linear method to calculate monomer reactivity ratios by using high conversion copolymerization data: terminal model, Polymer (Guildf). 34 (1993) 1709–1715. https://doi.org/10.1016/0032-3861(93)90331-4.

[232] D. Chen, Y. Huang, S. Xu, H. Jiang, J. Wu, X. Jin, X. Zhu, Self-Assembled Polyprodrug Amphiphile for Subcutaneous Xenograft Tumor Inhibition with Prolonged Acting Time In Vivo, Macromol. Biosci. 17 (2017) 1700174. https://doi.org/10.1002/mabi.201700174.

[233] S. Kozuka, K. Kuroda, K. Ishihara, S. Yusa, Interpolymer association of amphiphilic diblock copolymers bearing pendant siloxane and phosphorylcholine groups, J. Polym. Sci. Part A Polym. Chem. 57 (2019) 1500–1507. https://doi.org/10.1002/pola.29407.

[234] S.J. Byard, C.T. O'Brien, M.J. Derry, M. Williams, O.O. Mykhaylyk, A. Blanazs, S.P. Armes, Unique aqueous self-assembly behavior of a thermoresponsive diblock copolymer, Chem. Sci. 11 (2020) 396–402. https://doi.org/10.1039/C9SC04197D.

[235] M. Arotçaréna, B. Heise, S. Ishaya, A. Laschewsky, Switching the Inside and the Outside of Aggregates of Water-Soluble Block Copolymers with Double Thermoresponsivity, J. Am. Chem. Soc. 124 (2002) 3787–3793. https://doi.org/10.1021/ja012167d.

[236] T. Shimizu, T. Goda, N. Minoura, M. Takai, K. Ishihara, Super-hydrophilic silicone hydrogels with interpenetrating poly(2-methacryloyloxyethyl phosphorylcholine) networks, Biomaterials. 31 (2010) 3274–3280.

https://doi.org/https://doi.org/10.1016/j.biomaterials.2010.01.026.

[237] X.-H. Qin, B. Senturk, J. Valentin, V. Malheiro, G. Fortunato, Q. Ren, M. Rottmar, K. Maniura-Weber, Cell-Membrane-Inspired Silicone Interfaces that Mitigate Proinflammatory Macrophage Activation and Bacterial Adhesion, Langmuir. 35 (2019) 1882–1894. https://doi.org/10.1021/acs.langmuir.8b02292.

[238] A.U. Alam, M.M.R. Howlader, M.J. Deen, The effects of oxygen plasma and humidity on surface roughness, water contact angle and hardness of silicon, silicon dioxide and glass, J. Micromechanics Microengineering. 24 (2014) 035010. https://doi.org/10.1088/0960-1317/24/3/035010.

[239] Y. Iwasaki, M. Ijuin, A. Mikami, N. Nakabayashi, K. Ishihara, Behavior of blood cells in contact with water-soluble phospholipid polymer, J. Biomed. Mater. Res. 46 (1999) 360–367. https://doi.org/10.1002/(SICI)1097-4636(19990905)46:3<360::AID-JBM8>3.0.CO;2-Z.

[240] Y. Iwasaki, K. Akiyoshi, Design of Biodegradable Amphiphilic

Polymers: Well-Defined Amphiphilic Polyphosphates with Hydrophilic Graft Chains via ATRP, Macromolecules. 37 (2004) 7637–7642. https://doi.org/10.1021/ma049043g.

[241] D. Ihara, Y. Higaki, N.L. Yamada, F. Nemoto, Y. Matsuda, K. Kojio, A. Takahara, Cononsolvency of Poly[2-(methacryloyloxy)ethyl phosphorylcholine] in Ethanol–Water Mixtures: A Neutron Reflectivity Study, Langmuir. 38 (2022) 5081–5088. https://doi.org/10.1021/acs.langmuir.1c01762.

[242] S.M.T. Chan, C.P. Neu, G. DuRaine, K. Komvopoulos, A.H. Reddi, Atomic force microscope investigation of the boundary-lubricant layer in articular cartilage, Osteoarthr. Cartil. 18 (2010) 956–963. https://doi.org/10.1016/j.joca.2010.03.012.

[243] H. Wan, K. Ren, H.J. Kaper, P.K. Sharma, A bioinspired mucoadhesive restores lubrication of degraded cartilage through reestablishment of lamina splendens, Colloids Surfaces B Biointerfaces. 193 (2020) 110977. https://doi.org/10.1016/j.colsurfb.2020.110977.

[244] M. Caligaris, G.A. Ateshian, Effects of sustained interstitial fluid pressurization under migrating contact area, and boundary lubrication by synovial fluid, on cartilage friction, Osteoarthr. Cartil. 16 (2008) 1220–1227. https://doi.org/10.1016/j.joca.2008.02.020.

[245] Y. Wang, W. Zhai, H. Zhang, S. Cheng, J. Li, Injectable Polyzwitterionic Lubricant for Complete Prevention of Cardiac Adhesion, Macromol. Biosci. 23 (2023) 2200554. https://doi.org/10.1002/mabi.202200554.

[246] V. Klimavicius, V. Klimkevicius, K. Aidas, S. Balčiūnas, J. Banys, R. Makuska, V. Balevicius, Fine structural features and proton conduction in zwitterionic poly(2-methacryloyloxyethyl phosphorylcholine) (PMPC): Multinuclear solid-state NMR, impedance and FTIR spectroscopy study, React. Funct. Polym. 192 (2023) 105727.

https://doi.org/10.1016/j.reactfunctpolym.2023.105727.

[247] A. Naderi, J. Iruthayaraj, T. Pettersson, R. Makuška, P.M. Claesson, Effect of Polymer Architecture on the Adsorption Properties of a Nonionic Polymer, Langmuir. 24 (2008) 6676–6682. https://doi.org/10.1021/la800089v.

[248] M. Kohri, S. Yamazaki, S. Irie, N. Teramoto, T. Taniguchi, K. Kishikawa, Adhesion Control of Branched Catecholic Polymers by Acid Stimulation, ACS Omega. 3 (2018) 16626–16632. https://doi.org/10.1021/acsomega.8b02768.

[249] S.A. Siddiqui, A. Dwivedi, P.K. Singh, T. Hasan, S. Jain, N. Sundaraganesan, H. Saleem, N. Misra, Vibrational dynamics and potential energy distribution of two well-known neurotransmitter receptors: Tyramine and dopamine hydrochloride, J. Theor. Comput.

Chem. 8 (2009) 433–450.

https://doi.org/10.1142/S0219633609004861.

[250] A. Lagutschenkov, J. Langer, G. Berden, J. Oomens, O. Dopfer, Infrared spectra of protonated neurotransmitters: Dopamine, Phys. Chem. Chem. Phys. 13 (2011) 2815–2823.

https://doi.org/10.1039/c0cp02133d.

[251] W. Pohle, M. Bohl, H. Böhlig, Interpretation of the influence of hydrogen bonding on the stretching vibrations of the PO-2 moiety, J. Mol. Struct. 242 (1991) 333–342. https://doi.org/10.1016/0022-2860(91)87145-8.

[252] E. Navakauskas, G. Niaura, S. Strazdaite, Effect of deuteration on a phosphatidylcholine lipid monolayer structure: New insights from vibrational sum-frequency generation spectroscopy, Colloids Surfaces B Biointerfaces. 220 (2022) 112866.

https://doi.org/10.1016/j.colsurfb.2022.112866.

[253] N. Aktaş, N. Şahiner, Ö. Kantoğlu, B. Salih, A. Tanyolaç, Biosynthesis and Characterization of Laccase Catalyzed Poly(Catechol), J. Polym. Environ. 11 (2003) 123–128.

https://doi.org/10.1023/A:1024639231900.

[254] T. López, J.L. Bata-García, D. Esquivel, E. Ortiz-Islas, R. Gonzalez, J. Ascencio, P. Quintana, G. Oskam, F.J. Álvarez-Cervera, F.J. Heredia-López, J.L. Góngora-Alfaro, Treatment of parkinson's disease: Nanostructured sol-gel silica-dopamine reservoirs for controlled drug release in the central nervous system, Int. J. Nanomedicine. 6 (2011) 19–31. https://doi.org/10.2147/IJN.S13223.

[255] A. Thakur, S. Ranote, D. Kumar, K.K. Bhardwaj, R. Gupta, G.S. Chauhan, Synthesis of a PEGylated Dopamine Ester with Enhanced Antibacterial and Antifungal Activity, ACS Omega. 3 (2018) 7925–7933. https://doi.org/10.1021/acsomega.8b01099.

[256] K. Czamara, K. Majzner, M.Z. Pacia, K. Kochan, A. Kaczor, M. Baranska, Raman spectroscopy of lipids: A review, J. Raman Spectrosc. 46 (2015) 4–20. https://doi.org/10.1002/jrs.4607.

[257] N.B. Colthup, L.H. Daly, S.E. Wiberley, Introduction to infrared and Raman spectroscopy, Academic Press, Inc., 1990.

[258] M. Talaikis, O. Eicher-Lorka, G. Valinčius, G. Niaura, Water-induced structural changes in the membrane-anchoring monolayers revealed by isotope-edited SERS, J. Phys. Chem. C. 120 (2016) 22489–22499. https://doi.org/10.1021/acs.jpcc.6b07686.

[259] J. Lipkowski, Chapter One - Biomimetic Membrane Supported at a Metal Electrode Surface: A Molecular View, in: A. Iglič, C.V.B.T.-A. in P.L.B. and L. Kulkarni (Eds.), Academic Press, 2014: pp. 1–49. https://doi.org/https://doi.org/10.1016/B978-0-12-418698-9.00001-0.

[260] A.P. Shivabalan, F. Ambrulevicius, M. Talaikis, V. Pudzaitis, G. Niaura, G. Valincius, Effect of pH on Electrochemical Impedance Response of Tethered Bilayer Lipid Membranes: Implications for Quantitative Biosensing, Chemosensors. 11 (2023). https://doi.org/10.3390/chemosensors11080450.

SANTRAUKA

Įvadas

Biomedžiagos yra tokios natūralios arba sintetinės medžiagos, kurios gali sąveikauti su įvairiomis biologinėmis sistemomis. Paprastai šios medžiagos pasižymi tokiomis savybėmis, kaip biosuderinamumas, biologinis aktyvumas, cheminis stabilumas, ir kai kuriais atvejais – bioinertiškumas. Pastaroji savybė itin svarbi biomedžiagų taikymui įvairių paviršių modifikavimui, kurių pagrindinis tikslas – baltymų atstūmimas nuo modifikuoto paviršiaus. Baltymų adsorbcija gali sukelti kraujo krešėjimą, uždegimą, imunoreakcijas, bakterijų sukibimą, ląstelių sukibimą ir ląstelių diferenciaciją. Būtent dėl šių priežasčių siekiama rasti tokias sintetines medžiagas, kurios galėtų užkirsti kelią baltymų adsorbcijai ant tam tikrų paviršių. Didelė pažanga, siekiant įveikti šią problemą, buvo padaryta sukūrus cviterjoninę fosforilcholino funkcinę grupę turintį monomerą 2-metakriloiloksietilfosforilcholiną (MPC). Turėdamas panašumų į fosfatidilcholiną, esantį eukariotų ląstelių plazminėse membranose, MPC pasižymi ne tik puikiu biosuderinamumu, bet ir bioinertinėmis savybėmis. Šių savybių priežastis yra cviterjoninė fosforilcholino (PC) grupė, kuriai būdingos vidinės elektrostatinės sąveikos ir ją supantis hidratinis apvalkalas.

Fosforilcholino polimerai yra reikšmingi biomedžiagų moksle dėl savo unikalių savybių – priešuždegiminio poveikio, biologinio suderinamumo, biolubrikacinio poveikio, kas yra labai svarbu tokias medžiagas taikant biomedicinos inžinerijoje. Tokie polimerai bent iš dalies imituoja ląstelių membranas, todėl tinkami medicininiams implantams, dangoms ir vaistų tiekimo sistemoms. Dėl išvardytų savybių MPC pagrindu susintetinti polimerai yra naudojami ir tyrinėjami įvairiose mokslo srityse, ypač biomedicinoje. Poli(2-metakriloiloksietilfosforilcholinas) (pMPC) yra populiariausias ir plačiausiai ištirtas cviterjoninis polimeras, o jo pirmtakas MPC monomeras yra komerciškai prieinamas. Viena iš daugiausiai dėmesio sulaukiančių MPC polimerų taikymo sričių yra tokių polimerų nanosluoksnių suformavimas. Siekiant modifikuoti paviršius pMPC monosluoksniu, būtina sintetinti diblokinius kopolimerus, sudarytus iš pMPC bloko ir kito polimerinio bloko, pasižyminčio skirtingomis savybėmis. Pageidautina, kad kitas polimerinis blokas turėtų tokias funkcines grupes, kurios užtikrintų gerą sukibimą su paviršiumi. Naudojant tokius kopolimerus, galima modifikuoti įvairių medicinos prietaisų paviršius, siekiant padidinti biologinį suderinamumą ir sumažinti baltymų adsorbciją.

Darbo mokslinis naujumas

Pirmą kartą buvo ištirta cviterjoninio monomero MPC ir makromonomero polietilenoksido metiletermetakrilato (PEOMEMA) su gana ilga PEO grandine (19 etileno oksido grandžių) RAFT kopolimerizacijos kinetika ir susintetinti kopolimerai p(MPC-*grad*-PEOMEMA). Nustatyti MPC ir PEOMEMA santykiniai aktyvumai r_1 ir r_2 RAFT kopolimerizacijoje ir įrodyta gradientinė kopolimerų struktūra. Pirmą kartą RAFT polimerizacijos būdu susintetinti numatytos struktūros hidrofiliniai diblokiniai kopolimerai pMPC-*b*-pPEOMEMA ir amfifiliniai diblokiniai kopolimerai pMPC-*b*-pDOPMA. Įvertintos gradientinių ir diblokinių MPC ir PEOMEMA kopolimerų lubrikacinis efektyvumas PDMS-stiklo ir kremzlės-stiklo sistemose. Diblokinių kopolimerų pMPC-*b*-pDOPMA su apsaugotomis ir neapsaugotomis katecholinėmis grupėmis adsorbcija ant auksuoto paviršiaus ištirta naudojant ATR-FTIR, paviršiaus sustiprintą infraraudonąją absorbcijos spektroskopiją (SEIRAS) ir atspindžio-absorbcijos infraraudonąją spektroskopiją (RAIRS). Kopolimerai su apsaugotomis katecholio grupėmis pasižymėjo greita fizine adsorbcija ir lengva desorbcija, o kopolimerai su neapsaugotomis katecholio grupėmis pasižymėjo chemine adsorbcija su lėtesne dinamika, tačiau stipresne sąveika su aukso paviršiumi.

Darbo tikslas – naujų norimos struktūros MPC grandis turinčių kopolimerų sintezė ir jų tirpalų savybių bei adsorbcijos tyrimas. Disertacijos tikslui pasiekti buvo iškelti šie **uždaviniai**:
1. Ištirti MPC ir PEOMEMA RAFT kopolimerizacijos kinetiką;
2. Susintetinti norimos struktūros MPC diblokinius kopolimerus su PEOMEMA ir DOPMA;
3. Apibūdinti MPC kopolimerus ir įvertinti jų tirpalų savybes;
4. Ištirti lubrikacines MPC ir PEOMEMA kopolimerų vandeninių tirpalų savybes;
5. Ištirti MPC ir DOPMA diblokinių kopolimerų adsorbcijos ant aukso paviršiaus dinamiką.

Pagrindiniai ginamieji disertacijos teiginiai:
1. RAFT kopolimerizacijos būdu susintetinti MPC ir PEOMEMA kopolimerai turi aiškiai išreikštą gradientinę mikrostruktūrą.
2. MPC ir DOPMA amfifiliniai diblokiniai kopolimerai gali būti sėkmingai susintetinti paeiliui vykdant MPC ir acetonidu apsaugoto DOPMA RAFT polimerizaciją metanolyje.

3. Gradientiniai ir diblokiniai MPC ir DOPMA kopolimerai pasižymi superhidrofiliškumu, jiems būdingas konetirpumas mišriuose vandens ir etanolio tirpaluose.

4. MPC ir PEOMEMA gradientiniai ir diblokiniai kopolimerai veikia kaip efektyvūs lubrikantai PDMS-stiklo ir kremzlės-stiklo sistemose.

5. MPC ir DOPMA diblokiniai kopolimerai pasižymi chemine adsorbcija ant aukso paviršiaus, po kurios vyksta adsorbuotų sluoksnių persiorientavimas.

Medžiagos ir metodai

RAFT grandinės perdavos agentas 4-((((butiltio)karbonotioil)tio)-4-cianopentano rūgštis) (GPA) ir acetonidu apsaugotas dopamino metakrilamidas (ADOPMA) buvo sintetinami pagal žinomas metodikas ir naudojami šviežiai paruošti. Gradientiniai ir blokiniai MPC kopolimerai buvo sintetinami vykdant RAFT (ko)polimerizaciją metanolio arba metanolio-vandens tirpaluose, GPA ir iniciatoriaus moliniam santykiui esant 3:1. (Ko)polimerizacijos eiga buvo sekama naudojant molekulinių sietų chromatografiją (MSC) ir/arba ^{1}H BMR spektroskopiją. Susintetinti kopolimerai buvo gryninami vykdant dializę ir liofilizuojant. Apsauginė acetonido grupė DOPMA grandyse buvo nuimama naudojant trifluoroacto rūgštį dichlormetano ir vandens mišinyje.

Susintetinti kopolimerai buvo apibūdinti naudojant įvairius analitinius instrumentinius metodus. Naudojant molekulinių sietų chromatografijos sistemą *Viscotek TDAmax* su 4 jutikliais, buvo nustatyta polimerų vidutinė skaitinė molekulinė masė (M_n) ir dispersiškumo indeksas (Đ). Naudojant ^{1}H BMR spektroskopiją (Bruker 400 Ascend™), buvo įrodyta susidarančių polimerų struktūra, nustatyta kopolimerų sudėtis. Dinaminės šviesos sklaidos (DLS) matavimai naudojant *Zetasizer Nano ZS* sudarė galimybes įvertinti polimerų tirpumą ir agregaciją. Kopolimerų vandeninių tirpalų paviršiaus įtempis buvo nustatytas naudojant tenziometrą *K100 MK2*, o kopolimerų hidrofiliškumas (vandens kontaktinis kampas) – optinį tenziometrą *Theta Lite*. Lubrikacinės MPC ir PEOMEMA kopolimerų savybės buvo tiriamos Groningeno universiteto Medicinos centro prof. P. Sharma grupėje (Olandija), atliekant tribologinius bandymus PDMS-stiklo ir kremzlės-stiklas sistemose. MPC ir DOPMA kopolimerų adsorbcijos ant aukso paviršiaus dinamika buvo tiriama Fizinių ir technologijos mokslų centre (prof. G. Niauros grupė), naudojant atspindžio-absorbcijos infraraudonųjų spindulių spektroskopiją (RAIRS) ir paviršiaus sustiprintos infraraudonųjų spindulių absorbcijos spektroskopiją (SEIRAS).

1. MPC ir PEOMEMA RAFT kopolimerizacijos kinetikos tyrimas

Kopolimerų p(MPC-*ko*-PEOMEMA) sintezės schema, vykdant MPC ir PEOMEMA RAFT kopolimerizaciją, pateikta 1a paveiksle. Yra žinoma, kad RAFT kopolimerizacijos metu galima gauti statistinį arba gradientinį kopolimerą. Kopolimerų struktūra priklauso nuo monomerų santykinių aktyvumų, kuriuos galima nustatyti tiriant kopolimerizacijos kinetiką. MPC ir PEOMEMA RAFT kopolimerizacijos kinetika buvo tirta ^{1}H BMR spektroskopijos (1b pav.) ir MSC metodais. Vykdant RAFT kopolimerizaciją, iš reakcijos mišinio periodiškai buvo imami mėginiai ir analizuojami MSC ir/arba ^{1}H BMR spektroskopijos metodais. Eliuentas MSC kolonėlėje buvo toks pat kaip tirpiklis sintetinant kopolimerus, t.y. MeOH:vanduo = 3:1 v/v.
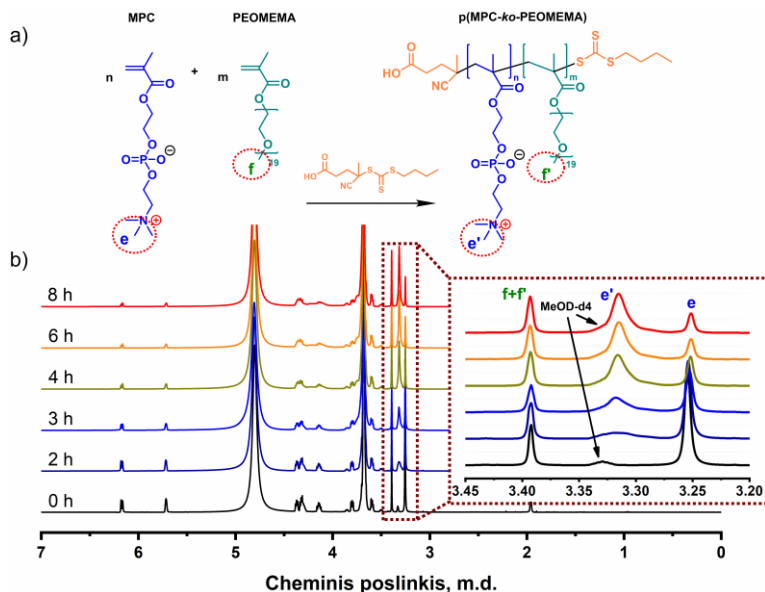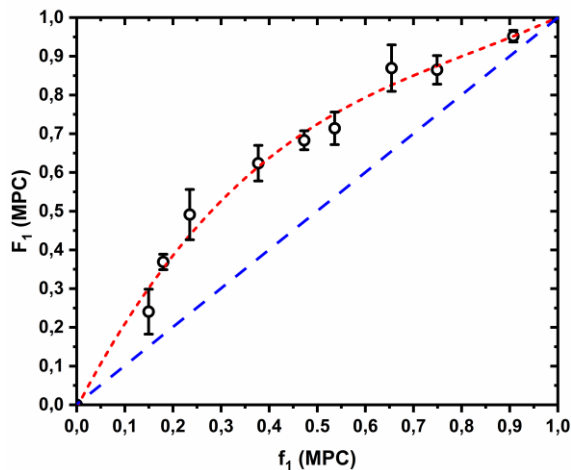

1 pav. MPC ir PEOMEMA RAFT kopolimerizacijos schema (a) ir reakcijos mišinio [MPC]$_0$:[PEOMEMA]$_0$ = 53:47 mol.% [1]H BMR spektrai (b); intarpas dešinėje – išplėsta spektrų sritis ties 3,15-3,45 m.d.

1b paveiksle pateikti reakcijos mišinio ^{1}H BMR spektrai, užrašyti mėginiai buvo paimti iš reakcijos mišinio prieš polimerizaciją ir praėjus 2, 3, 4, 6 ir 8 valandoms po polimerizacijos pradžios. Monomerų vinilgrupės protonų cheminiai poslinkiai matomi ties 5,71 m.d., 6,16 m.d. ir 6,17 m.d., tačiau dėl abiejų monomerų cheminių poslinkių dalinio persidengimo jų

negalima panaudoti monomerų koncentracijos pokyčiams įvertinti. Šių cheminių poslinkių intensyvumo mažėjimas duoda galimybę apskaičiuoti bendrą monomerų konversiją. Cheminis poslinkis ties 3,39 m.d. priskiriamas -OCH_3 grupei, esančiai tiek PEOMEMA monomere, tiek jo kopolimere. MPC monomere esančios -$N(CH_3)_3$ grupės protonų cheminis poslinkis yra ties 3,25 m.d., o tos pačios grupės, esančios kopolimere, cheminis poslinkis yra ties 3,31 m.d.; deja, pastarasis signalas nėra tinkamas kopolimerizacijos kinetikai tirti dėl persidengimo su deuteruoto metanolio signalu. Kita vertus, monomere esančios -$N(CH_3)_3$ grupės signalo intensyvumo mažėjimas duoda galimybę apskaičiuoti monomero sunaudojimą ir kopolimero sudėtį tam tikru laiko momentu.

Reakcijos mišinių prieš kopolimerizaciją tyrimas BMR spektroskopijos metodu parodė, kad faktinis monomerų santykis šiek tiek skyrėsi nuo apskaičiuoto. Pvz., ruošto kaip ekvimolinis monomerų mišinio sudėtis buvo [MPC]:[PEOMEMA] = 53:47 mol.%. Kopolimerizacija buvo vykdoma deuterintuose tirpikliuose BMR ampulėse, reakciją nutraukiant esant mažoms konversijoms (3-21 %). Pradinė monomerų mišinio ir kopolimero sudėtis apskaičiuota pagal ^{1}H BMR spektrus. Kopolimero sudėties priklausomybė nuo pradinio monomerų mišinio sudėties pateikta 2 pav.; matyti, kad, lyginant su naudojamu monomerų mišiniu, kopolimere yra daugiau MPC grandžių.


2 pav. Teorinė (raudona punktyrinė kreivė) ir eksperimentinė (taškai su paklaidų ribomis) MPC ir PEOMEMA kopolimerų, susintetintų vykdant RAFT kopolimerizaciją, sudėties F_1 priklausomybė nuo pradinės komonomerų mišinio sudėties f_1. Teorinė priklausomybė apskaičiuota naudojant monomerų santykinius aktyvumus $r_1 = 2{,}48$, $r_2 = 0{,}40$.
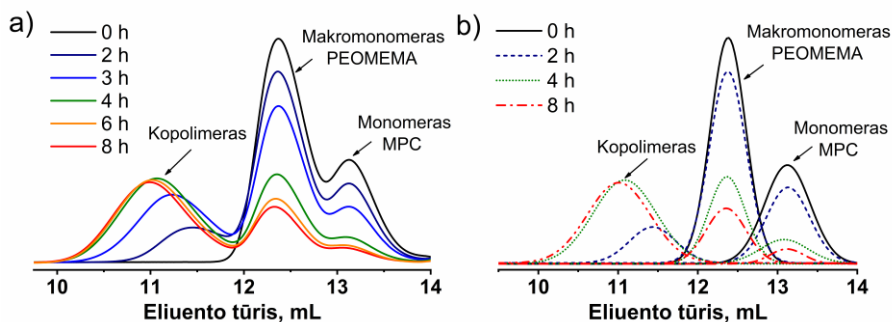
3 pav. Reakcijos mišinių MSC eliuogramos (a) ir dekonvoliuotų MSC eliuogramų kitimas (b) MPC ir PEOMEMA RAFT kopolimerizacijos metu. Eliuentas MeOD-*d4*:D_2O (3:1, v/v), kuriame yra 0,1 M $NaNO_3$; $[MPC]_0$: $[PEOMEMA]_0 = 53:47$ mol.%.

MPC (M_1) ir PEOMEMA (M_2) santykiniai aktyvumai kopolimerizacijoje r_1 ir r_2 nustatyti naudojant Mejerio ir Lowry metodą, $r_1 = 2,48$ ir $r_2 = 0,40$. Kopolimerizacijos eiga – monomerų koncentracijos mažėjimas ir kopolimero koncentracijos didėjimas – buvo sekama naudojant molekulinių sietų chromatografiją (MSC) (3 pav.). Pradinio ruošto kaip ekvimolinis monomerų mišinio analizė ^{1}H BMR spektroskopijos ir MSC metodais parodė, kad šiais metodais buvo nustatyta labai skirtinga monomerų mišinio sudėtis – 53 mol.% MPC (BMR) ir 69 mol.% MPC (MSC). Padidintas MPC kiekis kopolimere, nustatytas MSC metodu, galėtų būti aiškinamas padidintu MPC hidrodinaminiu tūriu, priklausančiu nuo fosforilgrupės hidratacijos. Monomerų mišinio sudėtis, nustatyta ^{1}H BMR ir MSC metodais, sutapo, padarius prielaidą, kad kiekviena MPC molekulė sulaiko maždaug 15 vandens molekulių, t.y. hidratuotos MPC molekulinė masė yra 565.

Eksperimentinės ir teoriškai apskaičiuotos momentinės kopolimero sudėties kitimo kopolimerizacijos eigoje kreivės labai skiriasi tarpusavyje, o tai rodo, kad teorinis modelis prastai aprašo faktinę RAFT metodu sintetinamų kopolimerų p(MPC-*co*-PEOMEMA) mikrostruktūrą. Tikėtina, kad šį neatitikimą lemia skirtingi monomerų sunaudojimo greičiai grįžtamosios deaktyvacijos radikalinėje kopolimerizacijoje, lyginant su įprasta radikaline kopolimerizacija. Tiksliau, RAFT kopolimerizacijos aktyvavimo ir deaktyvavimo greičio konstantos priklauso nuo to, kokia grandis yra augančios grandinės gale – MPC ar PEOMEMA; MPC aktyvavimo greičio konstanta didesnė, todėl šis monomeras sunaudojamas greičiau, todėl susidaro gradientinė kopolimero mikrostruktūra.
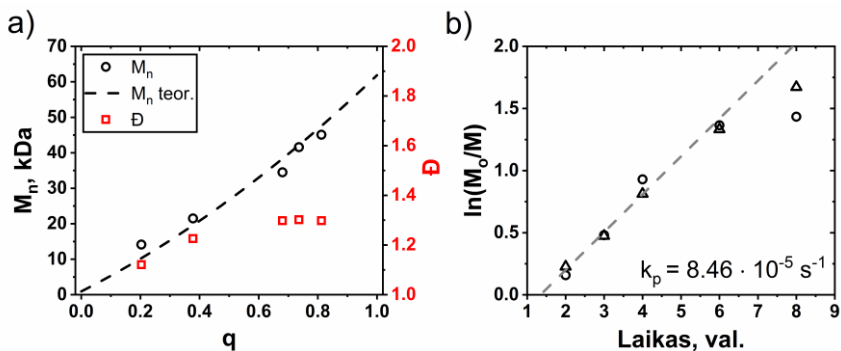
4 pav. Kopolimerų molekulinės masės (○) ir dispersiškumo (□) kitimas RAFT kopolimerizacijos metu (a); punktyrinė linija – teorinė (apskaičiuota) kopolimerų molekulinės masės priklausomybė nuo konversijos; MPC ir PEOMEMA RAFT kopolimerizacijos greičio konstantos nustatymas (b); eksperimentiniai taškai gauti MSC (Δ) ir ^{1}H BMR spektroskopijos (○) metodais. [MPC]$_0$: [PEOMEMA]$_0$ = 53:47 mol. %, MeOD-*d4*:D$_2$O (3:1 v/v).

4a pav. parodytas kopolimerų molekulinės masės ir dispersiškumo kitimas RAFT kopolimerizacijos metu. MSC metodu nustatyta kopolimerų molekulinė masė artima teorinėms (apskaičiuotoms) vertėms, o tai reiškia, kad kopolimerizacija yra kontroliuojama. Galima konstatuoti, kad vykdant MPC ir PEOMEMA RAFT kopolimerizaciją ir naudojant tritiokarbonato tipo grandinės perdavos agentą (GPA), gaunami gradientiniai kopolimerai, kurių molekulinė masė prognozuojama, o dispersiškumas yra pakankamai mažas (Đ ≤ 1,3). Monomerų sunaudojimo kopolimerizacijos metu greitis, nustatytas tiek ^{1}H BMR spektroskopijos, tiek ir MSC metodais, sutapo ir buvo gerai aprašomas pseudopirmosios eilės kinetine lygtimi (4b pav.). Šie rezultatai patvirtino, kad MSC yra tinkamas metodas RAFT kopolimerizacijos kinetikai tirti. Artimo ekvimoliniam mišinio RAFT kopolimerizacijos greičio konstanta yra gana didelė ir lygi 8,46×10^{-5} s^{-1}.

1 lentelė. Kopolimerų p(MPC-*grad*-PEOMEMA) sudėtis ir molekuliniai rodikliai ([M]$_0$:[CTA]$_0$:[ACVA]$_0$ = 240:3:1, τ = 24 h).

Bandinio numeris	[MPC]$_0$/ [PEOMEMA]$_0$	Išeiga, %	Kopolimero sudėtis, MPC mol.%	M$_n$, kDa	PL	Đ
1	25:75	51	31,9	39,4	61	1,30
2	50:50	64	59,7	34,1	65	1,25
3	75:25	70	77,4	33,7	73	1,19

Vykdant RAFT kopolimerizaciją, buvo susintetinta skirtingos sudėties gradientinių kopolimerų p(MPC-*grad*-PEOMEMA) serija (1 lentelė). Kopolimerizaciją vykdant 24 val., buvo gauti kopolimerai, kurių polimerizacijos laipsnis PL 60-70, o dispersiškumo indeksas Đ 1,2-1,3. Didžiausias dispersiškumas (Đ 1,30) buvo būdingas šepetiniam kopolimerui, turinčiam didžiausią PEOMEMA monomerinių grandžių kiekį.

2. MPC ir PEOMEMA diblokinių polimerų sintezė

Diblokiniai kopolimerai pMPC-*b*-p(PEO$_{19}$MEMA) buvo sintetinami pirmiausia susintetinant pMPC, ir vėliau pratęsiant šio polimero, turinčio aktyvią galinę tritiogrupę, grandinę PEOMEMA grandimis. MPC ir PEO$_{19}$MEMA diblokinių polimerų sintezės schema pateikta 1 schemoje.
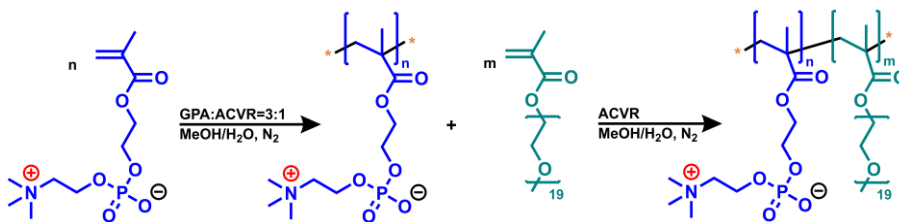

Schema 1. Diblokinio kopolimero pMPC-*b*-p(PEO$_{19}$MEMA) sintezės schema.

MPC RAFT polimerizacija buvo vykdoma mišriame tirpiklyje MeOH/vanduo = 3/1 v/v. Keičiant MPC ir GPA santykį, buvo susintetinti įvairios molekulinės masės pMPC. MPC RAFT polimerizacija buvo gerai kontroliuojama, gauti polimerai su labai mažu dispersiškumo indeksu – Đ apie 1,1. Trys skirtingos molekulinės masės (PL 18, 27 ir 41) pMPC mėginiai buvo panaudoti kaip makroGPA grandinei pratęsti jų tirpale vykdant PEO$_{19}$MEMA arba PEO$_9$MEMA RAFT polimerizaciją. Grandinės pratęsimas (antrojo bloko, sudaryto iš PEOMEMA grandžių, susidarymas) buvo stebimas registruojant reakcijos mišinių MSC eliucijos kreives.

5 pav. pateiktos reakcijos mišinių, paimtų baigus MPC RAFT polimerizaciją ir pMPC grandinę pratęsus PEO$_9$MEMA arba PEO$_{19}$MEMA grandimis, MSC eliucijos kreivės. Visose eliucijos kreivėse yra matomos polimero ir nesureagavusio monomero smailės. Prailginant pMPC grandinę, nesureagvusio PEOMEMA monomero lieka gana daug, ženkliai daugiau nei pirmojoje polimerizacijos stadijoje. Tai reiškia, kad PEOMEMA monomero konversija buvo mažesnė, nei MPC. Nepaisant to, blokiniam kopolimerui

priskiriamos smailės eliucijos kreivėse buvo vienmodalės ir pasislinkusios į mažesnį eliuento tūrį, palyginti su pMPC smailėmis (5 pav.). Tai įrodo, kad susidarė blokiniai kopolimerai, kurių molekulinė masė yra ženkliai didesnė už pMPC molekulinę masę. Diblokinių kopolimerų dispersiškumas pakankamai mažas, apie 1,2 – 1,3.
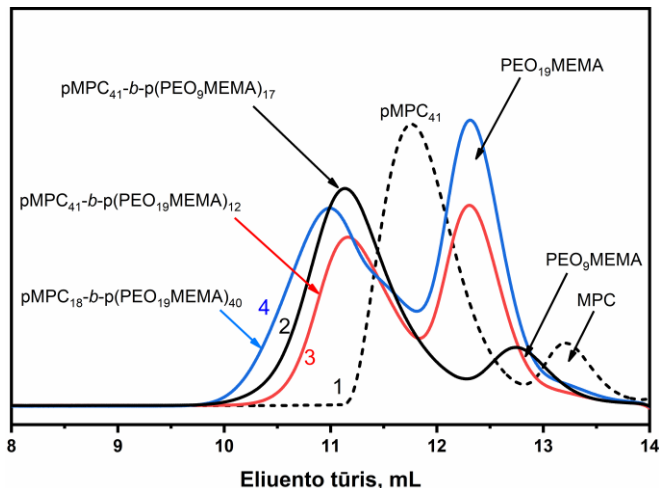
5 pav. Reakcijos mišinių MSC eliuogramos, užrašytos po 8 valandų MPC polimerizacijos (1) ir 24 valandų PEO_9MEMA (2) arba $PEO_{19}MEMA$ (3,4) polimerizacijos, pratęsiant pMPC grandinę. Eliuentas $MeOH:H_2O$ (3:1, v/v) plius 0,1 M $NaNO_3$.

6 pav. pateikti pMPC ir diblokinių kopolimerų pMPC-*b*-pPEOMEMA ^{1}H BMR spektrai. Kopolimero sudėčiai apskaičiuoti tinkamiausi buvo cheminiai poslinkiai ties 3,33 m.d. ir 3,37 m.d., kurie priskirti atitinkamai MPC ir PEOMEMA grandims (6 pav., intarpas).

Pirmojo bloko ilgis buvo artimas teoriniam (apskaičiuotam), PL nuo 18 iki 41. pPEOMEMA bloko ilgis buvo apskaičiuotas dviem metodais – iš diblokinių kopolimerų ir pMPC MSC duomenų ir iš kopolimerų ^{1}H BMR spektrų, atsižvelgiant į MSC metodu nustatytą pirmojo bloko PL. Abiem metodais apskaičiuotas antrojo bloko PL buvo panašus. Antrojo bloko PL buvo nedidelis, dažniausiai nuo 20 iki 40. Susintetinta serija diblokinių kopolimerų pMPC-*b*-pPEOMEMA su skirtingu abiejų blokų ilgiu.
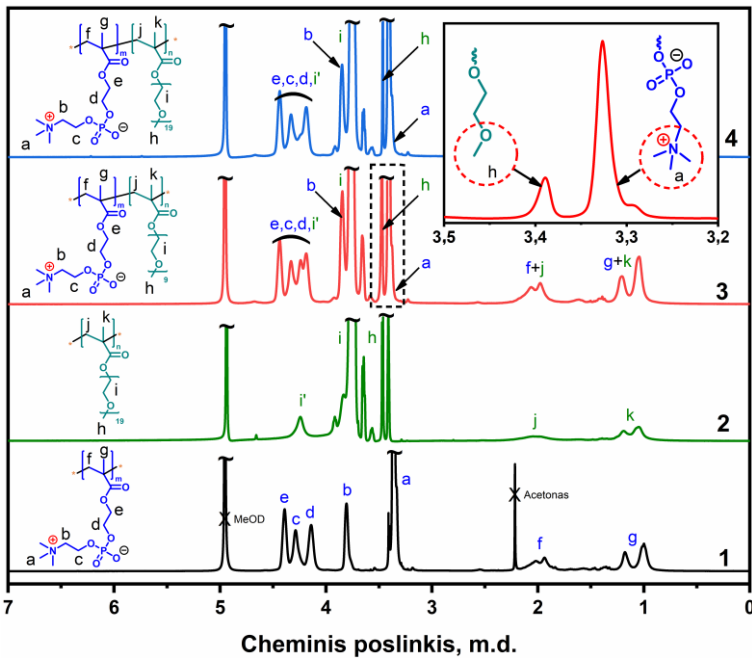
6 pav. ^{1}H BMR spektrai: pMPC (1), pPEO$_{19}$MEMA (2), pMPC$_{41}$-*b*-p(PEO$_9$MEMA)$_{17}$ (3) ir pMPC$_{41}$-*b*-p(PEO$_{19}$MEMA)$_{12}$ (4) MeOD-*d4* tirpaluose. Intarpas – pMPC$_{41}$-*b*-p(PEO$_9$MEMA)$_{17}$ spektro išplėtimas 3,2–3,5 m.d. ribose.

3. MPC ir DOPMA diblokinių polimerų sintezė

MPC ir DOPMA diblokinių kopolimerų su acetonidu apsaugotomis katecholio grupėmis (pMPC-*b*-pADOPMA) ir neapsaugotomis katecholio grupėmis (pMPC-*b*-pDOPMA) sintezės eiga pateikta 2 schemoje.
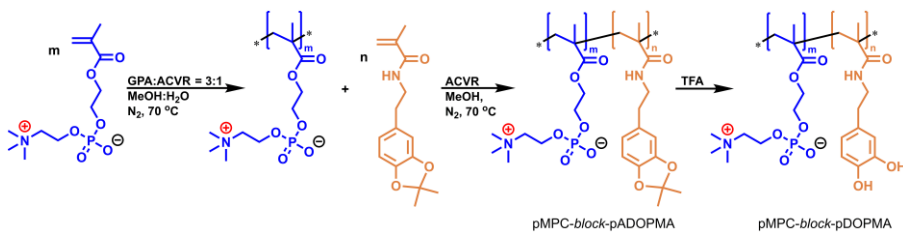
**Schema 2**. Diblokinio kopolimero pMPC-*b*-pDOPMA sintezės schema.

Mažo dispersiškumo pMPC (Đ 1,10) buvo panaudotas kaip makroGPA antrojo bloko sintezei, [ADOPMA]:[makroGPA] = 40:1. Skirtingai nei

pMPC-*b*-pPEOMEMA kopolimerų sintezės atveju, antrasis monomeras ADOPMA yra netirpus vandenyje, todėl pMPC grandinei pratęsti buvo išbandyti įvairūs tirpikliai, iš kurių labiausiai tinkamas buvo metanolis. Metanolis gerai tirpina pMPC bloką, tačiau ribotai – pADOPMA bloką; dėl šios priežasties pADOPMA PL buvo mažas – iki 13.

Blokiniam pMPC-*b*-pADOPMA kopolimerui, sudarytam iš hidrofilinio pMPC bloko ir hidrofobinio pADOPMA bloko, nėra galimybių parinkti MSC eliuento, todėl antrojo bloko PL buvo nustatytas naudojant ^{1}H BMR spektrus. [1]H BMR spektrai buvo naudojami ir kopolimero sudėčiai apskaičiuoti. Kadangi amfifilinių diblokinių kopolimerų ^{1}H BMR spektruose kai kurie cheminiai poslinkiai „pasislepia" ar sumažėja jų intensyvumas, kopolimerų sudėtis buvo nustatyta ir kitu metodu – užrašius kopolimerų tirpalų UV-VIS spektrus. Abiem metodais nustatyta kopolimero sudėtis labai gerai sutampa, paklaida mažiau nei 1 %.
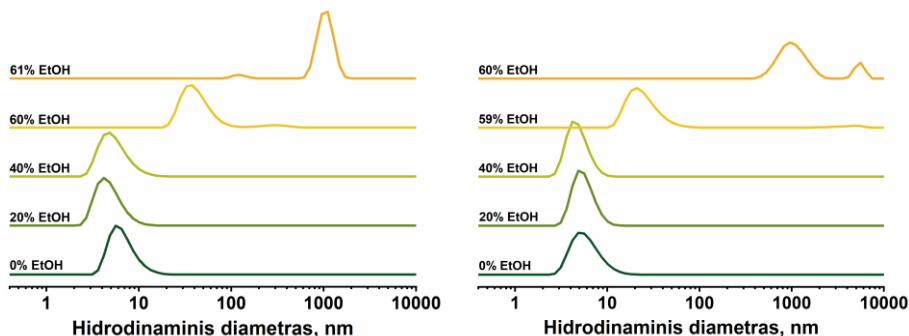
4. MPC kopolimerų savybės

Kopolimerų p(MPC-*grad*-PEOMEMA), kuriuose yra mažai ir santykinai daug MPC grandžių, hidrofiliškumas buvo įvertintas matuojant kopolimero dangos vandens kontaktinį kampą (VKK). Kopolimeru padengus stiklo paviršių, vandens kontaktinis kampas sumažėjo nuo 35° iki 7° (7 pav.). Nustatyta, kad kopolimerų VKK nepriklauso nuo kopolimero sudėties ir yra labai mažas, apie 7°, o tai reiškia, kad kopolimerus p(MPC-*grad*-PEOMEMA) galima laikyti superhidrofiliniais. Diblokinio kopolimero pMPC-*b*-pDOPMA danga ant aukso taip pat buvo labiau hidrofilinė (VKK lygus 29°), lyginant su acetonidu apsaugoto kopolimero pMPC-*b*-pADOPMA danga (VKK 54°).
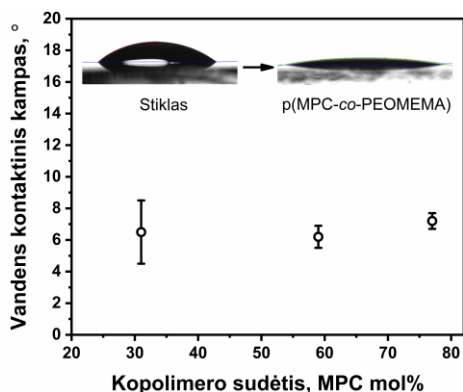
7 pav. Vandens kontaktinio kampo priklausomybė nuo kopolimero p(MPC-*grad*-PEOMEMA) sudėties. Intarpas – VKK nustatymo vizualizacija.

Gradientiniai kopolimerai p(MPC-*grad*-PEOMEMA) gerai tirpsta vandenyje ir etanolyje, tačiau tampa netirpiais vandens-etanolio mišiniuose, kuriuose etanolio yra daugiau kaip 60 tūrio % (8 pav.). Buvo parodyta, kad konetirpumas yra būdingas ne tik pMPC, bet ir p(MPC-*grad*-PEOMEMA) kopolimerams nepriklausomai nuo jų sudėties. Vandens-etanolio tirpaluose etanolio kiekiui pasiekus 60 tūrio %, susidaro maži (20–40 nm skersmens) stabilūs agregatai; etanolio kiekiui didėjant, agregatai tampa dideliais (>800 nm).

Diblokiniai MPC ir PEOMEMA kopolimerai pasižymėjo paviršiniu aktyvumu, jų kritinė micelizacijos koncentracija vandenyje 0,01 mg/mL. Diblokiniai kopolimerai pMPC-*b*-pADOPMA yra tirpūs metanolyje (hidrodinaminis skersmuo d = 4-5 nm), tačiau vandenyje sudaro micelinius agregatus (d = 10-40 nm).

8 pav. Kopolimerų p(MPC-*grad*-PEOMEMA), kuriuose yra 32 mol.% (kairėje) ir 77 mol.% (dešinėje) MPC grandžių, dalelių pasiskirstymas pagal tūrį vandens ir vandens-etanolio mišiniuose.
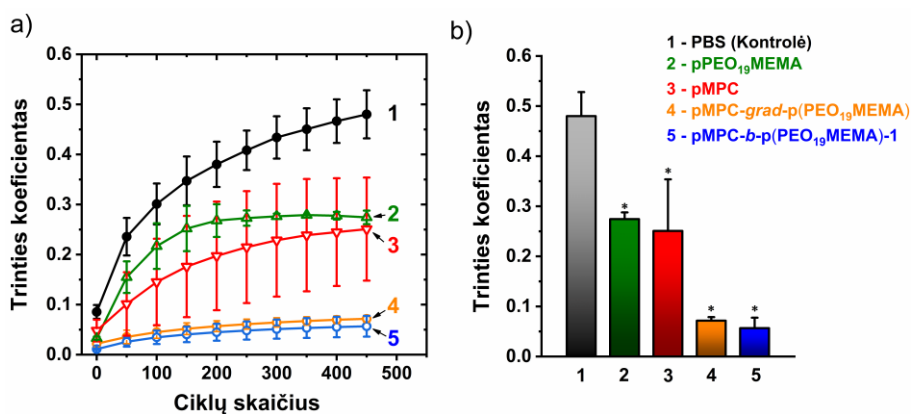
5. MPC ir PEOMEMA kopolimerų lubrikacinės savybės

Kopolimerų lubrikacinėms savybėms įvertinti buvo pasirinktos PDMS-stiklo ir kremzlės-stiklo sistemos. Tribologiniuose bandymuose naudotų (ko)polimerų rodikliai pateikti 2 lentelėje. Siekiant nustatyti optimalią MPC ir PEOMEMA kopolimerų koncentraciją sąnario kremzlės tepimui, pirmiausia buvo atlikti tribologiniai bandymai PDMS-stiklo sistemoje. Rezultatai parodė, kad visi kopolimerų tirpalai ženkliai (keliasdešimt ar net šimtą kartų) sumažino trinties koeficientą (TK). Geriausiai lubrikavo gradientinis kopolimeras p(MPC-*grad*-PEO$_{19}$MEMA), kuris sumažino TK iki 0,004 ± 0,002.

2 lentelė. Tribologiniuose bandymuose naudotų MPC ir PEOMEMA (ko)polimerų rodikliai.

| (Ko)polimeras	Kopolimero sudėtis, MPC mol%	M_n, kDa	Đ	PL
pMPC	100	23,3	1,10	41
p(PEO$_{19}$MEMA)	0	59,1	1,37	62
pMPC-*b*-p(PEO$_{19}$MEMA)-1	77,4	31,8	1,33	41 + 12
pMPC-*b*-p(PEO$_{19}$MEMA)-2	31,0	47,6	1,57	18 + 40
pMPC-*b*-p(PEO$_9$MEMA)	70,7	31,5	1,38	41 + 17
pMPC-*grad*-p(PEO$_{19}$MEMA)	59,8	49,9	1,41	69

9 pav. TK pokytis kremzlės-stiklo sistemoje, lubrikacijai naudojant pMPC, p(PEO$_{19}$MEMA) ir MPC-PEOMEMA kopolimerų (0,4 mg/mL) tirpalus PBS: a) TK priklausomybė nuo ciklų skaičiaus; b) TK pasiekus 450 ciklų.

Atliekant bandymus kremzlės-stiklo sistemoje (9 pav.), TK priklausomai nuo ciklų skaičiaus didėjo, ypač kontroliniame PBS tirpale. Kopolimerų p(MPC-*grad*-PEO$_{19}$MEMA) ir pMPC-*b*-(PEO$_{19}$MEMA)-1 tirpalai pasižymėjo labai geromis lubrikacinėmis savybėmis, nes po 450 ciklų TK vertės padidėjo nežymiai ir liko mažos, atitinkamai 0,072 ± 0,007 ir 0,057 ± 0,021. Taigi, diblokiniai ir gradientiniai MPC ir PEO$_{19}$MEMA kopolimerai pasižymi geresnėmis lubrikacinėmis savybėmis, lyginant su atitinkamais homopolimerais pMPC ir p(PEO$_{19}$MEMA). Puikios diblokinių ir gradientinių MPC ir PEOMEMA kopolimerų lubrikacinės savybės buvo paaiškintos tuo, kad pPEOMEMA blokai sorbuojasi stiklo paviršiuje, o pMPC blokai orientuojasi statmenai paviršiui, sukurdami lubrikacinį sluoksnį.

6. Blokinių MPC ir DOPMA kopolimerų adsorbcijos ant aukso paviršiaus dinamika
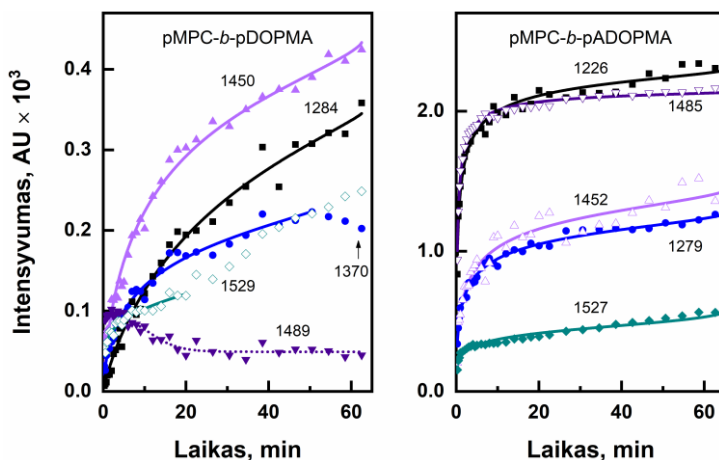
Diblokinių kopolimerų pMPC-*b*-pADOPMA ir pMPC-*b*-pDOPMA adsorbcija ant aukso paviršiaus buvo tiriama įvairiais infraraudonosios spektroskopijos metodais, t. y. taikant visiško atspindžio ATR FTIR, paviršiaus sustiprintą infraraudonąją absorbcijos spektroskopiją (SEIRAS) ir atspindžio absorbcijos infraraudonąją spektroskopiją (RAIRS). Tiriamųjų polimerų ATR-FTIR spektrai pavaizduoti 10 pav.
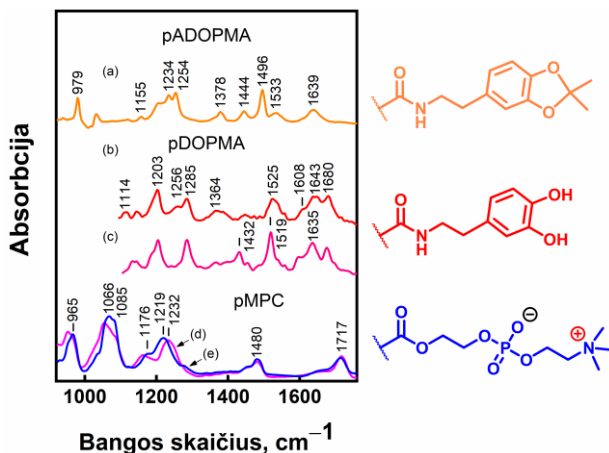
10 pav. ATR-FTIR spektrai: pADOPMA ištirpintas CH_3OH (a), pDOPMA ištirpintas CH_3OH (b) ir CH_3OD (c), pMPC miltelių formoje (d) ir ištirpintas vandenyje (e). Dešinėje, nuo viršaus į apačią, pavaizduoti acetonidu apsaugoto dopamino (pADOPMA), dopamino (pDOPMA) ir fosforilcholino (pMPC) fragmentai.

pMPC monomerinės grandys turi fosforilcholino grupę, kuriai būdingos sugerties juostos ties 1080 ir 1230 cm^{-1}, atitinkančios simetrinį ir asimetrinį fosfatinės grupės virpesius. Asimetrinis virpesys $\nu_{as}(PO_2)$ yra jautrus hidratacijos laipsniui, todėl šios sugerties juostos bangos skaičius pasislinko 30 cm^{-1}. Nepaisant to, kad MPC monomerinių grandžių yra 3,5 karto daugiau nei DOPMA, SEIRAS spektruose dominuoja DOPMA sugerties juostos ties 1255, 1284, 1369 ir 1529 cm^{-1}. Tai rodo, kad sąveikoje su paviršiumi pirmiausia dalyvauja katecholio hidroksigrupės, o ne fosforilcholinas, kurio fosfatinės grupės virpesių juostos yra silpnos; tikėtina, kad PO_2 grupės yra nutolusios nuo paviršiaus.

SEIRAS spektrų kitimas laike parodė, kad reikšminga sorbciją ir molekulinis persiorientavimas įvyksta per pirmąsias 10 minučių (11 pav.). Analizuojant skirtuminį spektrą, gautą iš SEIRAS spektro po 60 min. atėmus spektrą po 1 min., nustatyta, kad padidėjo sugerties juostos ties 1280 cm^{-1}, susijusios su DOPMA, intensyvumas ir sumažėjo sugerties juostos ties 1481 cm^{-1}, susijusios su MPC C-H ryšių deformacija, intensyvumas. Tai reiškia, kad sorbcijos pradžioje cviterjoniniai pMPC blokai yra netoli aukso paviršiaus (spektras po 1 min.), tačiau vėliau (po 2-16 min.) aukso paviršiuje esantis diblokinis kopolimeras keičia konformaciją – pDOPMA blokas atsiduria prie aukso paviršiaus, o pMPC blokas nuo paviršiaus nutolsta.

11 pav. Diblokinių kopolimerų pMPC-*b*-pDOPMA ir pMPC-*b*-pADOPMA kai kurių SEIRAS spektro sugerties juostų intensyvumo kitimas laike. Eksperimentiniai duomenys aproksimuoti modifikuota Langmuiro-Freundlicho izoterma (ištisinės linijos).

Nustatyta, kad diblokinis kopolimeras pMPC-*b*-pADOPMA su acetonidu apsaugotomis katecholio grupėmis pasižymėjo fizisorbcija, kuriai būdinga greita adsorbcija ir palyginti lengva desorbcija, o kopolimeras pMPC-*b*-pDOPMA pasižymėjo chemine adsorbcija, kuri vyksta lėčiau, tačiau sąveika su aukso paviršiumi stipresnė. Naudojant SEIRAS ir RAIRS spektroskopiją pavyko įrodyti diblokinių kopolimerų persiorientavimą adsorbcijos metu, kai ir po tam tikro laiko pMPC blokas yra nukreipiamas į vandeninę fazę, o pDOPMA blokas lieka prie aukso paviršiaus.

Išvados

1. ^1H BMR spektroskopijos ir molekulinių sietų chromatografijos (MSC) metodais buvo ištirta cviterjoninio monomero 2-metakriloiloksietilfosforilcholino (MPC, M_1) kopolimerizacijos su makromonomeru PEO metakrilatu (PEOMEMA, M_2) RAFT kopolimerizacijos kinetika. Vidutinės kopolimero sudėties priklausomybė nuo monomerų konversijos ženkliai skyrėsi nuo apskaičiuotos pagal radikalinės kopolimerizacijos galinės grandies modelį, pagrįstą eksperimentiškai nustatytais monomerų santykiniais aktyvumais $r_1 = 2,48$ ir $r_2 = 0,40$. Kopolimerams p(MPC-*grad*-PEOMEMA) buvo būdinga stipriai išreikšta gradientinė mikrostruktūra. Nepaisant gradientinės mikrostruktūros, kopolimerų dispersiškumas buvo gana mažas (Đ < 1,3), o molekulinė masė artima teoriškai numatytai.

2. Hidrofiliniai diblokiniai šepetiniai kopolimerai, kuriuose yra ir fosforilcholino grupių, ir PEO šoninių grandinių, buvo susintetinti pirmiausia vykdant cviterjoninio monomero MPC RAFT polimerizaciją, o po to – makromonomero PEOMEMA RAFT polimerizaciją pMPC tirpale. pMPC blokas pasižymėjo labai mažu dispersiškumu (Đ ≤ 1,1), o diblokinių kopolimerų dispersiškumas buvo vidutinis, Đ apie 1,3-1,6. Antrojo bloko polimerizacijos laipsnis buvo kontroliuojamas ir kito nuo 10 iki 70.

3. Vykdant RAFT polimerizaciją buvo susintetinti amfifiliniai diblokiniai kopolimerai pMPC-*b*-pDOPMA, kuriuos sudaro pMPC blokas, pasižymintis unikaliomis savybėmis apsaugant paviršius nuo nespecifinės baltymų adsorbcijos ir gerinant lubrikaciją vandeninėje terpėje, ir pDOPMA blokas, puikiai prikimbantis prie įvairių paviršių. Sintezei buvo naudojamas DOPMA monomeras su acetonidu apsaugota katecholio grupe (ADOPMA), kuri padėjo išvengti nepageidaujamų šalutinių reakcijų polimerizacijos metu ir apsaugoti susintetintus kopolimerus nuo oksidacijos laikymo metu. Kopolimerų diblokinė struktūra buvo įrodyta užrašius ^1H BMR ir ^{13}C BMR spektrus ir atlikus jų tirpalų tyrimus DLS metodu.

4. Mišriuose etanolio ir vandens tirpaluose hidrofiliniams gradientiniams ir diblokiniams MPC ir PEOMEMA kopolimerams buvo būdingas konetirpumo reiškinys. Amfifiliniai diblokiniai MPC ir DOPMA kopolimerai tirpo metanolyje, tačiau vandeniniuose tirpaluose sudarė miceles. Gradientiniai kopolimerai p(MPC-*grad*-PEOMEMA), nepriklausomai nuo sudėties, pasižymėjo superhidrofiliškumu (vandens kontaktinis kampas apie 7°), o

diblokiniai kopolimerai pMPC-*b*-pPEOMEMA pasižymėjo paviršiniu aktyvumu (kritinė micelizacijos koncentracija 0,01 mg/mL).

5. MPC ir PEOMEMA diblokinių ir gradientinių kopolimerų lubrikacinės savybės įvertintos atliekant tribologinius matavimus sistemose PDMS-stiklas ir kremzlė-stiklas. Geriausią lubrikaciją vandeninėse terpėse užtikrino kopolimerai, turintys santykinai daug MPC grandžių. Vidutinis dinaminis trinties koeficientas (TK) sistemoje PDMS-stiklas, kai kopolimerų koncentracija 0,4 mg/mL, buvo tik 0,004-0,007, o kopolimerų TK vertės sistemoje kremzlė-stiklas po 450 slydimo ciklų buvo 0,06-0,07. Puikios diblokinių ir gradientinių MPC ir PEOMEMA kopolimerų lubrikacinės savybės aiškinamos tuo, kad pPEOMEMA blokai sorbuojasi stiklo paviršiuje, o pMPC blokai orientuojasi statmenai paviršiui, sukurdami lubrikacinį sluoksnį.

6. Diblokinių kopolimerų pMPC-*b*-pADOPMA ir pMPC-*b*-pDOPMA adsorbcija ant aukso paviršiaus buvo tiriama naudojant įvairius infraraudonosios spektroskopijos metodus, t. y. ATR-FTIR, SEIRAS ir RAIRS. Kopolimeras su acetonidu apsaugotomis katecholio grupėmis pMPC-*b*-pADOPMA pasižymėjo greita ir intensyvia fizisorbcija bei lengva ultragarso sukelta desorbcija. Priešingai, kopolimerui su neapsaugotomis katecholio grupėmis pMPC-*b*-pDOPMA buvo būdinga chemisorbcija su lėtesne dinamika ir stipresne sąveika su substratu.

7. Spektriniai duomenys rodo, kad pirmajame adsorbcijos etape cviterjoninės fosforilcholino grupės daugiausia buvo išsidėsčiusios netoli aukso paviršiaus, tačiau vėliau vyko diblokinių kopolimerų persiorientavimas paviršiuje, dėl to prie paviršiaus atsiduria pDOPMA blokas. SEIRAS matavimai, atlikti esant skirtingiems elektriniams potencialams, ir vandens kontaktinio kampo kitimas parodė ypatingą fosforilcholino grupių hidrofiliškumą ir vandens molekulių pritraukimą. Šie duomenys netiesiogiai įrodė, kad adsorbuotuose diblokinių kopolimerų pMPC-*b*-pDOPMA sluoksniuose pDOPMA blokas buvo prie aukso paviršiaus, o hidrofilinis pMPC blokas buvo nukreiptas tolyn nuo paviršiaus, sudarydamas labai hidratuotą sluoksnį.

Acknowledgements

Firstly, I would like to express my gratitude towards my supervisor and mentor Prof. Dr. Ričardas Makuška for an invitation to continue scientific career, and for his invaluable guidance, authority, support, and encouragement during the entire phD period.

Special recognition is dedicated to Assoc. Prof. Dr. Vaidas Klimkevičius for his help with processing the data, publishing articles, leadership in synthesis planning, and for being an inspiration of a true scientist.

I would like to thank coauthors dr. Martynas Talaikis, dr. Vaidas Pudžaitis, prof. dr. Gediminas Niaura for contributing in research, supervision, experimental ideas, and publishing a scientific article.

I would also like to express my appreciation to students Agnė Uscilaitė and Austėja Šimkutė for support and generously sharing their data on the solubility properties of copolymers.

I would like to thank all the colleagues of Vilnius University, Faculty of Chemistry and Geosciences and Center for Physical sciences and Technology, particularly my friends Martynas Malikėnas and Edvin Parafjanovič for their unwavering support, willingness to help, and engaging philosophical discussions over a cup of coffee.

I am also grateful to the reviewers for their suggestions and tips.

Finally, I want to express my deepest gratitude to my family – my wife Emilija and my son Steponas – for their unwavering love, encouragement, smiles, and support. Their constant inspiration has guided me in pursuing my goals. I'm also thankful to my dear relatives and friends for their immense help, love, and support over the past four years.

CURRICULUM VITAE

Personal information

Name, Surname	Marijus Jurkūnas
Date of birth and place	1994-03-15 Panevėžys, Lithuania
E-mail address	marijus.jurkunas@gmail.com

Education

2009-2013	Juozas Balčikonis gymnasium, Panevėžys
2013-2017	Bachelor degree of Science in Chemistry, Vilnius University
2017-2019	Master degree of Science in Chemistry, Vilnius University

Work experience

2017-2019	Engineer, Center for Physical Sciences and Technology
2022-2023	Project expert, Vilnius University
2023-2024	Laboratory technician, Vilnius University
2024-present	R&D scientist III, manufacturing sciences, Thermo Fisher Scientific Baltics

LIST OF PUBLICATIONS AND CONFERENCE PARTICIPATION

Articles in journals included in the thesis:

1. M. Jurkūnas, V. Klimkevičius, A. Uscilaitė, R. Makuška. Synthesis of Superhydrophilic Gradient-Like Copolymers: Kinetics of the RAFT Copolymerization of Methacryloyloxyethyl Phosphorylcholine with PEO Methacrylate. *European Polymer Journal* 183 (2023) 111764. https://doi.org/10.1016/j.eurpolymj.2022.111764

2. M. Jurkūnas, M. Talaikis, V. Klimkevičius, V. Pudžaitis, G. Niaura, R. Makuška. Diblock Copolymers of Methacryloyloxyethyl Phosphorylcholine and Dopamine Methacrylamide: Synthesis and Real-time Adsorption Dynamics by SEIRAS and RAIRS. *Langmuir* 40 (2024) 5945–5958. https://doi.org/10.1021/acs.langmuir.3c03925

3. M. Jurkūnas, K. Ren, P. K. Sharma, R. Makuška. Synthesis and articular cartilage biolubricating properties of nature inspired polymethacrylate-type copolymers containing phosphorylcholine moieties and poly(ethylene oxide) brushes. Submitted to the journal *Friction.*

Articles in journals not included in the thesis:

1. M. Kirsnytė, M. Jurkūnas, Ž. Kancleris, et al. Investigation of in situ formed conductive polymer composite in adhesive matrix, *Synthetic Metals* 258 (2019) 116181.
https://doi.org/10.1016/j.synthmet.2019.116181

2. A. Taha, F. Casanova, P. Šimonis, J. Jonikaitė-Švėgždienė, M. Jurkūnas, M. Gomaa, A. Stirkė. Pulsed electric field-assisted glycation of bovine serum albumin/starch conjugates improved their emulsifying properties. *Innovative Food Science & Emerging Technologies* 82 (2022) 103190.
https://doi.org/10.1016/j.ifset.2022.103190

3. A. Taha, F. Casanova, M. Talaikis, V. Stankevič, N. Žurauskienė, P. Šimonis, V. Pakštas, M. Jurkūnas, M. Gomaa, A. Stirkė. Effects of Pulsed Electric Field on the Physicochemical and Structural Properties of Micellar Casein. *Polymers* 15 (2023) 3311.
https://doi.org/10.3390/polym15153311

Attended conferences on the subject of the thesis:

1. M. Jurkūnas, V. Klimkevičius, R. Makuška. Synthesis of Brush Copolymers Carrying Phosphorylcholine Moieties, 23rd International Conference-School *Advanced Materials and Technologies 2021*, Palanga, June 8-10, 2021.

2. M. Jurkūnas, V. Klimkevičius, A. Uscilaitė, R. Makuška. Phosphorylcholine-based Diblock and Random Brush Copolymers, *Chemistry and Chemical Technology 2021*, Vilnius, September 20-22, 2021.

3. M. Jurkūnas, V. Klimkevičius, R. Makuška. Kinetics of RAFT Copolymerization of 2-Methacryloyloxyethyl Phosphorylcholine with PEO Macromonomer, *Baltic Polymer Symposium 2022*, Tallinn, May 10-12, 2022.

4. M. Jurkūnas, V. Klimkevičius, R. Makuška. Synthesis of Adhesive Block Brush Copolymers Carrying Phosphorylcholine Moieties, 24th International Conference-School *Advanced Materials and Technologies 2022*, Palanga, September 5-7, 2022.

5. M. Jurkūnas, V. Klimkevičius, R. Makuška. Diblock Copolymers with Gradient Distribution of Zwitterionic and Brush Fragments, and Containing Catechol Moieties for Surface Modification, *Open Readings 2023*, Vilnius, March 14-16, 2023.

6. M. Jurkūnas, V. Klimkevičius, R. Makuška. Diblock Copolymers of Methacryloyloxyethyl Phosphorylcholine and Dopamine Methacrylamide: Synthesis and Solution Properties, *Baltic Polymer Symposium 2023*, Jelgava, June 7-9, 2023.

NOTES

NOTES